INTER-AMERICAN TROPICAL TUNA COMMISSION

SCIENTIFIC ADVISORY COMMITTEE

13TH MEETING

(by videoconference)

16-20 May 2022

DOCUMENT SAC-13 INF-S

STOCK ASSESSMENT OF SOUTH PACIFIC ALBACORE TUNA

SCIENTIFIC COMMITTEE

SEVENTEENTH REGULAR SESSION

Online meeting

11–19 August 2021

Stock assessment of South Pacific albacore tuna

WCPFC-SC17-2021/SA-WP-02

August 10 2021 Rev 2

C. Castillo Jordán[1], J. Hampton[1], N. Ducharme-Barth[1], H. Xu[2], T. Vidal[1], P. Williams[1], F. Scott[1], G. Pilling[1] and P. Hamer[1]

[1]Oceanic Fisheries Programme, Pacific Community (SPC), Nouméa, New Caledonia
[2]Inter-American Tropical Tuna Commission, La Jolla, United States

Revision 1:

Revision one of this paper includes an updated Appendix 6 that now includes stock projections based on both catch and effort. There is a minor addition to the last conclusions dot point on page 42. Some axis labels were corrected, i.e. Fig. 12 bottom graph Y-axis is now labelled correctly as depletion. The caption in Fig. 46 had indicated that the blue point was the median, this was meant to be the diagnostic case model.

Revision 2:

Revision 2 has the addition of data bars to represent the 'recent' and 'latest' median values, and uncertainty quantiles, for $SB/SB_{F=0}$ to Figure 44. It also includes an additional table 5 in Appendix 6 that has the alternative "status quo" values of catch and effort used for the stock projections.

Contents

1 Executive Summary

This paper describes the 2021 stock assessment of albacore tuna (*Thunnus alalunga*) across the South Pacific ocean (south of the equator), incorporating the Convention areas of the Western and Central Pacific Fisheries Commission (WCPFC) and the Inter American Tropical Tuna Commission (IATTC). A further three years of data are available since the last stock assessment was conducted in 2018; the model time period now extends from 1960–2019. The 2018 assessment was restricted to the convention area under the jurisdiction of the WCPFC (Tremblay-Boyer et al., 2018a). This assessment is the first complete attempt at a spatially structured South Pacific wide assessment, although a previous assessment applied an areas-as-fleets approach to the stock across the entire South Pacific (Hoyle et al., 2012).

Key changes made in the progression from the 2018 reference case to the 2021 diagnostic case model include:

- Updating all data to the end of 2019 and applying a new version of Multifan-CL (2.0.8.2)
- Refinements to the geostatistical approach for standardisation of longline CPUE for the index fisheries.
- Moving to a South Pacific-wide four region spatial structure with simplification of the model regions for the WCPFC area and use of an areas-as-fleet approach to stratify fisheries in the IATTC area.
- Applying an areas-as-fleets approach to stratify fisheries within the 'overlap' area between the WCPFC and IATTC Convention areas (previous assessments defined separate model regions for this area).
- Applying re-analysed otolith ageing data and a new approach to generating natural mortality (M)-at-age based on growth parameters.
- Combining growth and M into a single axis of uncertainty, with two options; one involved growth parameters estimated from the reanalysed otoliths external to the model and the other used growth parameters estimated from the length frequency data external to the model. The previous assessment applied a conditional-age-at-length approach.
- Inclusion of structural uncertainty axes for movement probabilities and recruitment distribution. This assessment used SEAPODYM model outputs to inform movement coefficients and recruitment distributions, along with alternative approaches that were similar to those of the previous assessment.

In addition to the diagnostic case model, we report the results of one-off sensitivity models to explore the relative impacts of key data and model assumptions on the stock assessment results and conclusions. We also undertook a structural uncertainty analysis (model grid) for consideration in developing management advice, where all possible combinations of the axes of uncertainty were included. It is recommended that management advice is formulated from the results of the structural uncertainty grid. The results from this assessment are not directly comparable to the previous assessment due to the different geographical extent of the assessment and regional/fishery structures applied. Recognising the interest in separating reference points between the two convention areas, results for the key depletion based reference points are provided for the WCPFC Convention Area (WCPFC-CA) (which includes the 'overlap' region) and for the IATTC region (referred to as the EPO), along with the entire assessment region.

Across the range of models run in this assessment, the most important factor when evaluating stock status was the hypothesis related to age-specific movement probabilities among the model regions, an uncertainty that was not examined in the 2018 assessment because movement was estimated in the model. The size data weighting and to a lesser degree the combined growth/M hypotheses had some influence on uncertainty in management quantities, but the steepness and recruitment distribution hypotheses had minimal influence on depletion.

Applying the regional movement probabilities predicted from the SEAPODYM model resulted in more pessimistic estimates of spawning potential and depletion. While the SEAPODYM movement probabilities may incorporate more biological 'realism', it is unclear what is the most appropriate movement hypothesis to apply. More work is required to reduce this uncertainty for South Pacific-wide albacore assessments that use spatially explicit models.

The general results of this assessment are as follows:

- Spawning Potential: Spawning potential for the South Pacific albacore stock declined from 1960 until the early 1980s after which it stabilised for a period, before declining more gradually as catches increased from the 1990s until 2010. A more notable decline in spawning potential is estimated to have occurred since 2015.
- Depletion: The terminal depletion levels estimated by this assessment for the South Pacific stock as a whole are the most pessimistic across the model time period with $SB_{recent}/SB_{F=0}$ median of 0.47 (0.40 - 0.56, 10^{th} and 90^{th} percentiles) and $SB_{latest}/SB_{F=0}$ median of 0.36 (0.27 - 0.44, 10^{th} and 90^{th} percentiles). However, none of the 72 models exceeded the WCPFC limit reference point (LRP) of $20\%SB_{F=0}$. There is no target reference point applied for the stock at the scale of the entire South Pacific.
- Fishing Morality: A steady increase in the South Pacific wide fishing mortality on adult age-classes is estimated to have occurred over most of the assessment period, accelerating since the 1990s, with a rapid increase in the last five years. Juvenile fishing mortality increased until around 1990, and has remained stable at a comparatively low level since that time. Recent fishing mortality is estimated to be below F_{MSY} ($F_{recent}/F_{\text{MSY}}$ median 0.26; 0.16 - 0.38, 10^{th} and 90^{th} percentiles) and none of the 72 models had recent F exceeding F_{MSY}.
- WCPFC-CA: For the WCPFC-CA, estimated spawning biomass had become more depleted since the end of the previous assessment (i.e. data to 2016). Median estimates of depletion are below the interim TRP of 0.56 ($SB_{recent}/SB_{F=0}$ median=0.47; 0.42 - 0.58, $SB_{latest}/SB_{F=0}$ median=0.36; 0.28 - 0.43, 10^{th} and 90^{th} percentiles), but no models estimated the stock to be below $20\%SB_{F=0}$. Relative to the interim TRP, some individual models estimated depletion above the interim TRP when considering 'recent' depletion levels, but most (86%, 62 of 72 models) indicated that $SB_{recent}/SB_{F=0}$ was less than the TRP, and all models estimated depletion below the interim TRP when considering 'latest' depletion levels. In relation to management objectives for the WCPFC-CA southern longline fishery, this assessment estimated that the median 'latest' (2019) and 'recent' (2016-2019) longline vulnerable biomass for the WCPO are 60% and 78% of the 2013+8% target level that defined the interim TRP.

Summary: The 2021 South Pacific albacore stock assessment provided results consistent with the previous assessment; that is, a decline in estimated spawning potential over most of the assessment period, and in particular, within the most recent years. The addition of the EPO region into the

current assessment did not notably alter the main assessment outcomes, and similar trajectories and terminal depletion were estimated in both RFMO regions. The most influential uncertainty of those considered in this assessment was the assumption related to movement of fish among the model regions. Further research on albacore movement and population mixing across the entire South Pacific should be a priority. Given the difficulty of tagging albacore, genetic and otolith based approaches are recommended. However, perhaps of greatest concern for this assessment is the lack of contrast in the standardised CPUE indices, and greater reliance on size composition to inform population scale. We note the development of the Close Kin Mark Recapture (CKMR) methods that can provide information on population scale and stock structure, along with other fishery-independent information on uncertain biological processes, and we strongly recommend that this approach is considered for South Pacific albacore, noting that the feasibility of this method for South Pacific albacore is now outlined in Bravington et al. (2021).

Uncertainty in the most recent estimates of the South Pacific albacore stock status are highlighted, given they are reliant on sparse information until the older age-classes are observed in longline fishery catches.

The potential stock consequences of fishing at alternative "status quo" conditions (i.e. at recent average fishing levels) were evaluated through stochastic projections, using the uncertainty framework approach previously endorsed by SC. The results are included in Section 18.

2 Introduction

This paper presents the 2021 stock assessment of South Pacific albacore tuna (*Thunnus alalunga*). The Scientific Committee (SC) of the Western and Central Pacific Fisheries Commission (WCPFC) requested that the 2021 assessment cover the entire South Pacific, the previous assessment being restricted to the WCPFC Convention Area (WCPFC-CA) south of the equator (Tremblay-Boyer et al., 2018a). This assessment covers the albacore fisheries from the equator to 50°S in the Pacific Ocean, incorporating the convention areas of the WCPFC and the Inter American Tropical Tuna Commission (IATTC) (Figure 1). Since 1999, South Pacific albacore has been assessed regularly for the WCPFC convention area (Hoyle and Davies, 2009; Hoyle et al., 2012; Harley et al., 2015; Tremblay-Boyer et al., 2018a), with one assessment that covered the entire South Pacific (Hoyle et al., 2012). There has been no previous stand-alone assessment of albacore in the south eastern Pacific Ocean region (herein referred to as the EPO) under the jurisdiction of the IATTC. The 2012 assessment conducted by Hoyle et al. (2012) included the EPO as a fishery stratum in a single region areas-as-fleets model. The 2021 assessment is the first attempt at a fully spatially structured assessment of albacore across the South Pacific Ocean, requiring collaboration between scientists from the Pacific Community (SPC, the Scientific Services Provider for the WCPFC) and the IATTC.

The 2021 assessment continues the development of stock assessment models for South Pacific albacore, facilitated by the ongoing development of the statistical stock assessment software, known as MULTIFAN-CL[3] (Fournier et al., 1998; Hampton and Fournier, 2001; Kleiber et al., 2019), that is routinely used by SPC for assessments of tuna and tuna-like species. The move to a spatially structured South Pacific-wide assessment necessitated a revision of the spatial and fishery structures applied in the previous assessment (discussed in detail in Section 4.1). Further, each new assessment can involve updates to fishery input data, implementation of new features in

[3] www.multifan-cl.org

the MULTIFAN-CL modelling software, and consideration of new information on biology, population structure and other population parameters. These changes are an important part of efforts to improve the modelling procedures to more accurately estimate stock status, fishing impacts, and biological and population processes. However, they can result in changes to the estimated status of the stock and fishing impacts from previous assessments. It is important to recognise that each new assessment represents a new estimation of the historical population dynamics, impacts of fishing and stock status. Advice from the SC on previous assessments, and the annual pre-assessment workshops (PAW) (Hamer et al., 2021) guide this ongoing process.

The objectives of this assessment are to estimate population parameters, such as time series of recruitment, biomass, biomass depletion and fishing mortality, which indicate the stock status and impacts of fishing. We summarize the stock status in terms of reference points adopted by the WCPFC for routine reporting in tuna assessments. The methodology used for the assessment is based on the general approach of integrated modelling (Fournier and Archibald, 1982), which is carried out using MULTIFAN-CL, and implements a size-based, age- and spatially-structured population model. Model parameters are estimated by maximizing an objective function, consisting of both likelihood (data) and prior information components (penalties). The assessment uses an 'uncertainty grid' of models as the basis for management advice. The uncertainty grid is a group of models that are selected to explore the interactions among key axes of uncertainty that relate to plausible biological assumptions, data inputs and data treatment. The variation in estimates of the key management quantities across the uncertainty grid represents the current appreciation of uncertainty in stock status and should be considered carefully by managers.

This assessment report should be read in conjunction with several supporting papers, listed below:

- Background analysis and data inputs for the 2021 South Pacific albacore tuna stock assessment (Vidal et al., 2021)
- Ageing of South Pacific albacore (Project 106) (Farley et al., 2021)
- Report from the SPC Pre-assessment Workshop - March 2021 (Hamer et al., 2021)

3 Background

3.1 Stock structure

Albacore are distributed globally with separate stocks in the Indian, Atlantic and Pacific Oceans (Nikolic et al., 2017, 2020). In the Pacific Ocean, albacore are thought to comprise discrete stocks north and south of the equator (Nikolic et al., 2017). In the South Pacific, the stock structure is not fully resolved. Tag recapture data for releases in the southern region of the Western and Central Pacific Ocean (WCPO, refers to west of 130°W) show a high level of latitudinal mixing, and provide some evidence of individual movements from the WCPO to the southern EPO (Figure 2). The longest period at liberty for a recaptured tagged albacore in the South Pacific is 11 years, and for the North Pacific 15 years (ISC Albacore Working Group, 2011). Tagging mortality is thought to be high in albacore and, as a result, there have been limited tagging programs for this species and it is, therefore, not an ongoing focus of tuna tagging in the South Pacific. The earlier tagging programmes that targeted albacore in the South Pacific occurred in the early 1990s and again in 2009-2011. For both these programmes the tag releases were all in the southern temperate latitudes (south of 30°S), with most releases being immature fish (<80 cm FL), and most recapture displacements occurring in a northerly direction (Figure 2). There have

been no tagging studies in the EPO. Tagging with PSATs (pop-up satellite tags) in the south western Pacific showed the capacity for large movements, with one individual moving more than 1000 km in 50 days (Williams et al., 2015).

The south-north mixing, and the prevalence of smaller albacore in the southern region of the WCPO suggests a southern juvenile feeding/nursery area, south of 30°S, with increased northerly movements and residency with age (Farley et al., 2014; Nikolic et al., 2017). In the WCPO, spawning and larval stages mostly occur where surface water temperatures (SST) are >24°C, and typically north of 35°S (Farley et al., 2014; Nikolic et al., 2017). In the EPO, size composition data also show a pattern of smaller juveniles occurring where SST is <24°C, typically closer to South America (see appendix E in Vidal et al. (2021)). Although spawning areas in the EPO are not documented, similar to the WCPO, larger fish appear to be more abundant in catches where SST is >24°C (Vidal et al., 2021). The level of mixing between the WCPFC and IATTC convention areas is poorly known. Significant spatial variation in growth and observed length-at-age with longitude has been observed, which suggests a more complex spatial structure with longitude (Williams et al., 2012). Otolith chemistry studies have suggested that fish caught near French Polynesia in the central South Pacific were from a separate larval source than fish caught further west (Macdonald et al., 2013). Similarly, for five sample groups from the western, central and southern Pacific, Anderson et al. (2019) provided evidence of population structuring at adaptive loci, particularly a differentiation of samples from French Polynesia. Further studies are needed to resolve the level of mixing between the WCPO and EPO regions to better inform assessments at the scale of the entire South Pacific.

Adult longline catch data indicate that they also appear to migrate seasonally between tropical and sub-tropical waters (Langley, 2004; Nikolic et al., 2017). These data show that albacore in the southern hemisphere are most abundant in sub-equatorial waters during December-January and May-July, indicating that albacore migrate south during early summer, and north during winter. This movement tends to correspond with the seasonal shift in the 23–28°C sea surface temperature isotherm.

Understanding the potential extent of mixing across the South Pacific may also be informed by recent developments in quantitative modelling of the spatial dynamics of South Pacific albacore across life history stages (SEAPODYM) (Lehodey et al., 2015; Senina et al., 2020). The SEAPODYM modelling framework is highly spatially resolved and provides predictions on spatio-temporal exchange of biomass by age class (in numbers and months), forced by environmental/habitat variables. SEAPODYM can potentially be used to predict the exchange rates among model regions to inform transfer rates in the stock assessment model. The idea of applying SEAPODYM outputs to informing movement between model regions by 'quarter' and 'age' was discussed at the Pre-assessment Workshop (Hamer et al., 2021), and is explored in the 2021 assessment.

3.2 Vertical movement behaviour

An important aspect of albacore behaviour for understanding their ecology and how they interact with fishing gear is vertical movement. For example, vessels that target albacore tuna at warmer latitudes typically set longlines at depths between 100 and 400 m (Bigelow et al., 2006), while those at cooler latitudes typically set at shallower depths of around 100 m, and the troll fishery targeting smaller fish around New Zealand typically fishes at <10 m depth (Williams et al., 2015). Williams et al. (2015) used PSAT tags to study vertical movement behaviour of individual

albacore tagged near New Caledonia, Tonga and New Zealand (tagged fish were 89-107 cm fork length, FL). They found that for the tropical latitudes (i.e., New Caledonia and Tonga), albacore tuna showed a distinct diurnal pattern in vertical habitat use, occupying shallower, warmer waters above the mixed layer depth (MLD) at night (e.g., <150 m deep), and deeper, cooler waters below the MLD during the day (e.g., 200-300 m deep). However, there was little evidence of a diurnal pattern of vertical migration behaviour in albacore at temperate latitudes (New Zealand), with fish staying in shallow waters above the MLD (e.g., <150 m deep) almost all of the time. This latitudinal variation in vertical migration was reflected in diets with the surface dwelling fish near New Zealand consuming a low diversity of prey consisting primarily of crustaceans, but albacore in the more tropical regions consuming primarily fish, with significantly more deeper-water species and a greater diversity of prey species.

3.3 Biology

3.3.1 Reproductive biology

Albacore spawn in tropical and sub-tropical waters between latitudes 10°S and 30°S during the austral summer (Farley et al., 2014). In the South Pacific, Farley et al. (2013b) and Farley et al. (2014) estimated ages at 50% and 100% maturity of 4.5 and 7 years respectively. The minimum reported size of mature females was 74 cm FL with the length at 50% maturity of approximately 85 cm FL, and the length at 100% maturity was 94 cm FL. Juveniles are caught in surface fisheries in New Zealand's coastal waters, and in the vicinity of the sub-tropical convergence zone (STCZ, at about 40°S) in the South Pacific, at about one year old and at a size of 40–50 cm FL.

3.3.2 Growth

Daily otolith growth increments indicate that initial growth is rapid (Renck et al., 2014; Farley et al., 2021), with albacore reaching 45–50 cm FL in their first year (Williams et al., 2012; Farley et al., 2021). Subsequent growth is slower, at approximately 12 cm per year from 2 to 4 years age, and declining thereafter (Williams et al., 2012; Farley et al., 2021). Maximum recorded length is about 120 cm FL but sex-combined von Bertalanffy growth models for both the South and North Pacific albacore predict an L_∞ of around 105 cm (Williams et al., 2012; Farley et al., 2013a, 2014). Maximum age is around 15 years for males and females (Williams et al., 2012; Farley et al., 2021). Recent analyses of age-at-length from otolith data have identified important patterns in South Pacific albacore growth (Williams et al., 2012; Farley et al., 2021). Males grow to larger sizes than females, and their lengths-at-age begin to diverge above 85 cm FL, when they reach maturity. Lengths-at-age of both sexes also appear to vary with longitude, with growth rates and maximum sizes increasing toward the east. In the New Zealand troll fishery, there are clear 10 cm modes in the length frequency data for juveniles between 50 and 80 cm. These modes are likely to represent annual growth, based on the annual spawning peaking in January (Farley et al., 2014). Farley et al. (2021) re-analysed otoliths from Farley et al. (2013b) and applied a new decimal age algorithm (developed for WCPO Pacific bigeye and yellowfin) to obtain updated decimal age estimates for albacore. The updated growth estimates based on these data are used in the 2021 assessment.

3.3.3 Natural mortality

The instantaneous natural mortality (M) rate is thought to be between 0.2 and 0.5 per year, with significant numbers of fish living 10 years or more. The default M of 0.4 used in previous

assessments was updated in 2015 to 0.3 to match that used in other stocks, including the North Pacific. However, a recent meta-analysis of mortality for the North Pacific stock indicated M should be closer to 0.4, higher for females, and age-specific (Kinney and Teo, 2016). The value of M is an important biological uncertainty that is estimated again for the current assessment based on the revised age-at-length data in Farley et al. (2021) and is discussed further below.

3.4 Fisheries

Distant-water longline fleets from Japan, Korea, Chinese Taipei, and China, and the domestic longline fleets from a number of Pacific Island Countries and Territories (PICTs), catch albacore over a large area of the South Pacific (Figure 4, Figure 5). Most of the catch is taken by longline. Smaller albacore have been targeted by a troll fishery around New Zealand (model region WCPO3) since the 1960s, the United States troll fishery fishing further east, and a small fishery occurs along the east coast of Australia. Catches from the troll fishery are relatively small, generally less than 10,000 mt per year. The Chinese Taipei fleet, in particular, has targeted albacore consistently since the 1960s (Figure 5). Since the mid-1990s, longline catch and effort (Figure 6) has increased considerably with the development and expansion of longline fisheries targeting albacore in several Pacific Island EEZs, notably those of American Samoa, Cook Islands, Fiji, French Polynesia, New Caledonia, Samoa, Solomon Islands, Tonga, and Vanuatu. Driftnet vessels from Japan and Chinese Taipei also targeted albacore in the central Tasman Sea and in the central Pacific near the sub-tropical convergence zone for a short period during the 1980s and early 1990s (Figure 4). Driftnet catch reached approximately 22,000 mt in 1989, but rapidly declined to zero following a United Nations moratorium on industrial-scale drift-netting.

The areas of highest albacore catch rates have typically been in waters between 10–35°S in the WCPO. The spatial pattern of CPUE has been relatively consistent over time, although overall CPUE has reduced (Figure 6).

Longline fisheries operate throughout the year, although there is a strong seasonal trend in the catch distribution by latitude, with the fishery operating in southern latitudes (south of 35°S) during late summer and autumn, moving northwards during winter. Surface troll fisheries around New Zealand are highly seasonal, occurring mainly from December-April.

4 Data compilation

Data used in this South Pacific albacore assessment consist of fishery-specific catch, effort and length-frequency data, tag release-recapture data, and age-length observations. Details of these data and their stratification are described below. A summary of the available data is in Table 2.

4.1 Spatial stratification

The 2021 assessment is the first attempt at a spatially structured assessment of albacore across the entire South Pacific. The 2012 assessment (Hoyle et al., 2012) was the last that considered the entire South Pacific. That assessment was a single region model with the fisheries stratified into six areas (i.e. an areas-as-fleets approach). The 2015 assessment (Harley et al., 2015) introduced a fully spatially structured model for the WCPFC-CA region south of the equator with eight regions, however, there were difficulties with the complexity of this structure and the spatial structure was therefore simplified to five regions for the 2018 assessment focussing on the WCPFC-CA (Tremblay-Boyer et al., 2018a).

We continue with the spatially structured approach for the 2021 assessment and further simplify the WCPFC-CA regions by the removal of the boundary between regions 2-4 and 3-5 applied in the 2018 model structure (i.e. longitude 150°W, Figure 1). This boundary was used in previous assessments primarily to separate the 'overlap' region of the WCPFC and IATTC convention areas into separate model regions. A separate model region for the overlap area is problematic given the limited data or other population structure information to support this. We have dealt with the overlap region in this assessment by applying an areas-as-fleets approach to stratify fishing effort in this region (described below). Overall, the information from tagging (Figure 2) and length composition data (Vidal et al., 2021) show smaller fish being more prevalent in catches from cooler waters, and moving to warmer waters as they grow (Nikolic et al., 2017). This life-history movement pattern underpinned the latitudinal boundary between regions 2 and 3 for the WCPFC-CA in the previous two assessments, placed at 25°S (Figure 1). For the 2021 assessment we maintain this boundary. The boundary between regions 1 and 2 in the WCPFC-CA was set at 10°S for the previous two assessments. This corresponds to the southern boundary of the WCPFC-CA tropical longline fishery (20°N – 10°S) and seems logical from a fishery structure, targeting practice, data and management perspective. As this boundary was also supported at previous Pre-assessment Workshops (PAWs) and there have been no changes to the tropical longline fishery region of operation, we retain this model region boundary for the WCPFC-CA in the 2021 assessment. Due to the poor understanding of life-history-related changes in movement behaviour for albacore in the EPO, and limited historical composition data across large areas of that region, we apply a single spatial region to encompass the entire southern EPO (Figure 1). However, acknowledging that there is spatial fishery structure in the EPO we apply an areas-as-fleets approach to stratify the fisheries in that region (Vidal et al., 2021). The fishery strata were identified using the methods described by Lennert-Cody et al. (2010, 2013). Briefly, a regression tree approach was used to explore spatial and seasonal structure in length-frequency distributions. Predictors were quarter; cyclic quarter; 5° latitude and 10° longitude. Year was not used as a predictor. The analysis showed spatial structure in length composition was strong, was more important than seasonal variation, and supported a three area stratification of the EPO fisheries (Figure 3). This structure explained 22.3% of the variability in the length composition and was better suited to the spatial catch and compositional data distribution than more complex structures that only explained a minor amount of additional variation.

Finally, fishing opportunities in the overlap region between the WCPFC and IATTC convention areas could be influenced by Conservation and Management Measures implemented by either RFMO and fleets operating in that region in existing CMMs have the option to nominate that their catches are managed under WCPFC or IATTC measures. There is also a considerable area of high seas in this region. As such it is useful to have the capability to explore, for example in projection studies, the implications of different management measures influencing this region for both the WCPFC and IATTC areas. To accommodate this, as mentioned above, we include separate fishery strata as areas-as-fleets (Waterhouse et al., 2014) in the overlap region. In summary, the spatial stratification for the 2021 South Pacific-wide assessment includes four spatial regions and nine fishery strata (Figure 3).

4.2 Temporal stratification

The time period covered by this assessment is the first quarter of 1960 to the final quarter of 2019. Within this period, data were compiled by quarter (Jan-Mar, Apr-Jun, Jul-Sep, and Oct-Dec). This period and the quarterly time-step is consistent with the 2018 assessment except

with the addition of data for the years 2017–2019. The assessment does not include data from the most recent complete calendar year as these are considered incomplete at the time of formulating the assessment inputs. Recent year data are also often subject to significant revisions post-SC, in particular the longline data on which this assessment depends.

4.3 Fisheries definitions

MULTIFAN-CL requires all catch and effort to be allocated to fisheries. Ideally, the defined fisheries have selectivity and catchability characteristics that do not vary greatly over time. For most tuna assessments, fisheries can be defined according to gear type, fishing method, flag and region or fishery area strata. The move to a South Pacific-wide assessment, and related modifications to the spatial regions, with inclusion of areas-as-fleets strata, necessitated some changes to the fishery definitions applied in the 2018 assessment. Further, consistent with the 2018 assessment we apply the 'extraction' and 'index' fisheries approach (Tremblay-Boyer et al., 2018a). "Extraction" fisheries are used to account for fishery removals and do not influence the abundance index. To achieve this they have all their effort removed and the model estimates catches perfectly. The "index" fisheries are constructed from the combined fleets CPUE data to provide the indices of abundance for each model region. These fisheries then are assigned a trivial amount of catch (i.e. 1 fish per quarter) so that they are in effect non-extractive fisheries (i.e. akin to a survey). The index fisheries are used to inform the model on relative abundance of older albacore over time and among regions (Methot and Wetzel, 2013). Given the dynamic and patchy effort of longline fleets in the South Pacific over time, there are distinct advantages to developing index fisheries from a combined-fleets dataset. This makes maximum use of the fully integrated, multi-fleet standardised CPUE analyses by providing the best possible spatial and temporal coverage for the indices of relative abundance in the assessment, and avoids assigning the multi-fleet standardised CPUE time series to only one fleet component within the assessment. In addition, this approach allows the size data to be used to remove fish at the proper sizes and also to inform the model on fluctuations in abundance and size composition. The multi-fleet regional abundance indices were calculated using the VAST R package for implementing spatial delta-generalized linear mixed models (Thorson et al., 2015) and is discussed further below and in the supporting paper by Vidal et al. (2021).

4.3.1 Extraction fisheries

The fishery definitions for the 2021 assessment are detailed in Table 1. In summary there are 21 extraction fisheries, that include groupings of longline fisheries for the Distant Water Fishing Nations (DWFNs), PICTs, and Australia (AU)/New Zealand (NZ), along with troll and driftnet fisheries. The extraction fisheries are stratified according to the model regions and spatial fishery strata in Figure 3, resulting in 17 fisheries for the WCPFC-CA and four fisheries for the EPO (IATTC) region.

4.3.2 Index fisheries

We defined one index fishery for each of the four model regions, for which catchability was assumed constant across years and fleets. These index fisheries were constructed from the full, multi-fleet longline CPUE analyses. The effort for each time step was adjusted such that the original standardised CPUE from the supporting analysis (Vidal et al., 2021) was preserved. There was considerable overlap in the fleet composition for each of the four index regions, but

there were also some differences. Data for each of the index fisheries spanned the full time series, 1960-2019, but with variable effort by the participating fleets. Specifically:

- **Region 1:** There were 18 active fleets with fishing activity in region 1 including Japan, Korea, Chinese Taipei, Solomon Islands, Vanuatu, French Polynesia, Fiji, Papua New Guinea, United States, China, Tonga, Cook Islands, Niue, Tuvalu, Indonesia, Kiribati, Federated States of Micronesia (FSM), and Samoa. Based upon data available, Japan was the only active fleet from 1960-1962. In 1963 and 1964, Korea and Chinese Taipei began longline fishing in the region, respectively. The data series among the fleets varied from that for the full time series (240 quarters), to a single quarter of fishing effort (Niue), with an average of 71 quarters fished by the individual fleets.
- **Region 2:** There were data from 21 active fleets in Region 2, many of which overlapped with those fishing in Region 1 to the north. Data from the DWFNs (Japan, Korea, Chinese Taipei) were the main information until the 1980s. Solomon Islands, Tonga, New Caledonia, Australia, and Fiji began reporting longline fishing in this region in 1980s and have continued through the present day. During the 1990s, French Polynesia, Papua New Guinea, United States, Samoa, and China began reporting fishing data in the area, and all, excepting the US, continue to this day. In the latter part of the time series, some of the smaller PICTs have increased their participation, although with inconsistent effort. Niue and Indonesia have not fished in the most recent years, and based upon available data, New Zealand fished in the region for the first time in 2019. On average, the participating fleets fished 91 quarters over the time series.
- **Region 3:** This is the most southern region within the WCPFC-CA and has experienced similar fleet dynamics as described for the two other WCPFC-CA index fisheries. There were data from 18 fleets participating across the time series. Australia and New Zealand were more active in this region as compared to those to the north. Korea began fishing in the region in 1963 but did not have any reported effort (in the filtered data set) beyond 1998. There has been recent and ephemeral effort from 2015 on by vessels flagged to Indonesia, Portugal, Papua New Guinea, and Samoa.
- **Region 4**: As described in Vidal et al. (2021), the only fleet retained for the EPO (index fishery 4) was the Japanese fleet, which spanned from 1960-2019, but with very little effort since 2018. Fishing occurred during 236 of the 240 quarters included in the analysis.

4.4 Catch and effort data

Catch and effort data were compiled according to the fisheries defined in Table 1. All catches were expressed in numbers of fish, with the exception of the driftnet fishery, where catches were expressed in weight (metric tonnes). For longline fisheries, effort (hooks set) was standardized as described below, while for troll and driftnet fisheries, the number of vessel days of fishing activity was used.

Annual catches by flag for the South Pacific, and the WCPO and EPO regions are provided in Figure 5 and historically by gear across model regions in Figure 4. Catch for the entire South Pacific has generally been between 80,000–100,000 mt since 2009, after an increasing trend from 1990. The majority of the catch has always been from the WCPO, and mostly from model region 2, although the catch from the EPO has been increasing since 2000, most notably since 2010. Catches in the EPO peaked at around 20,000 mt in 2014, largely due to increased catches by the

Chinese fleet since 2010. The catch is almost all by taken longline, except for the troll catches primarily around New Zealand (Figure 4). Driftnet catches only occurred over a few years in the late 1980s.

In terms of the spatial patterns of catch and effort over time (Figure 6), most of the recent catch and effort has occurred in region 2, the area almost exclusively comprised of EEZs between 10-25° S in the WCPFC-CA. Over the last two decades, catch and effort has increased in the south-central pacific extending into the overlap and EPO region

4.4.1 Longline effort and CPUE

CPUE standardisation for the index fishery data was conducted using a spatiotemporal modelling approach implemented in the VAST R package (Thorson et al., 2015). This approach is consistent with the previous assessment and is described in detail in Vidal et al. (2021). Briefly, the VAST framework was used to implement a spatiotemporal delta generalized linear mixed model (GLMM), from which area-weighted abundance indices were generated after 'standardising out' the influence of the catchability covariates. The modelling approach explicitly addresses the spatial structure in the response variable, that is, the fact that observations closer in space are more likely to be similar. This allows the spatial autocorrelation to be accounted for, which increases the precision in estimates and in some instances makes it easier to identify a relationship between the response and candidate explanatory variables.

The final model used to generate the CPUE indices included targeting cluster and vessel flag as catchability covariates. We explored models with combinations of targeting cluster, flag, and hooks between floats (HBF) fitted as a spline as catchability covariates. The models with HBF did not converge, and therefore were not considered. The model that included both flag and targeting cluster demonstrated a slightly improved fit over the model with targeting cluster as the only catchability covariate.

Targeting clusters were defined from the relative proportion of albacore, bigeye, and yellowfin tuna, and swordfish catch, and hooks between floats (HBF). For this assessment, targeting cluster was derived in a similar manner as in 2018 (Tremblay-Boyer et al., 2018b), except that the k-means clustering algorithm was applied to the full data set simultaneously, as opposed to the index regions separately. This minor change is expected to better capture the relative targeting practices across the entire region. The model was fit to data from 1960-2019, and as a result, there were limited data available to inform gear or vessel-based characteristics and unique vessel identity associated with each set in the earlier years. To account for these data gaps, data imputation was required to model the full data set. For HBF we used a random forest approach (Breiman, 2001) to predict the missing values, based on data for which HBF values were assumed to be reported accurately.

Flag was predicted to be an important covariate as there can be fleet effects and differences in fishing strategies employed. There was concern around potential confounding of the abundance signal with the flag effect because there are strata where Japan is the only fleet fishing (e.g. early part of the time series and in the EPO). However, the main impact of the flag effect was an increase in the predicted indices in the WCPFC-CA regions during the early part of the time series, the time period for which Japan was the only active fleet. For most of the remaining time series, the model with and without flag predicted nearly indistinguishable index trends.

In all regions, the standardized trends in relative abundance showed a decline from the early part

of the time series to relatively stable trends since approximately the 1980s. Recent estimates of relative abundance remain below the long-term mean, with some indication of increased seasonality in the abundance signal (Figure 7).

Since a single spatiotemporal model was used to generate the standardized CPUE, the CVs for the standardized effort assigned to the index fisheries were rescaled to an average level of 0.2 across all regions and time periods, consistent with the approach used in the most recent assessments for bigeye and yellowfin tuna (Ducharme-Barth et al., 2020; Vincent et al., 2020). This was done to more appropriately capture the relative differences in uncertainty, due in part to varying levels of sampling intensity, across spatial and temporal strata. In this way, MULTIFAN-CL is able to account for the time-varying nature of the CVs such that the fit to the CPUE data is given greater influence in the likelihood in time-steps with more precise estimates of abundance.

Regional scaling weights were based upon the analysis of fleet-combined operational longline catch and effort data and derived from the area-weighted standardized abundance indices (Vidal et al., 2021). The aim of the analysis was to standardize the data in such a way that spatial differences in CPUE across the entire model domain reflects differences in relative abundance. Regional weights were calculated as the time-varying proportion of biomass estimated for each index region in each time period, based upon the analysis of fleet-combined operational longline catch and effort data and derived from the area-weighted standardized abundance indices (Vidal et al., 2021).

4.5 Size data

Available length-frequency data for each of the defined fisheries were compiled into 100, 1-cm size classes (30–129 cm). Data were collected from a number of sources and can be summarized as follows.

4.5.1 Longline

Albacore catch size composition data have been routinely collected from the longline fishery though observer and port sampling programmes since the early 1960's. These data are characterized in Vidal et al. (2021).

4.5.2 Troll and other surface fisheries

New Zealand domestic troll size composition data (fishery in region WCPO3) were collected from port sampling programmes conducted by the New Zealand Ministry of Fisheries and, more recently, the New Zealand National Institute of Water and Atmospheric Research (NIWA).

Length-frequency data from troll fishing operations in the STCZ were collected and compiled through the Albacore Research Tagging Project (1991-1992) and by port sampling programmes in Levuka, Fiji; Pago Pago, American Samoa; and Papeete, French Polynesia; and, during the 1990–1991 and 1991–1992 seasons, by scientific observers.

Driftnet data were provided by the NRIFSF for Japanese driftnet vessels. Data from Japanese vessels were also collected by observers and by port sampling in Noumea, New Caledonia. It is assumed that these data are representative of all driftnet activity.

4.6 Re-weighting of size composition data

Statistical correction of size composition data is required as length and weight samples are often collected unevenly in space and time. The methods for re-weighting of the size composition data are detailed in Vidal et al. (2021) and are based on those developed by McKechnie (2014) for longline extraction fisheries, and Tremblay-Boyer et al. (2018a) for longline index fisheries.

For the extraction fisheries, re-weighting of composition data is required to ensure that sampling biases in space, time, and the fleets providing data, are minimised so that size composition data better reflect the composition of the overall removals. Strata-specific size data samples are therefore re-weighted by catch for the extraction fisheries. For the index fisheries, re-weighting of composition data is required to ensure that the size composition of the abundance indices reflect the size component of the population that is being sampled by the index fisheries through time. Strata specific samples are therefore re-weighted by relative abundance using the CPUE.

Given that the same composition data were used for both the extraction and index fisheries, the observed number of size-frequency samples input into the assessment was divided by two for both the extraction and index fisheries.

4.7 Tagging data

Tagging data are extremely limited for South Pacific albacore, but were nevertheless included as a data source in previous assessments. Initial model runs, and a sensitivity analysis excluding the tagging data from the 2018 assessment (Tremblay-Boyer et al., 2018a) in the stepwise model development, indicated minimal impact of including or excluding tagging data on the key stock assessment quantities of interest. We therefore opted in this assessment to exclude the tagging data, which resulted in some degree of model simplification and substantially faster run times. However, we verified that this exclusion did not unduly impact model estimates, including management quantities of interest, in a sensitivity analysis in which the tagging data, compiled as in previous assessments, were included (see Section 16). No further discussion of tagging data is included in the body of this report.

4.8 Age-at-length data

Age-length data from otolith readings were available from a recent ageing study of South Pacific albacore by Farley et al. (2021). The work used the previously collected and prepared otoliths (collected in 2009-2010) (Farley et al., 2013a) with the addition of new data on daily ages from 60 small fish (43-47 cm FL) sampled from NZ waters and the re-reading and measuring of increment zones on 600 previously collected 'high confidence' otoliths from the WCPO. Three recently recaptured OTC stained otoliths were also aged, and supported the previous observations that increment formation was annual. The reanalysis applied a new age algorithm (developed for WCPO bigeye and yellowfin) (Farley et al., 2020) to obtain updated decimal age estimates for albacore that were applied in the assessment. Details of the new ageing analysis can be found in the supporting paper (Farley et al., 2021).

5 Model description

5.1 General characteristics

The model can be considered to consist of several components, (i) the dynamics of the fish population; (ii) the fishery dynamics; (iii) the dynamics of tagged fish; (iv) the observation models for the data; (v) the parameter estimation procedure; and (vi) stock assessment interpretations. Detailed technical descriptions of components (i)–(iv) are given in Hampton and Fournier (2001) and Kleiber et al. (2019). In addition, we describe the procedures followed for estimating the parameters of the model and the way in which stock assessment conclusions are drawn using a series of reference points. In this section, model settings primarily refer to those used within the 'diagnostic case' model.

5.2 Population dynamics

The model partitions the population into four spatial regions (under the 2021 regional structure) and 48 quarterly age-classes. The last age-class comprises a 'plus group' in which mortality and other characteristics are assumed to be constant. The population is 'monitored' in the model at quarterly time steps, extending through a time window of 1960–2019. The main population dynamics processes are as follows.

5.2.1 Recruitment

Recruitment is defined as the appearance of age-class 1 (quarter) fish (i.e. fish averaging $\sim$ 35-45 cm (Farley et al., 2021)) in the population. In contrast to the tropical tunas, spawning of South Pacific albacore occurs during the Austral summer. Recruitment was allowed to occur in each quarter although it would be expected that the data would support recruitment occurring across a more restricted period due to the seasonal spawning pattern. It was assumed that recruitment occurs instantaneously at the beginning of each quarter. This is a discrete approximation to continuous recruitment, but provides sufficient flexibility to allow a range of variability to be incorporated into the estimates as appropriate.

Spatially-aggregated (over all model regions) recruitment was assumed to have a weak relationship with spawning potential *via* a Beverton and Holt stock-recruitment relationship (SRR) with a fixed value of steepness (h). Steepness is defined as the ratio of the equilibrium recruitment produced by 20% of the equilibrium unexploited spawning potential to that produced by the equilibrium unexploited spawning potential (Francis, 1992; Harley, 2011). Typically, fisheries data are not very informative about the steepness parameter of the SRR parameters (ISSF, 2011); hence, the steepness parameter was fixed at a moderate value (0.80) and the sensitivity of the model results to the value of steepness was explored by setting it to lower (0.65) and higher (0.95) values. The values of 0.65, 0.80 and 0.95 were included in the uncertainty grid.

In the diagnostic case model, it was assumed that annual recruitment was related to annual mean spawning potential, as recommended by the 2011 Bigeye Tuna Peer Review (Ianelli et al., 2012) and implemented for previous South Pacific albacore assessments (Harley et al., 2015; Tremblay-Boyer et al., 2018a) and recent WCPFC tropical tuna assessments.

The SRR was incorporated mainly so that yield analyses, equilibrium- and depletion-based reference points and population projections could be undertaken for stock assessment purposes. We therefore applied a weak penalty (equivalent to a CV of 0.7) for deviation from the SRR so

that it would have negligible effect on recruitment and other model estimates (Hampton and Fournier, 2001), but still allow the estimation of asymptotic recruitment. This approach was recommended by the review of the 2011 bigeye stock assessment (Ianelli et al., 2012). A higher CV (2.2) was assumed in the previous South Pacific albacore assessment, but we found that this setting occasionally resulted in model instability, which the CV of 0.7 was able to avoid. Recruitment deviations were estimated on the log scale for the full model period, excluding the nine terminal quarterly recruitments (which are not freely estimated and assumed to be zero), acknowledging that these estimates are poorly supported by data and, if unconstrained, can vary widely, with potentially large consequences for stock projections.

Two options for recruitment distributions were explored in this assessment. The first option involved specifying that all recruitment occurs in regions 3 and 4, and allowed the proportions for these regions to be estimated as part of the overall MULTIFAN-CL parameter estimation. The alternative was to use a fixed distribution of recruitment based on the average distribution obtained from the SEAPODYM model (Senina et al., 2020). These two option are discussed in Section 6.2.6. For both recruitment distribution hypotheses, the distribution was assumed to be time invariant.

5.2.2 Initial population

The population age structure in the initial time period in each region was assumed to be in equilibrium and determined as a function of the average total mortality during the first 20 quarters. This assumption avoids having estimate the initial age structure, which is generally poorly determined, as independent parameters in the model. As noted above, the population is partitioned into quarterly age-classes with an aggregate class for the maximum age (plus-group). The aggregate age class makes the accumulation of old and large fish possible, which is likely in the early years of the fishery when exploitation rates were low.

5.2.3 Growth

The standard assumptions for WCPFC assessments fitted in MULTIFAN-CL were made concerning age and growth: i) the lengths-at-age are normally distributed for each age-class; ii) the standard deviations of length for each age-class are a log-linear function of the mean lengths-at-age; and 3) the probability distributions of weights-at-age are a deterministic function of the lengths-at-age and a specified weight-length relationship. These processes are assumed to be regionally and temporally invariant.

This assessment incorporated two approaches for specifying growth: (i) an externally estimated von Bertalanffy (VB) growth curve based on age estimates from otoliths; and (ii) an externally estimated VB growth curve based on fitting to the size composition data used in the assessment. These alternative growth formulations are discussed in detail in Section 6.2.3.

5.2.4 Movement

Movement was assumed to occur instantaneously at the beginning of each quarter *via* movement coefficients that connect regions sharing a common boundary. Note that fish can move between non-contiguous regions in a single time step due to the 'implicit transition' computational algorithm employed (see Hampton and Fournier, 2001 and Kleiber et al., 2019 for details). Movement is parameterised as the proportion of fish in a given region that move to the adjacent region.

There is limited empirical information on broad scale movement rates of albacore across the South Pacific. Tag-recapture data discussed previously provide some information on north to south movements in the WCPO, but is limited in space and time, with low recapture numbers and localised release locations. Tag recovery effort was also focussed on fisheries in the WCPO. While we include the tagging data as a sensitivity on the 2021 diagnostic case model, consistent with the previous assessment, it had negligible influence on management quantities was not retained in the 2021 diagnostic case model or the uncertainty grid. In the absence of suitably informative tag-recapture data we applied two approaches to movement in the current assessment, that are described in detail in Section 6.2.5. Briefly for the first approach, **M1**, quarterly movement coefficients were estimated internally by MULTIFAN-CL - this was applied for the diagnostic case. The alternative approaches involved the use of SEAPODYM (Spatial Ecosystem and Population Dynamics Model) to provide information on spatial movement rates across life stages for South Pacific albacore (Senina et al., 2020).

5.2.5 Natural mortality

As with previous assessments, the level of natural mortality was considered a key area of uncertainty. For this assessment, we have adopted an approach for specifying natural mortality-at-age (M-at-age) that uses a combination of life history information and M-at-age theory (Lorenzen, 1996). The approach applied has been developed by Mark Maunder and colleagues and is described in Section 13. The method integrates the following information to provide estimates of M-at-age:

- VB growth parameters
- L_{mat}, the length at which albacore first begin to spawn, which we took as the 5% maturity level from the maturity-at-length curve, 80.81 cm
- W_{mat}, the equivalent weight at first maturity, 10.243 kg
- L_{50}, the length at 50% maturity, 85.71 cm
- Beta, a parameter of the maturity-at-length curve, -0.575
- M_{juv}, the M at first maturity, which is assumed as $3 * (Wmat^{-0.288})$
- Lambda, the shape parameter of the Lorenzen curve, which is fixed at 1.0
- M_{mat}, the M-at-length of mature albacore, which is assumed to be =1/(1+EXP(Beta*(Len-L_{50}))

As discussed above we apply two approaches for growth estimation in this assessment. In turn we apply the growth parameters from the two approaches to generate two M-at-age options (Figure 10) as described in Section 6.2.4.

5.2.6 Sexual maturity, or reproductive potential-at-age

The reproductive potential ogive is an important component of the assessment structure as it translates model estimates of total population biomass to the relevant management quantity, spawning potential biomass (SB). Reproductive output at age, which is used to derive spawning potential, attempts to provide a measure of the relative contribution of fish at different ages to the next generation. The maturity function is routinely input to stock assessment models as a fixed vector of age-specific values as there is very little information to inform the model of its

shape. MULTIFAN-CL allows input of length-based spawning potential, which is then converted internally within the model to an age-based vector dependent upon the growth model Figure 11. We specified spawning potential-at-length as the product of sex ratio and maturity-at-length, rescaled to a maximum of one. Sex ratio at length was obtained by fitting a spline to observed sex-ratio from SPC-held longline observer data, stratified by flag and 10° cell and weighted by longline catch to account for uneven observer coverage amongst fleets in space. Longline observer data only covered lengths from 70 to 110 cm so we extrapolated to cover the stock assessment range by: (1) setting sex ratio for lengths < 70 cm at the 70 cm value and (2) assuming sex ratio for females declined linearly from the value observed at 110 cm to 0 at 130 cm. The maturity proportion at length was obtained from the weighted maturity ogives presented in Farley et al. (2014), smoothed via a logistic curve.

5.3 Fishery dynamics

The interaction of the fisheries with the population occurs through fishing mortality. Fishing mortality is assumed to be a composite of several separable processes - selectivity, which describes the age-specific pattern of fishing mortality; catchability, which scales fishing effort to fishing mortality; and effort deviations, which are a random effect in the fishing effort - fishing mortality relationship.

5.3.1 Selectivity

Selectivity is fishery-specific and assumed to be time-invariant and length-based, but is modelled as age-based (Kleiber et al., 2019). Here we have used the same methods as the 2018 assessment which was based on cubic spline interpolation techniques. This is a form of smoothing, but the number of parameters for each fishery is the number of cubic spline 'nodes' that are deemed to be sufficient to characterise the selectivity over the age range. We used three nodes, which was sufficient to allow for reasonably complex selectivity patterns. All selectivities were constrained such that the selectivity of the last two age classes was equivalent.

In the current assessment, spatial structure and movement are explicitly modelled, which allows non-seasonal selectivity for longline fisheries to be employed. Explicitly specifying spatial structure also allowed simplifying assumptions to be made regarding the form of the selectivity curve for the longline fisheries in each region. For each fishery, we assumed that the oldest albacore were fully recruited. To encourage this behaviour, selectivity coefficients were penalized to be non-decreasing for successively older age-classes. For the index fisheries, we adopted the simplifying assumption that selectivity was shared. This assumes, therefore, that differences in size composition of index fisheries arise because of differences in the underlying size structure of the population in each region.

5.3.2 Catchability

Constant (time-invariant) catchability was assumed for the index fisheries. This assumption is similar to assuming that the CPUE for these fisheries indexes the exploitable abundance over time. Catchability of the index fisheries was shared, which provides the model with information on the relative population sizes among regions.

The assessment assumes a very high penalty on the fit to the catch which is essentially equivalent to treating the catch as "error-free" as done in "catch-conditioned" modelling approaches. Additionally, the effort deviates for the extraction fisheries did not attract likelihood

contributions, but were estimated such that the catch was predicted with high accuracy. As a result, there was no need to estimate both effort and catchability deviates for the extraction fisheries.

5.3.3 Effort deviations

Effort deviations were used to model the random variation in the effort - fishing mortality relationship, and are constrained by pre-specified 'prior' distributions (on the log-scale). The region specific CPUE indices implemented through the index fisheries represent the principal indices of stock abundance, and the extent to which the model can deviate from the indices is moderated by the penalty weights assigned to the standardized effort series. For these fisheries, the 'prior' was set to have a mean of zero and the CV was allowed to be time-variant and based on the variance estimates from the spatio-temporal standardization model. As explained previously, the regional differences in the estimated CVs from the spatio-temporal standardization model were preserved since they were generated from a unified analysis across regions. The CV across all index fisheries and time periods was rescaled to a value of 0.2. The resulting scaled CVs were transformed to an effort deviate penalty for each CPUE observation in MULTIFAN-CL. Penalties are inversely related to variance, such that lower effort penalties are associated with indices having high variance, consequently these indices are less influential in fitting the model.

5.4 Likelihood components

There are two main data components that contribute to the log-likelihood function for this assessment: the total catch data, and the length-frequency data. Fit to the CPUE data does not influence the fit as an explicit likelihood component but rather as a penalty on the effort deviates. There are various "other" grouped likelihood components that can have some influence. These appear dominated by the penalties on the movement coefficients (see Section 7.2.4).

The observed total catch data are assumed to be unbiased and relatively precise, with the SD of residuals on the log scale being 0.002. As noted, this is close to the 'catch conditioned' approach often used in other integrated assessments.

The probability distributions for the length-frequency proportions are assumed to be approximated by robust normal distributions, with the variance determined by the effective sample size (ESS) and the observed length-frequency proportion. Size frequency samples are assigned an ESS lower than the number of fish measured. Lower ESS values recognise that (i) length-frequency samples are not truly random (because of non-independence in the population with respect to size), and would have higher variance as a result; and (ii) the model does not include all possible process error, resulting in further under-estimation of variances. The observed sample sizes are capped at 1,000 (internal to MULTIFAN-CL), and in the diagnostic case model, these were further divided by 25 (i.e. size composition scalar of 25), resulting in a maximum ESS of 40 for each length sample for a fishery. Further scalars were applied in the uncertainty grid to upweight (divisor of 10) and downweight (divisor of 50) the size frequency data.

5.5 Parameter estimation and uncertainty

The parameters of the model were estimated by maximizing the log-likelihood of all data components plus the log of the probability density functions of the penalties specified in the model. The maximization to a point of model convergence was performed by an efficient optimization using exact derivatives with respect to the model parameters (auto-differentiation,

Fournier et al., 2012). Estimation was conducted in a series of phases, the first of which used relatively arbitrary starting values for most parameters. A bash shell script, "doitall", implements the phased procedure for fitting the model.

5.6 Diagnostics and uncertainty

Typically two types of uncertainty should be incorporated into the estimates of stock status used for management advice. One involves the statistical uncertainty of the estimates produced by individual models, often referred to as 'estimation' uncertainty. The second involves structural uncertainty, which is the uncertainty in the structural assumptions underpinning individual models, e.g. fixed M, steepness etc.. Tuna assessment delivered by SPC have typically attempted to calculate statistical uncertainty for the diagnostic case model, and present structural uncertainty, via a model grid, for the main results of importance for management. Ideally, both structural and statistical uncertainty would be incorporated into management advice, as has been done in the 2021 southwest Pacfic swordfish assessment (Ducharme-Barth et al., 2021; Ducharme-Barth and Vincent, 2021). However, due to the often large number of models in structural uncertainty grids, each with 1000s of parameters, calculation of statistical uncertainty across a grid can be impractical. Further, quantifying statistical uncertainty for individual models is facilitated by the calculation of a positive definite Hessian, which is often difficult to achieve for complex models with 1000s of parameters, many of which can be considered nuisance parameters. Indeed, we did not obtain a positive definite Hessian for the current version of the diagnostic case model, and the implications of this are discussed further in Section 7.2.5, as such we only include structural uncertainty for the key management quantities.

For highly complex population models fitted to large amounts of often conflicting data, it is common for there to be difficulties in estimating absolute abundance. Therefore, a likelihood profile analysis (see also above) was conducted for the marginal posterior likelihood in respect of the total average population biomass as a measure of population scaling, following the procedure outlined by McKechnie et al. (2017) and Tremblay-Boyer et al. (2017) for the 2017 bigeye and yellowfin tuna assessments.

Retrospective analyses are also undertaken as a general test of the stability of the model. A robust model, when rerun with data for the terminal year/s sequentially excluded (Cadigan and Farrell, 2005), should produce outputs that are variable across runs, but without a systematic pattern in either the scaling or time-series trends. The retrospective analyses for the 2021 diagnostic case model are presented in Section 17.

5.7 Stock assessment interpretation methods

Several ancillary analyses using the fitted model/suite of models were conducted in order to interpret the results for stock assessment purposes. The methods involved are summarized below and further details can be found in Kleiber et al. (2019).

5.7.1 Yield analysis

The yield analysis consists of computing equilibrium catch (or yield) and spawning potential, conditional on a specified basal level of age-specific fishing mortality (F_a) for the entire model domain, a series of fishing mortality multipliers (*fmult*), the natural mortality-at-age (M_a), the mean weight-at-age (w_a) and the SRR parameters. All of these parameters, apart from *fmult*, which is arbitrarily specified over a range of 0–50 (in increments of 0.1), are available from the

parameter estimates of the model. The maximum yield with respect to *fmult* can easily be determined using the formulae given in Kleiber et al. (2019), and is equivalent to the MSY. Similarly the spawning potential at MSY (SB_{MSY}) can also be determined. The ratios of the current (or recent average) levels of fishing mortality and spawning potential to their respective levels at MSY are determined for all models of interest, including those in the structural uncertainty grid, and so alternative values of steepness were assumed for the SRR in many of them. Note that in this case MSY quantities can only be estimated at the scale of the entire model domain, and not for individual regions, or separately for the WCPFC-CA and EPO.

Fishing mortality-at-age (F_a) for the yield analysis was determined as the mean over a recent period of time (2015–2018). We do not include 2019 in the average as fishing mortality tends to have high uncertainty for the terminal data year of the analysis and the terminal recruitments in this year are constrained to be the average over the full time-series, which affects F for the youngest age-classes.

MSY was also computed using the average annual F_a from each year included in the model (1960–2018). This enabled temporal trends in MSY to be assessed and a consideration of the differences in MSY levels under historical patterns of age-specific exploitation.

5.7.2 Depletion and fishery impact

Many assessments estimate the ratio of recent to initial biomass (usually spawning potential) as an index of fishery depletion. The problem with this approach is that recruitment may vary considerably over the time series, and if either the initial or recent biomass estimates (or both) are "non-representative" because of recruitment variability or general high uncertainty with early time series data, then the ratio may not measure fishery depletion reliably.

We assess fishery depletion by computing the unexploited spawning potential time series (at the region level) using the estimated model parameters, but assuming that fishing mortality was zero. Because both the estimated spawning potential SB_t (with fishing), and the unexploited spawning potential $SB_{F=0[t]}$, incorporate recruitment variability, their ratio at each quarterly time step (t) of the analysis, $SB_t/SB_{F=0[t]}$, can be interpreted as an index of fishery depletion. The computation of unexploited spawning potential includes an adjustment in recruitment to acknowledge the possibility of a reduction in recruitment for exploited populations through stock-recruitment effects. To achieve this the estimated recruitment deviations are multiplied by a scalar based on the difference in the SRR between the estimated fished and unfished spawning potential estimates.

A similar approach was used to estimate depletion associated with specific fisheries or groups of fisheries. Here, fishery groups of interest, Tropical longline (region 1), Sub-tropical longline (region 2), southern longline (region 3), EPO fisheries (region 4), troll and driftnet fisheries, are removed in-turn in separate simulations. The changes in depletion observed in these runs are then indicative of the depletion caused by each of the removed fisheries.

5.7.3 Reference points

The unfished spawning potential ($SB_{F=0}$) in each time period was calculated given the estimated recruitments and the Beverton-Holt SRR. This offers a basis for comparing the exploited population relative to the population subject to natural mortality only. The WCPFC adopted $20\%SB_{F=0}$ as a limit reference point (LRP) for the albacore stock, where $SB_{F=0}$ is calculated as

the average over the period 2006–2015. Stock status was referenced against these points by calculating $SB_{recent}/SB_{F=0}$ and $SB_{latest}/SB_{F=0}$, where SB_{latest} and SB_{recent} are the estimated spawning potential in 2019, and the mean over 2016–2019, respectively (Table 4).

The other key reference point, $F_{recent}/F_{\mathrm{MSY}}$ (Table 4), is the estimated average fishing mortality over the full assessment area over a recent period of time (F_{recent}; 2015–2018 for this stock assessment) divided by the fishing mortality producing MSY (as produced by the yield analysis and detailed in Section 5.7.1).

5.7.4 Majuro and Kobe plots

For the standard yield analysis (Section 5.7.1), the fishing mortality-at-age, F_a, is determined as the average over some recent period of time (2015–2018 herein). In addition to this approach the MSY-based reference points (F_t/F_{MSY}, and SB_t/SB_{MSY}) and the depletion-based reference point ($SB_t/SB_{F=0[t]}$) were also computed for each year included in the model (1960–2019, with no value calculated for the terminal year) by repeating the yield analysis for each year in turn. This enabled temporal trends in the reference point variables to be estimated taking account of the differences in MSY levels under varying historical patterns of age-specific exploitation. This analysis is presented in the form of dynamic Kobe plots and "Majuro plots", which have been presented for all recent WCPFC stock assessments.

6 Model runs

6.1 Developments from the last assessment

The progression of model development from the 2018 reference case to the model proposed as the diagnostic case in 2021 was incremental, with stepwise changes to the model made in-turn to ensure that the consequences of each modification could be assessed. Changes made to the previous assessment model include additional input data for the years 2016–2019, modified methods in producing the input files, new regional structures, updated biological information and data, updated default settings for the diagnostic case, and implementation of the new version of MULTIFAN-CL. The progression through the models is as follows:

- **Step 1** The 2018 reference case model
- **Step 2** Update 2018 diagnostic case model with the new MULTIFAN-CL executable (v2.0.8.0) (MFCL208).
- **Step 3** Apply new growth parameters (as fixed values) from the age-length re-analyses by Farley et al. (2021) (newGrowth18)
- **Step 4** Apply revised CPUE indices determined using the approach described in Vidal et al. (2021) (newCPUE).
- **Step 5** Exclude the tagging data (Notag).
- **Step 6** Include the troll fishery data by month, and apply the new region and fleet structure for the WCPFC-CA (regions 1, 2 and 3), for data up until 2016 (WCPFC16)
- **Step 7** Update all data until 2019 for the WCPFC-CA regions (WCPFC21).
- **Step 8** Add the new region (EPO - region 4) and fisheries (18, 19, 20, 21, 25) and include data up until 2019 (SPO21)

6.2 Sensitivity analyses

In developing the 2021 South Pacific albacore assessment sensitivities to key structural and data uncertainties were explored. These analyses informed the choice of axes to include in the structural uncertainty grid used for provision of management quantities. This section focuses on the set of uncertainty axes which are described in further detail below. These axes were used for 'one-off' changes from the diagnostic case model and, depending on the results of these alternative models, several of the settings were used in the structural sensitivity analyses. The latter process involves constructing a grid of model runs where all-possible combinations of the assumptions are explored (see Section 6.3).

The recommendations of the 2021 PAW informed consideration of one-off sensitivity analyses undertaken from the diagnostic case. Each of the one-off sensitivity runs was carried out by making a single change to the diagnostic case. Importantly, these model runs are not carried out to provide absolute estimates of management quantities but to demonstrate the *relative* changes that result from the different assumptions or hypotheses.

6.2.1 Steepness [*h0.65, h0.95*]

Steepness is a particularly difficult parameter to estimate in stock assessment models, but if it is fixed in the model, the choice of value may have significant influence on some reference points used in management. As with other recent WCPFC tuna assessments, we assumed a value of h0.8 for the diagnostic case, but examined values of 0.65 (*h0.65*) and 0.95 (*h0.95*) in sensitivity runs. This choice of values is consistent with the results of the meta-analysis conducted on tuna stock-recruitment data and has been well established in previous Scientific Committees.

6.2.2 Relative weighting of size-frequency data [*Size10, Size50*]

To assess the sensitivity of model results to the weighting of the length-frequency data, two alternative models were considered as sensitivities alongside the diagnostic case model. Divisors of 10 and 50 were used to upweight and downweight the data relative to the diagnostic case. These settings corresponded to a maximum effective sample size of 100 and 20 fish, respectively, while the diagnostic case downweights the data with a divisor of 25, corresponding to a maximum effective sample size of 40 fish.

6.2.3 Alternative growth functions [*Fixed otolith, Est. from length frequency*]

Fixed otolith growth: Initially, various growth curves (logistic, VB and Richards) were fitted to the revised decimal years age-length data (combining spatial strata and sexes in external analyses), with the logistic model providing the best fit to the data. Logistic growth is not currently available in MULTIFAN-CL, therefore a choice between the VB and Richards growth was required. The Richards and VB models provided very similar fits to the data out to at least age 10 years, but the additional (inflection) parameter of the Richards model converged to its upper bound. We therefore opted to use the VB model for the assessment, the estimated parameters of which were:

- L_{inf}=110.2 cm
- $k = 0.268 yr^{-1}$
- $t_0 = -1.24$ yr

These parameters were converted to the parameterisation used for the 48 quarterly age-class model used in the assessment: $L_1 = 41.07$ cm, $L_{max} = 107.23$ cm and $k = 0.067 qtr^{-1}$. According to this growth model, the age of the first age class (of mean length L_1) was 0.5 yr.

This VB model was used as a fixed growth specification in the assessment. We did not incorporate the otolith-based data as a conditional age-at-length data set and estimate growth internally in the assessment model as was done in the 2018 assessment. There were two reasons for this. First, for the otolith-based growth hypothesis we chose to apply a growth model based only on otolith ageing, rather than one jointly estimated from both otolith conditional age-at-length and length-frequency data. Secondly, our approach for specifying natural mortality-at-age in the assessment (see below) is dependent, among other things, on the VB growth parameters, making a fixed growth specification more practical. An alternative would have required a complicated iterative approach or, ideally, incorporating the growth/M-at-age relationship into the assessment software. This approach was not possible given time constraints.

Length frequency: As an alternative to the otolith-based growth hypothesis, we developed a growth curve estimated by fitting to the length-frequency data alone. The reason for this was to include a growth model that was able to reproduce the clear modal structure in the NZ troll fishery size data. While the otolith-based growth curve improved the fit to these data considerably compared to the 2018 assessment, the VB formulation of the otolith-based growth curve generally implied around nine months between length modes rather than the expected one year. The length-frequency growth analysis was undertaken using the MULTIFAN-CL software in much the same way as it is used in an assessment, with the following exceptions:

- The length-frequency data were up-weighted by setting the effective sample size equal to the observed sample size for the NZ troll fishery and to one-fifth of the observed sample size for all other fisheries.
- The other main data components – effort deviations and catch – were down-weighted as much as possible.
- Deviations from VB growth for age classes 2-12 were estimated as separate parameters with a moderate penalty to enhance the fit to the size data.
- Selectivity deviations for the first 12 age quarterly classes were also estimated with a moderate penalty to further enhance the fit to the size data.

For this analysis, L_1 and k were estimated, with L_{max} being held fixed at the estimate derived from the otolith-based growth curve (107.23 cm). The rationale for this was to retain a link to the otolith-based growth curve for the age of the largest fish, but to allow different estimates of early growth to better fit the troll fishery length-frequency data. The estimates obtained for L_1 and k were 46.07 cm and 0.053 qtr^{-1}, respectively.

A comparison of the two growth curves is shown in Figure 8, which shows the slightly slower early growth for the length-frequency-based growth curve. Fits of both growth models to several samples of the NZ troll fishery data (chosen to demonstrate the consistency with the clear modal structure) are shown in Figure 9. Note that the length-frequency-based model fits the troll size data better, and is consistent with the annual structure of the length modes (4 quarterly age classes per mode), whereas the otolith-based growth curve fits less well and is closer to 3 quarterly age classes per mode.

6.2.4 Natural mortality [*Nat-M1, Nat-M2]*

As discussed previously we applied two M-at-age options both estimated using the approach of Maunder et al. (Section 13) with different paramterisations based on the alternative growth models. The M-at-age functions are compared in Figure 10.

6.2.5 Movement [*M1, M2]*

Two movement options were explored:

- **Model estimated - M1**: quarterly movement coefficients were estimated internally by MULTIFAN-CL, initially without age-class dependency. This involved estimating two movement coefficients for each of the five region boundaries (1-2, 1-4, 2-3, 2-4, 3-4) for each quarter, thus requiring the estimation of 40 (2x5x4) movement parameters. Movement was assumed to be invariant across years. Trial fits indicated that substantial improvement in fit to size and CPUE data could be obtained by allowing movement to be age-dependent via a simple log-linear relationship. This involved the estimation of an additional parameter for each movement coefficient, increasing the final number of movement parameters to be estimated to 80. A prior of 0.1 was assumed for all movement coefficients, allowing some unpenalized movement among regions. A low penalty was applied to deviations from this prior.
- **SEAPODYM - M2**: SEAPODYM was used in this assessment as an option for providing information on spatial movement rates across life stages for South Pacific albacore (Senina et al., 2020). SEAPODYM is highly spatially resolved and provides predictions on spatio-temporal exchange of biomass by age class (in numbers and months), forced by environmental/habitat variables. For the **M2** movement hypothesis, we computed movement probability matrices based on estimates from the SEAPODYM model. The probability matrices were computed by year quarter and quarterly age class, and averaged over years to match the MULTIFAN-CL movement structure. The matrices were specified in MULTIFAN-CL as fixed parameters.

A graphical representation of **M1** for the diagnostic case model and **M2** is provided in Figure 29. The estimated movements in **M1** simply represent the estimates that minimize the log-likelihood of the data and various penalties in the model; there is no guarantee of biological realism. For the **M2** estimates based on the SEAPODYM model output, some degree of biological realism is expected, since the SEAPODYM model is driven by the interaction of albacore biology and various environmental parameters (Senina et al., 2020).

6.2.6 Recruitment distribution [*R1, R2]*

The average (over time) distribution of recruitment among the model regions needs to be specified as a set of fixed proportions, or estimated as part of the model parameter estimation. Initial trials in which we attempted to estimate the average recruitment proportion for each region did not produce sensible estimates. We therefore implemented two recruitment distribution hypotheses for this assessment.

In hypothesis **R1**, we applied a fixed distribution of recruitment based on the average distribution obtained from the SEAPODYM model (Senina et al., 2020). This indicated a large proportion (0.6) of recruitment occurring in the southern-most region 3, which was consistent with expectation as this is the main region where age-class 1 albacore are observed in catches.

As an alternative hypothesis **R2**, we specified that all recruitment occurs in regions 3 and 4, and allowed the proportions for these regions to be estimated as part of the overall MULTIFAN-CL parameter estimation.

The regional recruitment proportions for both hypotheses are shown in Figure 37, and Figure 38 with the **R1** estimates being for the diagnostic case model. For both recruitment distribution hypotheses, the distribution was assumed to be time invariant.

6.3 Structural uncertainty

Stock assessments of tuna for the WCPFC have recently included an approach to assess the structural uncertainty in the assessment model by running a 'grid' of models to explore the interactions among selected 'axes of uncertainty'. The grid contains all combinations of two or more parameter settings or assumptions for each uncertainty axis.

The structural uncertainty grid for the 2021 assessment was constructed from 5 axes, listed below. Because M-at-age options (M1 and M2) were derived from alternative growth models (G1 and G2), M and growth could not be separate axes in the grid and were combined into one axis with the two combinations of growth and M-at-age.

Axes in the 2021 South Pacific albacore assessment are shown below, with bold font used to indicate settings applied in the diagnostic case:

- **Steepness**: 0.65, **0.80**, 0,95
- **Movement**: **M1 (model estimated, age dependent)**, M2 (SEAPODYM)
- **Size data weighting**: 50 (low), **25** (medium), 10 (high)
- **Recruitment distribution**: **R1 (SEAPODYM)**, R2 (Regions 3 and 4)
- **Growth/M combinations**: **(Fixed otolith growth and associated M-at-age)**, (Length frequency and associated M-at-age)

The final grid thus consisted of 72 models (Table 3).

7 Results

7.1 Consequences of key model developments

The progression of model development from the 2018 reference case model to the 2021 diagnostic case model is outlined in Section 6.1 and results are displayed in Figure 12 showing changes in the estimated spawning potential and the spawning potential relative to the unfished level (i.e. spawning potential depletion, $SB/SB_{F=0}$). A summary of the consequences of this progression through the models is as follows:

- Step 1 (ALB18): We re-ran the 2018 reference case model with the original data, MULTIFAN-CL version used and settings from that assessment, achieving the same results (Tremblay-Boyer et al., 2018a).
- Step 2 (MFCL208): The 2018 reference case model (black line) refitted with the latest version of MULTIFAN-CL (2.0.8.0) (red line), produced almost identical results to the 2018 reference case for both spawning potential and spawning depletion.

- Step 3 (newGrowth18): The 2018 model refitted in MULTIFAN-CL 2.0.8.0 and with the updated otolith growth data as fixed parameters (purple line) resulted in decreased initial and final estimates of spawning potential and depletion, although temporal variation and trends were consistent with the previous model.
- Step 4 (new CPUE): Updating the 2018 assessment with the refined 2021 CPUE approach (dark blue line) resulted in a much lower initial spawning potential but a very similar final spawning potential to the original 2018 model. Similarly, although not as extreme as for spawning potential, spawning depletion was lower than the 2018 reference model for the initial years but similar in the final years.
- Step 5 (Notag): Removal of the tagging data (light blue line) had a very minor effect on both the spawning potential and the spawning depletion from the previous step, and showed the same variation and trend over time.
- Step 6 (WCPFC16) Using data until 2016, but adding the troll data by month, and applying the new region and fleet structure for the WCPO (regions 1, 2 and 3) (green line), increased the initial spawning potential from the previous step, but the final spawning potential was similar to the 2018 reference model, albeit with a downward trend in the final two years compared to the increasing trend for the same years in the 2018 reference model. A similar effect was observed for spawning depletion, which tracked the 2018 reference case model, but with the downward trend in the last two years.
- Step 7 (WCPFC21): Updating the data to 2019 for the WCPFC-CA three region model (yellow line) resulted in a further increase of the initial spawning potential to be similar to the 2018 reference model. This model also showed a similar trend and similar levels to the 2018 model in 2016 (i.e. the final year of the 2018 model). A declining trend in spawning potential occurred for the last three years for the updated dated (2016-2019). Similar changes also occurred for spawning depletion that tracked the 2018 reference model closely until the 1980s and then estimated a less depleted state from then on, but with similar levels in 2016 and the steep decline for the last three years.
- Step 8 (SPO21): The final step involved adding in the new region, data and fisheries/fisheries strata for the EPO (region 4, fisheries 18, 19, 20, 21, 25) (orange line). Not surprisingly, due the larger model region overall, this step resulted in a large increase in the spawning potential above the other model steps (which included the WCPFC-CA regions only), and finished at a higher level, but with similar trend and dynamics, including the sharp decline for the last three years. Spawning depletion also showed a less depleted state for the SPO21 model compared to the other steps, and more so post-1980, and again showed a decline in the last three years. SPO21 is the diagnostic case model.

Overall the 2021 South Pacific albacore diagnostic case model (SPO21) estimates higher levels but similar trends and variability of spawning potential and depletion to the previous 2018 model that only considered the WCPFC-CA. The declining trend in recent years shown by the new diagnostic case model is notable. This recent decline results in 2019 spawning potential and spawning depletion levels that are similar to those observed in the final year (2016) of the 2018 WCPFC-CA only model (i.e. compare orange and red/black lines; Figure 12).

7.2 Model fit for the diagnostic case model

This section discusses the model results for the diagnostic case model, defined by the final step in the stepwise model development (*SPO21*; Figure 12), in particular the fit to the various sources of data, and the biological and fisheries-related parameters. We do not present these results for all models in the structural uncertainty grid, because of the volume of material that this would entail. However, results for all models are available on request.

7.2.1 Catch data

Very high penalties were applied to the catch data for all fisheries and so as expected model-predicted catches fit to the observed catches very closely for all fisheries (Figure 13, Figure 14, Figure 15).

7.2.2 Standardised CPUE

The standardised indices were highly variable in the first two decades for each region and display a decreasing trend over the first 15-20 years, after which the CPUE remained relatively flat for all regions (Figure 7). On the whole the model fits to the index data were good, but there was a clear tendency to underestimate CPUE during the early period and overestimate in the latter period for region 1 (INDEX-LL-1) (Figure 16). In regions 2 and 4 there was a tendency for the model to overestimate the CPUE during the late 1960s-1970s. Region 3 showed the best model fit to its CPUE index.

The plots of effort deviates for each index fishery over time indicate an adequate fit to the CPUE indices for region 1, 2 and 3, but systematic bias in region 4, which also has the lowest effort deviation penalties, indicating the model had most trouble fitting to the region 4 index (INDEX-ll-4) (Figure 17).

7.2.3 Size frequency data

Model fit to the time-aggregated length frequency data for fisheries with adequate sample sizes, particularly the longline fisheries, were quite good (Figure 18). Poorer fits occurred for fisheries with low sample sizes and variable compositions (e.g. PICT-LL-3b), and for several DWFN fisheries (e.g. DWFN-LL-3a, DWFN-LL-3b) where the model had difficulty fitting the multimodal observations. For the longline fishery in the EPO with the highest size samples (i.e. DWFN-LL-4a) the data were fit reasonably well, while a poorer fit was obtained for the other EPO fisheries. This was particularly the case for DWFN-LL-4c where the model overestimated the size of fish captured.

The model had a satisfactory fit to the troll and drifnet fisheries composition with some minor misfit related to the multimodality of observations for these fisheries (Figure 19). For the troll fishery in the EPO (ALL-TR-4) there was a lack of fit to the larger sizes likely due to the low sample sizes available.

Fits to the index fisheries size compositions were all very good, assisted by the combined large sample sizes. The exception was for the region 3 index (INDEX-LL-3), that had a bimodal distribution due to the occurrence of smaller albacore in this region, and the model underestimated the proportion of fish smaller than 75 cm (Figure 20).

Fits to size composition were consistently good across the model period for all DWFNs with the

exception DWFN-LL-4c, where the model consistently overestimated the size of fish, but this fishery also had low samples sizes and patchy temporal coverage (Figure 21). Similarly for the PICT and AZ (Australia/New Zealand) fisheries (Figure 22), and the troll and driftnet fisheries (Figure 23), the model was able to fit the composition data consistently well over time, even where sample coverage was lower and patchy. The fit to the index fisheries composition was very good across time, with the exception of the early model period where the model tended to slightly overestimate the size composition compared to the observations (Figure 24).

7.2.4 Likelihood profile

The change in negative log-likelihood relative to the minimum is shown for the total likelihood (purple line) and the individual data components in Section 14. The total likelihood is influenced mostly by the length composition that seems to be mostly informing the population scale (blue line).The CPUE prefers a higher population size, but the 'other' miscellaneous likelihood components, which are comprised of various penalties but are dominated by the penalties on the movement coefficients, and particularly the age-dependent movement coefficients, appear to effectively constrain the population to a lower population size. The movement coefficient penalties appear to have some influence on population scaling, therefore we checked different settings of the prior to evaluate their impact more explicitly. For the diagnostic case model the movement coefficients are penalised for deviations from their specified prior mean of 0.1 with a penalty weight of 5 (equivalent to a CV of approximately 0.32) while the age-dependent movement coefficients are penalised for deviations from their specified prior mean of 0, also with a penalty weight of 5. To check the sensitivity to this prior setting we conducted comparisons among alternative settings (Section 15). This sensitivity analysis indicated very minor influence of the prior settings for movement scale, and somewhat more influence, albeit still fairly minor, of the prior settings for age dependency. The results of this comparison indicate that the estimated population scaling, as indicated by total average biomass, is fairly robust to the prior settings for the movement coefficients. It is possible that other penalties that make up the 'other' category in Section 14 are influential on population scaling, and this requires further investigation.

7.2.5 Hessian diagnostic

Despite a stable minimisation where the objective function had declined to an essentially constant level with no minimizer errors, the Hessian approximation of the diagnostic case model was non-positive definite, having negative eigenvalues, which may indicate the model is not well determined and that there may be some confounding among the parameters. The independent variables contributing most to these negative values included: effort deviate coefficients; and, movement parameters. As previously explained, the model was configured to be similar to a "catch-conditioned" model with no observed effort being supplied for the extraction fisheries. The estimated effort deviate coefficients therefore act mainly to produce the observed catch for these fisheries. Early versions of the diagnostic case model were tested by fixing the movement and effort deviate parameters, and these produced positive definite Hessians solutions with minor influence on the dependent variables. It is therefore possible that the confounding that is indicated among these parameters will not substantially influence those dependent variables used for formulating management advice. Unfortunately, attempts to formally diagnose the implications of the negative eigenvalues on the dependent variables of the diagnostic case model were unsuccessful. It is therefore not possible to definitively state the degree of influence on the dependent variables of management interest. However, this does not necessarily imply that a

small number of near-zero negative eigenvalues (out of over 4000 parameters estimated) largely related to parameters having a relatively minor role, is sufficient to ignore the advice derived from the model. Future model simplification, including reducing spatial complexity and moving to a fully catch conditioned approach may be beneficial in achieving a positive definite Hessian.

7.3 Model parameter estimates (diagnostic case)

Estimates from the diagnostic case are presented in this section, e.g. by fishery and region, so that model behaviour can be assessed.

7.3.1 Selectivity

Estimated selectivity functions were consistent with known operational characteristics of the different gear types; longline fisheries selecting larger, older individuals (Figure 25 and Figure 26) and the driftnet and troll fisheries selecting smaller, younger fish that are more prevalent in the surface fisheries of the southern regions (Figure 27). These latter fisheries displayed dome-shaped selectivities which increased rapidly from age 0 to maximum selectivity at, or below, 10 quarters of age (Figure 27). Slight differences among fisheries existed, with the driftnet fisheries selecting a slightly wider range of ages and a slightly higher modal age than the troll fisheries. The troll fishery in the EPO (All-TR-4) was estimated to have a higher modal age, and a slower decrease in selectivity at higher ages than the WCPO troll fishery (All-TR-3a), which was estimated to select very few fish above age 13 quarters.

All the longline fisheries were estimated to have asymptotic, or near-asymptotic selectivity (Figure 25 and Figure 26). Differences among longline fisheries were evident in the age at which fish began to be selected, and the slopes of the ascending limbs of the selectivity functions, that were largely determined by the flag grouping and region of operation of the fishery. Some general patterns were: fisheries in the southern region selected younger fish, often down to 10 quarters of age; some fisheries had more gradual increases in selectivity between the age of first selection and the age of maximum selection (e.g. AZ-LL-2a vs DWFN-LL-2a); there were also differences in the presence and magnitude of a descending right limb for fish older than the age of maximum selectivity among longline fisheries, presumably related to availability older and larger fish to some fisheries.

The selectivities of the index fisheries were very similar among regions, noting that these were all set to have non-decreasing (asymptotic) selectivities (Figure 28).

7.3.2 Movement

Figure 29 provides a graphical representation of the movement coefficients (probabilities) 'estimated' for the diagnostic case and the 'fixed' movement coefficients applied from the SEAPODYM model. The 'estimated' movements shows greater probability of moving among regions in season 2 and from age 13 quarters onwards than for the SEAPODYM fixed coefficients. However across all seasons the SEAPODYM probabilities force greater movement rates. For both scenarios there is very low movement from region 4 (EPO) to regions 1,2 or 3 in the WCPFC-CA. The fixed SEAPODYM movement also implies greater movement of the youngest age groups than the modal 'estimated' movement.

7.4 Stock assessment results

7.4.1 Recruitment

Temporal trends in recruitment by region are shown in Figure 30. Region 3 is estimated to contribute the highest amount of recruitment to the overall stock throughout the time period, followed by the EPO (region 4) and region 2, which make similar contributions. The relative contribution of the regions was consistent over the assessment period.

A period of higher, but also highly variable, recruitments was estimated in the first decade of the assessment period in all regions. Recruitment was then maintained at a relatively consistent level for the remaining period, with the most significant observation being a period of lower variability from about 1965-1985, followed by higher variability for the remainder of the assessment. Most notable is a period of low recruitment in recent years (2015-2017). The last recruitment estimated is for the end of 2017 (noting the final nine quarters are flat as they are set at average recruitment) and suggest a higher recruitment event, more in line with the average (Figure 30). More years of data will be required to confirm if the most recent recruitment estimations are reliable.

The spawner recruit relationship for the diagnostic case is displayed in Figure 31. The regional number of recruits has been relatively consistent throughout the assessment so the annual recruitment has shifted horizontally along the curve as spawning potential has declined. Consistent with the quarterly recruitment trends discussed above, the recent time period shows the lowest estimated recruitments.

7.4.2 Biomass for the diagnostic case model

The diagnostic case model shows that spawning depletion has declined continuously since 1960 in all model regions, and is now at it lowest estimated level since 1960 (Figure 32).

Spawning and total biomass declined rapidly from 1960s until the 1980s after which they stabilised until the late 1990s, when a further decline occurs until the mid-2000s (Figure 33). The spawning and total biomass then stabilises again until the very recent period, when they decline steeply to the lowest estimated levels since the start of the model period. The overall trend is consistent in each model region despite the estimated levels of biomass associated with each region differing substantially. Spawning potential is relatively evenly attributed across regions 2, 3, and 4, with a very low proportion in region 1. The majority of recruitment is consistently apportioned to region 3. For total biomass, region 3 and 4 account for most of the biomass, followed by region 2. Recruitment is estimated to be highest in the early model period, but relatively stationary with high short-term variability since the 1970s. A period of historically low recruitment is estimated to have occurred from 2015-2017, consistent with the recent decline in biomass (before being set to the average recruitment for the last 9 quarters).

7.4.3 Fishing mortality

A steady increase in estimated fishing mortality of adult age-classes is estimated to have occurred over most of the assessment period (Figure 34), accelerating since the 1990s. Adult fishing mortality has increased in recent years, and is now the highest estimated over the history of fishery. Juvenile fishing mortality increased until around 1990, with a large spike in the late 1980s due to the driftnet fishery, and has remained stable at a comparatively low level since that time. A small peak in juvenile fishing mortality is estimated to have occurred in the late 2010s.

7.5 Multimodel inference - stepwise model development, sensitivity analyses and structural uncertainty

7.5.1 One-off sensitivities from the structural uncertainty analysis

This section compares the spawning potential and depletion trajectories for the diagnostic case and one-off sensitivity runs from the structural uncertainty analysis.

Steepness [*h0.65*, ***h0.80***, *h0.95*]

Low penalties on fitting the SRR relationship mean that the value of steepness specified in the model has a minor effect on fit and time-series estimates of spawning potential. Steepness is more influential when spawning potential is low and levels of depletion are high, however, under the diagnostic case the stock remains above 40% depletion and changing the steepness value has no influence on spawning potential (Figure 35). For depletion the impact of steepness was a marginal reduction in spawning depletion for the lowest value of $h0.65$. Low and high steepness values lead to marginally more pessimistic and optimistic estimates of stock status, respectively (Figure 36).

Weighting of the size-frequency data [*Size10*, ***Size25***, *Size50*]

The three models with alternative size frequency data weighting (divisors of 10, 25 and 50) had differing impacts on spawning potential and depletion. With the lower divisor of 10 spawning potential was notably scaled higher than results from the models with size frequency data weighting set at 25 and 50, while the results from those two models were comparable. For spawning depletion the lower size frequency data weighting value of 10 resulted in a less depleted stock, with the values of 25 and 50 leading to very similar depletion levels and trends (Figure 35, Figure 36).

Alternative growth/natural morality models [***Fixed-otolith with M-at-age***, *Length frequency with M-at-age*]

The diagnostic scenario of fixing the VB growth parameters with associated M-at-age resulted in a slightly lower spawning potential and a slightly more depleted spawning potential than the growth estimated from length frequency data with associated M-at-age (Figure 35, Figure 36).

Alternative movement [***Movement estimated***, *SEAPODYM*]

The movement assumption proved to be the most influential sensitivity on both spawning potential and depletion. The fixed SEAPODYM movement estimated a notably lower spawning potential and more depleted status than when movement was estimated by the model, but in contrast to the gradual decline when movement was estimated, is showed a gradual increasing trend in spawning potential from the 1980s until the recent decline (Figure 35, Figure 36).

Alternative recruitment [***Recruitment estimated***, *SEAPODYM*]

The recruitment sensitivity showed no influence on spawning potential or depletion between the scenarios where recruitment was fixed to occur only from regions 3 and 4, and the SEAPODYM derived recruitment distributions that allocated recruitment to all regions, but higher in regions 3 and 4 (Figure 35, Figure 36).

The diagnostic case SEAPODYM recruitment distribution (Figure 37) shows that recruitment is higher in quarters 3 and 4, and from region 3, and that some recruitment is estimated to occur in all regions.

The alternative scenario where recruitment is only allowed to occur in region 3 and 4 showed the same quarterly pattern of increased recruitment in quarter 3 and 4 as the SEAPDODYM scenario, but no recruitment in regions 1 and 2 (Figure 38).

The recruitment distribution for all models in the uncertainty grid is shown in Figure 39. The pattern of recruitment distribution across the grid models is more similar to the SEAPODYM scenario, with recruitment occurring in all regions.

7.5.2 Structural uncertainty analysis

The results of the structural uncertainty analysis are summarised in several forms – time-series plots of spawning potential and spawning depletion for all models in the grid by each axis of uncertainty (Figure 40, Figure 41), and the overall model grid by region, WCPFC, and EPO regions and for the South Pacific as a whole (Figure 42 to Figure 45), plus the Majuro and Kobe plots showing the estimates of $F_{recent}/F_{\text{MSY}}$ and $SB_{latest}/SB_{F=0}$ (and $SB_{recent}/SB_{F=0}$ for comparison) across all models in the grid (Figure 46).

The general features of the structural uncertainty analysis are as follows:

- The grid contains 72 models showing a wide range of estimates of stock status. The largest influence on the model uncertainty is the parameterisation of movement, with all models applying the SEAPODYM option showing lower estimates of spawning potential and higher depletion (i.e. a more deleted status). The difference in estimates of stock status depending on the movement scenario are in the order of 10 percentage points, which is significant in terms of the management advice, and underscores the importance of reducing uncertainty in movement parameters.
- Compared to the influence of movement assumptions, the other uncertainties were less influential, with the size data weighting being the next most important. Unlike the previous assessment where natural mortality and growth assumptions made major contributions to uncertainty (Tremblay-Boyer et al., 2018a), the combined growth/M axis used in this assessment had a more subtle effect on the uncertainty of management quantities. This is likely due to the different M-at-age functions (Figure 10) only being influenced by the different growth parameters being applied in the Maunder et al. method (Section 13). These growth parameters did not differ greatly, i.e. otolith growth - k= 0.067 $qtr^{-}1$, length frequency growth k=0.053 $qtr^{-}1$), resulting in minor difference to the M-at-age curves (Figure 10).

Majuro and Kobe plots and comparisons with Reference Points

The recent and latest spawning potential depletion and fishing mortality (relative to F_{MSY}) from each model within the uncertainty grid is presented in Figure 46 for the South Pacific as a whole. All models indicated that the South Pacific albacore stock is not overfished ($SB_{recent}/SB_{F=0}$ and $SB_{latest}/SB_{F=0}$ >0.2), nor subject to overfishing ($F_{recent}/F_{\text{MSY}}$ <1). While $SB_{recent}/SB_{F=0}$ estimates tended to be above 35%, $SB_{latest}/SB_{F=0}$ estimates fell to 25% for the more pessimistic models (Table 5).

There was a greater spread of estimates for SB/SB_{MSY} than for $SB/SB_{F=0}$, indicating greater uncertainty in the MSY based quantities. For the Majuro plots there were also two clusters of model results that were separated mostly according to the estimated $SB/SB_{F=0}$, although the models with the most depleted status also had the highest estimates of $F_{recent}/F_{\text{MSY}}$. These more

pessimistic models all involved the SEAPODYM movement hypothesis.

Depletion estimates of stock status could also be derived specifically for the WCPFC-CA (regions WCPO1-3 of the assessment model; Table 6), and hence related to the interim target reference point for the stock in that region ($SB/SB_{F=0} = 0.56$). While results for the WCPFC-CA also indicated that the stock in this area was not overfished (the results of all models estimating $SB/SB_{F=0}$ >0.2), median $SB_{recent}/SB_{F=0}$ was 0.47 and median $SB_{latest}/SB_{F=0}$ was 0.36. Eight six percent of models estimated that $SB_{recent}/SB_{F=0}$ was less than the interim TRP.

Longline vulnerable biomass: WCPFC-CA

Longline vulnerable biomass apportions the total biomass to that which is vulnerable to longline gear. Vulnerable biomass is relevant to the management objectives for the southern longline fishery in the WCPFC-CA where an objective is to achieve a vulnerable biomass that is equivalent to or greater than the vulnerable biomass estimated in 2013+8%, the basis for the TRP. This assessment estimated that the median latest (2019) and recent (2016-2019) longline vulnerable biomass for the WCPFC-CA fisheries are 60% and 78% of the 2013+8% target level.

7.5.3 Further analyses of stock status

There are several ancillary analyses related to stock status that are typically undertaken on the diagnostic case model (dynamic Majuro analyses, and fisheries impacts analyses). The shift towards relying more on multimodel inference makes it difficult to present these results over a large number of model runs so these analyses are only provided for the diagnostics model in this paper, but those for other models can be provided if requested.

Dynamic Majuro and Kobe plots

The section summarising the structural uncertainty grid (Section 7.5.2) presents terminal estimates of stock status in the form of Majuro plots. Further analyses can estimate the time-series of stock status in the form of Majuro and Kobe plots, the methods of which are presented in Section 5.7.4. The large number of model runs in the structural uncertainty grid precludes undertaking and presenting this process for all runs, however an example for the diagnostic case model is presented in Figure 47. The equivalent dynamic Kobe plots are displayed in Figure 47. At the beginning of the assessment period the stock was estimated to be close to unexploited levels. Over the first several decades stock status declined steadily, with a small peak in fishing mortality around the time of the driftnet fishery. Depletion levels and fishing mortality subsequently continued to increase until the end of the assessment period. The stock is above both depletion and fishing mortality limit reference points (Figure 47).

Fishery impacts for example models

It is possible to attribute the fishery impact (with respect to depletion levels) to specific fishery components (grouped by fishery and gear-type), in order to estimate which types of fishing activity have had the most impact on spawning potential using the diagnostic case model (Figure 48). The majority of the fisheries depletion in each region over the entire assessment period can be attributed to longline fisheries, and in the terminal years of the assessment this is almost entirely the case. The sub-tropical longline fleet has the most impact overall, though in region 3 and 4 the temperate longline fleet has the major impact, and in region 4 there is an increased impact of the EPO longline fishery since 2000. In region 1 the longline impact is mostly split between that of the tropical and sub-tropical fleets, though in earlier years the temperate

longline fleet also had a significant impact. The driftnet fishery is estimated to have had a moderate impact on depletion over the years it operated and this impact occurred in all regions to a degree, despite the fishery only occurring in region 3, owing to the movement of fish among regions. The troll fisheries have had a relatively low impact on the stock.

8 Discussion

8.1 General remarks on the assessment

Stock status and management quantities of interest were evaluated against a range of assessment model assumptions. This structural uncertainty grid included combinations of different values for key parameters that were considered relevant for albacore, including: steepness of the stock recruitment relationship, movement among model regions, length composition data weighting, recruitment distribution, and growth and natural mortality. Evaluating a range of alternative, but plausible, models provides more robust scientific advice than using just a single model (Jardim et al., 2021). Future assessments should also seek to include the statistical uncertainty of individual models by applying an ensemble approach as done for the 2021 southwest Pacific swordfish assessment (Ducharme-Barth and Vincent, 2021; Ducharme-Barth et al., 2021).

Most of the models in the uncertainty grid estimated a steady decline in spawning potential and depletion over most of the assessment period, with a relatively steep decline in the most recent years. A notable exception were the models that applied the SEAPODYM movement which all showed a gradual increasing trend from the 1980s until the most recent period, when they too showed a decline in stock status. This decline appears to be the result of a low period of recruitment estimated from 2015–2017, potentially a consequence of an unfavourable period of oceanography and environmental conditions for albacore recruitment. Castillo-Jordán et al. (2016) indicated that potential linkages between recruitment and global environmental indices such as Interdecadal Pacific Oscillations (IPO), Southern Oscillation Index (SOI) and Southern Annular Mode (SAM) at sub-basin, basin, and multi-basin scales can play an important role for dynamics of important southern hemisphere fishery species. Exploration of environmental influences on South Pacific albacore spatial dynamics have involved the development and application of the SEAPODYM modelling framework (Senina et al., 2020). This work suggest that albacore are influenced by ocean temperature and other variables such as dissolved oxygen, currents and prey concentration. While it is likely that environmental drivers have influenced the recent poor recruitment the specific causal mechanisms behind the lower recruitment and the implications of fishing depletion are unclear. Environmental effects are not explicitly dealt with in this assessment.The recent decline in spawning potential and the increased depletion estimated by the new assessment are consistent with stock projections conducted by Hare et al. (2020) based on the 2018 assessment model (Tremblay-Boyer et al., 2018a).

The 2021 South Pacific albacore assessment spanned the entire South Pacific encompassing the southern hemisphere convention areas of the WCPFC and the IATTC. This new regional structure was a substantial change from the previous models used for assessment of South Pacific albacore in the WCPFC-CA. The last assessment that included the EPO was led by Hoyle et al. (2012) but that assessment applied an areas-as-fleets approach. Here, we have developed a spatially explicit assessment with a four region model structure that considered seasonal and age-specific movement, spatial structure of the population by age, and patterns of fishing activity and selectivity. In the diagnostic case model, movement was estimated internally within MULTIFAN-CL. However, due to limited knowledge on movement patterns for albacore, and a

lack of tagging data to inform this, the SEAPODYM model (Lehodey et al., 2008; Senina et al., 2020) was used for the first time as the basis for an alternative hypothesis for albacore movement in the South Pacific Ocean. This meant that alternative movement hypotheses where included in the grid of models proposed for management advice, which was not the case in the previous assessment.

Not surprisingly, the assumed movement probabilities with age and season were found to strongly influence estimated spawning potential and depletion, with the SEAPODYM estimates resulting in a more pessimistic estimated stock status. This result emphasises the important influence that assumptions on movement can have on the outcomes of spatial explicit models. Exploration of alternative plausible movement assumptions and inclusion of a range of options in model uncertainty grids, perhaps drawn from prior distributions (i.e. Ducharme-Barth and Vincent (2021)), is recommended for future spatially explicit assessments of South Pacific albacore. We encourage further biological research to improve our understanding of population structure and movements of albacore across the South Pacific.

Although SEAPODYM has potential to be useful in this context, some caution should be exercised with regard to these movement estimates and the implications for stock status. The SEAPODYM estimates are model derived quantities and have statistical and structural uncertainty that is not accounted for in the way they are applied to the current assessment. Developing more robust data sets on movement will help to refine and validate these estimates. On the other hand, the lack of spatial population structure and connectivity dynamics could lead to biased stock status indicators. Goethel and Berger (2017) suggest that a simpler spatial structure for assessment models may be preferable to complex spatial structuring when the true spatial dynamics are not well understood. A management strategy evaluation (MSE) approach could be beneficial to investigate the implications of including different degrees of spatial complexity on estimated stock dynamics and management robustness to spatial misspecifications. Furthermore the interactions between spatial complexity and misspecified movement rates could be explored with simulation studies.

Given the challenges in estimating steepness and the substantial uncertainty in stock assessment outputs and management quantities that can result (Lee et al., 2012), steepness was fixed at values (i.e. 0.65, 0.80, and 0.95) routinely used in WCPFC tuna assessments. The model results suggested minimal impact on the depletion based quantities of most interest given the range of steepness values evaluated (noting a greater impact on MSY-related metrics, as expected). Punt et al. (2021) found that steepness could compensate for a misspecification of natural mortality to some degree. Further investigation or simulation studies could improve our understanding of the influence steepness has on the albacore assessment and to assess the interaction between steepness and other potentially influential parameters such as natural mortality.

As for the 2018 assessment, the growth of South Pacific albacore remains an area of uncertainty. The otolith-based growth parameters used in the current assessment incorporated several improvements over previous estimates, including the addition of new otolith readings for smaller albacore using daily otolith increments and the use of an improved method for computing decimal age (Farley et al., 2021). The refined otolith growth data improved the interpretation of the modal structure of the New Zealand troll fishery when applying a logistic growth model. The age estimates by modal group for the otolith-sampled fish were 1.1 yr (43-55 cm), 1.9 yr (56-64 cm) and 2.9 yr (65-74 cm) (Farley et al., 2021), thereby confirming the annual nature of the clear length modes in the sample data. However, the logistic growth model is currently not available in Multifan-CL. The von Bertalanffy model (which provided a better fit than the Richards) was

fitted to the full otolith data set but did not fit the troll length composition modes as well as was indicated by Farley et al. (2021) using the logistic curve and reduced data set. This is likely due to some inadequacies of the von Bertalanffy model, and/or some latitudinal variability in growth that was present in the full otolith data set. To evaluate the potential impact of growth misspecification resulting from applying a single von Bertalanffy growth curve estimated from the full region-wide otolith data set, an alternative growth curve was estimated by fitting a flexible von Bertalanffy model (with length-at-age offsets estimated for the younger age classes) to the size data used in the assessment, but with the troll fishery data heavily up-weighted. This growth model provided an excellent fit to the troll fishery size data, with a consistent interpretation of annual length mode spacing, and therefore represented a reasonable alternative growth model to use in this assessment. It appears that the main difference in the two growth curves was the growth rate during the first 1-2 years of life, that was faster for the growth estimated from length composition data. Adding a logistic growth option, and potentially an option that allows fixed values for mean growth for each age-class, to Multifan-CL, coupled with further daily ageing of even smaller albacore, could help with improving the flexibility and fit of the otolith growth model to the troll fishery length modes. Further spatio-temporal analysis of growth is also required to understand how stable growth parameters are in space and time, acknowledging most of the otolith samples used to inform growth in this study were collected in 2009 and 2010.

This assessment adopted the approach recommend by Maunder et al. (Section 13) to natural mortality (M) by linking hypotheses about growth and M, with M-at-age being determined by life-history parameters, including growth, and theoretical considerations (Lorenzen, 1996). We consider this approach (discussed in-depth at the most recent CAPAM workshop – see *https://capamresearch.org/Natural-Mortality-Workshop*) to be a substantial improvement over that used in previous albacore assessments. The M-at-age estimates associated with the alternative growth models appear to be biologically plausible, with relatively high M for the youngest age classes, the lowest M estimated for the sub-adult age classes, and a moderate increase in M around the age at first maturity. We suggest that linking the growth and M-at-age is a desirable approach, which could be improved in future assessments through a more thorough exploration of uncertainty, such as the biological ensemble approach adopted by Ducharme-Barth et al. (2021) for the southwest Pacific swordfish assessment. The other advantages of combining growth and natural mortality into a single axis of uncertainty, are; 1) it removes unrealistic combinations of growth and mortality that might be included in a typical grid where the two uncertainties are separated, 2) it reduces the number of models in the grid which make it more computationally efficient. As currently modelled, the growth/natural mortality assumptions had a relatively small impact on spawning potential and depletion estimates, in contrast to the previous assessment where natural mortality was one of the most influential uncertainties. Although this approach was viewed as sensible, the overall uncertainty may not be fully captured.

The other influential area of uncertainty was the weighting of the size data within the model. A size data divisor of 10 (maximum effective sample size of 100) led to higher estimated spawning potential compared to the other weightings, although the impact on estimated depletion was not as notable. To improve the approach to data weighting within WCPFC tuna assessments, further testing of the feasibility of using Self-Scaling Multinomial with Auto-correlated Random Effects likelihood for the size composition data is recommended, and will be considered as part of the upcoming peer review of the 2020 yellowfin tuna assessment.

Finally, the results of the assessment appeared robust to the alternative hypotheses regarding distribution of recruitment amongst model regions.

8.2 Examining other key data inputs into this assessment

The approach to standardize the longline CPUE data for the index fisheries was similar to the previous assessment in that both used a spatiotemporal delta-GLMM modelling approach with a synthetic targeting cluster variable as a catchability covariate. In addition, vessel flag was included in the 2021 standardization approach, which offered some improvement in the model fit. The standardized trends tracked the nominal CPUE fairly well for much of the time series, suggesting minimal effect of the standardization procedure, which may be cause for concern. In addition, there was a notable spatial pattern in the residuals; likely an indication that potentially important explanatory variables are missing from the model. Preliminary analyses explored splitting the time series to allow for a more informed assessment model in the contemporary time period. These model enhancements were possible due to the availability of more detailed data regarding vessel and gear characteristics, as well as oceanographic covariates. Ultimately the split series were not adopted for the final model; however, given the data limitations for the historical time period, such an approach should be given additional consideration in future assessments, along with consideration of the best approach to bridging between split indices. Spatial stratification of the albacore stock by size has been observed, with smaller/younger fish more available in the southern regions of the assessment domain and the larger individuals more distributed throughout the sub-tropical waters. Standardizing the catch data by size class, or life stage (juveniles versus adults), could improve the estimation of selectivity for the index fisheries, which may differ from the catch selectivity. These alternative size-based approaches to CPUE index standardization (Maunder et al., 2020) could prove valuable for the next South Pacific albacore assessment.

While developments related to the CPUE standardisation methodology are important, perhaps more important is the need for greater focus on improving the scope of the data to support these analyses so indices of relative abundance are more representative of the true stock dynamics. Scientific observers collect detailed vessel, gear, and fishing strategy related information that could improve these analyses, but coverage levels are insufficient (generally less than 5%) to provide the spatial and temporal coverage needed for these analyses. Electronic monitoring for longline fisheries has shown great promise (Brown et al., 2021), and steps to expand and enhance these tools to better monitor the longline sector are encouraged. Lastly, developing collaborative partnerships and cooperative research programmes with the fishing industry is important to; 1) explore questions related to fishing strategy, gears, decision making, and other operational factors influencing catch rates, and 2) improve the understanding of fishery operations by the scientists tasked with conducting these analysis. Both of these would no doubt lead to improvements in the approaches for developing abundance indices from fishery dependent catch and effort data.

The South Pacific albacore assessment has relatively high uncertainty in the key model outputs, which is a consequence of the uninformative nature of the fishery data with respect to population scaling, notably the CPUE data which has little contrast. Indeed population scaling was more informed by the length composition data. The inability to achieve a positive definite Hessian solution for the diagnostic case model, in spite of a stable minimisation, while not ideal and likely related to nuisance parameters, is perhaps less concerning for this assessment than the lack of contrast in the abundance indices. While tag-recapture data provides information within other key tuna assessments, this information is lacking for South Pacific albacore given the challenges in successfully tagging this species; only one tag has been recovered in the region since 2017, and no new tagging data have been incorporated to the assessment since 2015. To improve information on population scale, a new approach utilising genetic markers should be seriously considered.

Close-kin mark-recapture (CKMR) is an approach that integrates genetic methods of population estimation that could be used to scale future South Pacific albacore stock assessments. CKMR offers an opportunity to provide fishery-independent information on absolute population size, natural mortality and other demographics parameters for albacore and others tuna species in the region, with the added bonus of information on population structure. We strongly recommend considering the approach outlined in Bravington et al. (2021).

8.3 Main assessment conclusions

The 2021 stock assessment provided results consistent with the previous assessment; that is, a decline in estimated spawning potential over most of the assessment period, in particular within the most recent years. The addition of the EPO into the current assessment did not result in notable changes to the main assessment outputs, and similar spawning potential trajectories and terminal depletion levels were estimated in the WCPFC-CA and EPO.

The uncertainty in the terminal year estimates of the albacore stock status are highlighted, given they are reliant on sparse information until the older age-classes are observed in the longline fishery catches. The results of the retrospective analysis (Section 17) and comparison of spawning potential estimated in terminal years of recent assessments with those estimated in subsequent estimates further highlight the greater uncertainty in the most recent years of the assessment period.

The main conclusions of this assessment are summarised as follows:

- Spawning potential has generally declined across the model period, with that decline increasing in the most recent years. The assessment indicates the stock is not overfished, and there was zero estimated risk of the stock being below $20\% SB_{F=0}$. However, decline in the latest estimated $SB_{latest}/SB_{F=0}$ (median 0.36; 0.27 - 0.44, 10^{th} and 90^{th} percentiles) are notably more pessimistic than those of $SB_{recent}/SB_{F=0}$ (median 0.47; 0.40 - 0.56, 10^{th} and 90^{th} percentiles). The general trends are consistent for estimates across all regions of the South Pacific stock, and for the WCPFC-CA only.
- For the WCPFC-CA regions only, $SB_{recent}/SB_{F=0}$ had a median of 0.47 (0.42 - 0.58, 10^{th} and 90^{th} percentiles) and $SB_{latest}/SB_{F=0}$ had a median 0.36 (0.28 - 0.43, 10^{th} and 90^{th} percentiles), both being below the interim target reference point of 0.56. Further, *86%* of models (62 out of 72 models) estimated that $SB_{recent}/SB_{F=0}$ was below the interim TRP. In relation to management objectives for the WCPFC-CA longline fishery, this assessment estimated that the median 'latest' (2019) and 'recent' (2016-2019) longline vulnerable biomass for the WCPFC-CA are 60% and 78% of the 2013+8% target level that defined the interim TRP.
- South Pacific-wide median estimates of $F_{recent}/F_{\mathrm{MSY}}$ indicate the stock was not subject to overfishing (median 0.26; 0.16 - 0.38, 10^{th} and 90^{th} percentiles).
- Uncertainty in movement and the size frequency data weighting are the major contributors to the overall assessment uncertainty. The bimodal nature of the assessments results, especially for regions 1, 2, and 4, were due mainly to the uncertainty of movement parameters. Further, the CPUE indices lacked contrast to inform population scale, which was more influenced by the size composition data.

9 Acknowledgements

We thank the various fisheries agencies and CCMs for the provision of the catch, effort and size frequency data used in this analysis, and gratefully acknowledge the hard work of the observers working throughout the region to gather data and biological samples. We thank Tom Peatman for assistance with analyses of size composition data, Jessica Farley and Page Eveson from CSIRO and Kyne Krusic-Golub of Fish Ageing Services for timely delivery of the updated otolith ageing data. We thank Cleridy Lennert-Cody for her analysis to inform stratification of the EPO fisheries, and Inna Senina for providing the movement probabilities from SEAPODYM. We also thank Fabrice Bouye for ensuring our Condor flock was up and flying when we needed it most. Sam McKechnie, as always provided valuable advice, reviews and reality checks along the way, and Matthew Vincent helped Claudio get going with MFCL, Multifan-data-generator and various other 'things' needed to tackle this assessment. Finally the MFCL development team of Dave Fournier and Nick Davies, your support and responsiveness to all our requests for advice is absolutely very much appreciated. The assessment was supported by the WCPFC secretariat through the funding contributions of CCMs.

10

References

Anderson, G., Hampton, J., Smith, N., and Rico, C. (2019). Indications of strong adaptive population genetic structure in albacore tuna (*Thunnus alalunga*) in the southwest and central Pacific Ocean. *Ecol Evol*, 9(18):10354–10364.

Bigelow, K., Musyl, M. K., Poisson, F., and Kleiber, P. (2006). Pelagic longline gear depth and shoaling. *Fisheries Research*, 77(2):173–183.

Bravington, M., Nicol, S., and Anderson, G. (2021). Feasability of Close-Kin-Mark-Recapture for albacore in the WCPO (project 100b). Technical Report WCPFC-SC17/SA-IP-14.

Breiman, L. (2001). Random forests. *Machine Learning*, 45(1):5–32.

Brown, C. J., Desbiens, A., Campbell, M. D., Game, E. T., Gilman, E., Hamilton, R. J., Heberer, C., Itano, D., and Pollock, K. (2021). Electronic monitoring for improved accountability in western Pacific tuna longline fisheries. *Marine Policy*, 132:104664.

Cadigan, N. G. and Farrell, P. J. (2005). Local influence diagnostics for the retrospective problem in sequential population analysis. *ICES Journal of Marine Science: Journal du Conseil*, 62(2):256–265.

Castillo-Jordán, C., Klaer, N. L., Tuck, G. N., Frusher, S. D., Cubillos, L. A., Tracey, S. R., and Salinger, M. J. (2016). Coincident recruitment patterns of Southern Hemisphere fishes. *Can. J. Fish. Aquat. Sci.*, 73(2):270–278.

Ducharme-Barth, N., Castillo-Jordan, C., Hampton, J., Williams, P., Pilling, G., and Hamer, P. (2021). Stock assessment of swordfish in the southwest Pacific Ocean. Technical Report WCPFC-SC17-2021/SA-WP-04.

Ducharme-Barth, N. and Vincent, M. (2021). Focusing on the front end: A framework for incorporating in uncertainty in biological parameters in model ensembles of integrated stock assessments. Technical Report WCPFC-SC17-2021-SA-WP-05.

Ducharme-Barth, N., Vincent, M., Hampton, J., Hamer, P., Williams, P., and Pilling, G. (2020). Stock assessment of bigeye tuna in the western and central Pacific Ocean. Technical Report WCPFC-SC16-2020/SA-WP-03 [REV3].

Farley, J., Krusic-Golub, K., and Eveson, P. (2021). Ageing of South Pacific Albacore: (Project 106). Technical Report WCPFC-SC17-SA-IP-10.

Farley, J., Krusic-Golub, K., Eveson, P., Clear, N., Rouspard, F., Sanchez, C., Nicol, S., and Hampton, J. (2020). Age and growth of yellowfin and bigeye tuna in the western and central Pacific Ocean from otoliths. Technical Report SC16-SA-WP-02.

Farley, J. H., Hoyle, S. D., Eveson, J. P., Williams, A. J., Davies, C. R., and Nicol, S. J. (2014). Maturity Ogives for South Pacific Albacore Tuna (Thunnus alalunga) That Account for Spatial and Seasonal Variation in the Distributions of Mature and Immature Fish. *PLoS ONE*, 9(1):e83017.

Farley, J. H., Williams, A. J., Clear, N. P., Davies, C. R., and Nicol, S. J. (2013a). Age estimation and validation for South Pacific albacore (Thunnus alalunga). *Journal of Fish Biology*, 82(5):1523–1544.

Farley, J. H., Williams, A. J., Hoyle, S. D., Davies, C. R., and Nicol, S. J. (2013b). Reproductive Dynamics and Potential Annual Fecundity of South Pacific Albacore Tuna (Thunnus alalunga). *PLoS ONE*, 8(4):e60577.

Fournier, D. and Archibald, C. P. (1982). A general-theory for analyzing catch at age data. *Canadian Journal of Fisheries and Aquatic Sciences*, 39(8):1195–1207.

Fournier, D., Hampton, J., and Sibert, J. (1998). MULTIFAN-CL: a length-based, age-structured model for fisheries stock assessment, with application to South Pacific albacore, Thunnus alalunga. *Canadian Journal of Fisheries and Aquatic Sciences*, 55:2105–2116.

Fournier, D. A., Skaug, H. J., Ancheta, J., Ianelli, J., Magnusson, A., Maunder, M. N., Nielson, A., and Sibert, J. (2012). AD Model Builder: using automatic differentiation for statistical inference of highly parameterized complex nonlinear models. *Optimization Methods and Software*, 27(2):233–249.

Francis, R. I. C. C. (1992). Use of risk analysis to assess fishery management strategies: A case study using orange roughy (ıt Hoplostethus atlanticus) on the Chatham Rise, New Zealand. *Canadian Journal of Fisheries and Aquatic Science*, 49:922–930.

Goethel, D. R. and Berger, A. M. (2017). Accounting for spatial complexities in the calculation of biological reference points: effects of misdiagnosing population structure for stock status indicators. *Canadian Journal of Fisheries and Aquatic Sciences*, 74(11):1878–1894.

Hamer, P., Castillo Jordon, C., Xu, H., Ducharme-Barth, N., and Vidal Cunningham, T. (2021). Report from the SPC Pre-assessment Workshop - March 2021. Technical Report WCPFC-SC17-2021/SA-IP-02, Pacific Community.

Hampton, J. and Fournier, D. (2001). A spatially-disaggregated, length-based, age-structured population model of yellowfin tuna (Thunnus albacares) in the western and central Pacific Ocean. *Marine and Freshwater Research*, 52:937–963.

Hare, S., Pilling, G., and Williams, P. (2020). Trends in the South Pacific albacore longline and troll fisheries. Technical Report WCPFC-SC16-2020/SA-IP-11.

Harley, S. J. (2011). A preliminary investigation of steepness in tunas based on stock assessment results. Technical Report WCPFC-SC7-2011/SA-IP-08, Pohnpei, Federated States of Micronesia, 9–17 August 2011.

Harley, S. J., Davies, N., Tremblay-Boyer, L., Hampton, J., and McKechnie, S. (2015). Stock assessment of south Pacific albacore tuna. Technical Report WCPFC-SC11-2015/SA-WP-06, Pohnpei, Federated States of Micronesia, 5–13 August 2015.

Hoyle, S., Hampton, J., and Davies, N. (2012). Stock assessment of albacore tuna in the South Pacific Ocean. Technical Report WCPFC-SC8-2012/SA-WP-04, Busan, Republic of Korea, 7–15 August 2012.

Hoyle, S. D. and Davies, N. (2009). Stock assessment of albacore tuna in the south Pacific Ocean. Technical Report WCPFC-SC5-2009/SA-WP-06, Port Vila, Vanuatu, 10–21 August 2009.

Ianelli, J., Maunder, M. N., and Punt, A. E. (2012). Independent review of the 2011 WCPO bigeye tuna assessment. Technical Report WCPFC-SC8-2012/SA-WP-01, Busan, Republic of Korea, 7–15 August 2012.

ISC Albacore Working Group (2011). Stock Assessment of Albacore Tuna in the North Pacific Ocean in 2011. Technical Report WCPFC-SC7-2011/SA-WP-10, Pohnpei, Federated States of Micronesia, 9–17 August 2011.

ISSF (2011). Report of the 2011 ISSF stock assessment workshop. Technical Report ISSF Technical Report 2011-02, Rome, Italy, March 14–17.

Jardim, E., Azevedo, M., Brodziak, J., Brooks, E. N., Johnson, K. F., Klibansky, N., Millar, C. P., Minto, C., Mosqueira, I., Nash, R. D. M., Vasilakopoulos, P., and Wells, B. K. (2021). Operationalizing ensemble models for scientific advice to fisheries management. *ICES Journal of Marine Science*, page fsab010.

Kinney, M. and Teo, S. (2016). Meta-analysis of north Pacific albacore tuna natural mortality. Technical Report ISC/16/ALBWG-02/07.

Kleiber, P., Fournier, D., Hampton, J., Davies, N., Bouye, F., and Hoyle, S. (2019). MULTIFAN-CL User's Guide. Technical report.

Langley, A. (2004). An examination of the influence of recent oceanographic conditions on the catch rate of albacore in the main domestic longline fisheries. Technical Report Working Paper SA-4., 17th Standing Committee on Tuna and Billfish. 9–18 August 2004. Majuro, Republic of Marshall Islands.

Lee, H.-H., Maunder, M. N., Piner, K. R., and Methot, R. D. (2012). Can steepness of the stock–recruitment relationship be estimated in fishery stock assessment models? *Fisheries Research*, 125-126:254–261.

Lehodey, P., Senina, I., and Murtugudde, R. (2008). A spatial ecosystem and populations dynamics model (SEAPODYM) – Modeling of tuna and tuna-like populations. *Progress in Oceanography*, 78(4):304–318.

Lehodey, P., Senina, I., Nicol, S., and Hampton, J. (2015). Modelling the impact of climate change on South Pacific albacore tuna. *Deep Sea Research Part II: Topical Studies in Oceanography*, 113:246–259.

Lennert-Cody, C. E., Maunder, M. N., Aires-da Silva, A., and Minami, M. (2013). Defining population spatial units: Simultaneous analysis of frequency distributions and time series. *Fisheries Research*, 139:85–92.

Lennert-Cody, C. E., Minami, M., Tomlinson, P. K., and Maunder, M. N. (2010). Exploratory analysis of spatial–temporal patterns in length–frequency data: An example of distributional regression trees. *Fisheries Research*, 102(3):323–326.

Lorenzen, K. (1996). The relationship between body weight and natural mortality in juvenile and adult fish: a comparison of natural ecosystem and aquaculture. *Journal of Fish Biology*, 42:627–647.

Macdonald, J. I., Farley, J. H., Clear, N. P., Williams, A. J., Carter, T. I., Davies, C. R., and Nicol, S. J. (2013). Insights into mixing and movement of South Pacific albacore Thunnus alalunga derived from trace elements in otoliths. *Fisheries Research*, 148:56–63.

Maunder, M. N., Thorson, J. T., Xu, H., Oliveros-Ramos, R., Hoyle, S. D., Tremblay-Boyer, L., Lee, H. H., Kai, M., Chang, S.-K., Kitakado, T., Albertsen, C. M., Minte-Vera, C. V., Lennert-Cody, C. E., Aires-da Silva, A. M., and Piner, K. R. (2020). The need for spatio-temporal modeling to determine catch-per-unit effort based indices of abundance and associated composition data for inclusion in stock assessment models. *Fisheries Research*, 229:105594.

McKechnie, S. (2014). Analysis of longline size frequency data for bigeye and yellowfin tunas in the WCPO. Technical Report WCPFC-SC10-2014/SA-IP-04, Majuro, Republic of the Marshall Islands, 6–14 August 2014.

McKechnie, S., Pilling, G., and Hampton, J. (2017). Stock assessment of bigeye tuna in the western and central Pacific Ocean. Technical Report WCPFC-SC13-2017/SA-WP-05, Rarotonga, Cook Islands, 9–17 August 2017.

Methot, Richard D., J. and Wetzel, C. R. (2013). Stock synthesis: A biological and statistical framework for fish stock assessment and fishery management. *Fisheries Research*, 142:86–99.

Nikolic, N., Montes, I., Lalire, M., Puech, A., Bodin, N., Arnaud-Haond, S., Kerwath, S., Corse, E., Gaspar, P., Hollanda, S., Bourjea, J., West, W., and Bonhommeau, S. (2020). Connectivity and population structure of albacore tuna across southeast Atlantic and southwest Indian Oceans inferred from multidisciplinary methodology. *Sci Rep*, 10(1):15657.

Nikolic, N., Morandeau, G., Hoarau, L., West, W., Arrizabalaga, H., Hoyle, S., Nicol, S. J., Bourjea, J., Puech, A., Farley, J. H., Williams, A. J., and Fonteneau, A. (2017). Review of albacore tuna, Thunnus alalunga, biology, fisheries and management. *Rev Fish Biol Fisheries*, 27(4):775–810.

Punt, A. E., Castillo-Jordán, C., Hamel, O. S., Cope, J. M., Maunder, M. N., and Ianelli, J. N. (2021). Consequences of error in natural mortality and its estimation in stock assessment models. *Fisheries Research*, 233:105759.

Renck, C., Talley, D., Wells, D., and Dewar, H. (2014). Regional growth patterns of juvenile albacore (Thunnus alalunga) in the eastern North Pacific. Technical Report CalCOFI Rep., Vol. 55.

Senina, I. N., Lehodey, P., Hampton, J., and Sibert, J. (2020). Quantitative modelling of the spatial dynamics of South Pacific and Atlantic albacore tuna populations. *Deep Sea Research Part II: Topical Studies in Oceanography*, 175:104667.

Thorson, J. T., Shelton, A. O., Ward, E. J., and Skaug, H. J. (2015). Geostatistical delta-generalized linear mixed models improve precision for estimated abundance indices for West Coast groundfishes. *Ices Journal of Marine Science*, 72(5):1297–1310.

Tremblay-Boyer, L., Hampton, J., McKechnie, S., and Pilling, G. (2018a). Stock assessment of South Pacific albacore tuna. Technical Report WCPFC-SC-14-2018/SA-WP-05, Busan, South Korea, 8-16 August 2018.

Tremblay-Boyer, L., McKechnie, S., and Pilling, G. (2018b). Background Analysis for the 2018 stock assessment of South Pacific albacore tuna. Technical Report WCPFC-SC14-2018/ SA-IP-07, Busan, South Korea, 8-16 August 2018.

Tremblay-Boyer, L., McKechnie, S., Pilling, G., and Hampton, J. (2017). Stock assessment of yellowfin tuna in the Western and Central Pacific Ocean. Technical Report WCPFC-SC13-2017/SA-WP-06, Rarotonga, Cook Islands, 9-17 August 2017.

Vidal, T., Castillo Jordan, C., Peatman, T., Ducharme-Barth, N., Xu, H., Williams, P., Lennert-Cody, C., and Hamer, P. (2021). Background analysis and data inputs for the 2021 South Pacific albacore tuna stock assessment. Technical Report WCPFC-SC17-SA-IP-03.

Vincent, M., Ducharme-Barth, N., Hamer, P., Hampton, J., Williams, P., and Pilling, G. (2020). Stock assessment of yellowfin tuna in the western and central Pacific Ocean. WCPFC-SC16-2020/SA-WP-04-Rev2.

Waterhouse, L., Sampson, D. B., Maunder, M., and Semmens, B. X. (2014). Using areas-as-fleets selectivity to model spatial fishing: Asymptotic curves are unlikely under equilibrium conditions. *Fisheries Research*, 158:15–25.

Williams, A. J., Allain, V., Nicol, S. J., Evans, K. J., Hoyle, S. D., Dupoux, C., Vourey, E., and Dubosc, J. (2015). Vertical behavior and diet of albacore tuna (Thunnus alalunga) vary with latitude in the South Pacific Ocean. *Deep Sea Research Part II: Topical Studies in Oceanography*, 113:154–169.

Williams, A. J., Farley, J. H., Hoyle, S. D., Davies, C. R., and Nicol, S. J. (2012). Spatial and sex-specific variation in growth of albacore tuna (Thunnus alalunga) across the South Pacific Ocean. *PLoS ONE*, 7(6):e39318.

11 Tables

Table 1: Definition of fisheries for the 2021 MULTIFAN-CL South Pacific albacore tuna stock assessment, refer to Figure 3.

Fishery Number	Gear	Model Code-Fleets	Flags	Model Region	Fleet area
1	LL	1-LL-DWFN	ALL	1	a
2	LL	2-LL-PICT	ALL	1	a
3	LL	3-LL-DWFN	ALL	2	a
4	LL	4-LL-PICT	ALL	2	a
5	LL	5-LL-AZ	AU/NZ	2	a
6	LL	6-LL-DWFN	ALL	3	a
7	LL	7-LL-PICT	ALL	3	a
8	LL	8-LL-AZ	AU/NZ	3	a
9	LL	9-LL-DWFN	ALL	1	b
10	LL	10-LL-PICT	ALL	1	b
11	LL	11-LL-DWFN	ALL	2	b
12	LL	12-LL-PICT	ALL	2	b
13	LL	13-LL-DWFN	ALL	3	b
14	LL	14-LL-PICT	ALL	3	b
15	TR	15-3a-All-TR	ALL	3	a
16	DN	16-3a-All-DN	ALL	3	a
17	DN	17-3b-All-DN	ALL	3	b
18	LL	18-LL-EPO1	ALL	4	a
19	LL	19-LL-EPO2	ALL	4	b
20	LL	20-LL-EPO3	ALL	4	c
21	TR	21-TR-EPO	ALL	4	a,b,c
22	LL	1-L-INDEX	INDEX	1	-
23	LL	2-L-INDEX	INDEX	2	-
24	LL	3-L-INDEX	INDEX	3	-
25	LL	4-L-INDEX	INDEX	4a	a*

Table 2: Summary of data available for the 2021 South Pacific albacore assessment by fisheries defined in table 1.

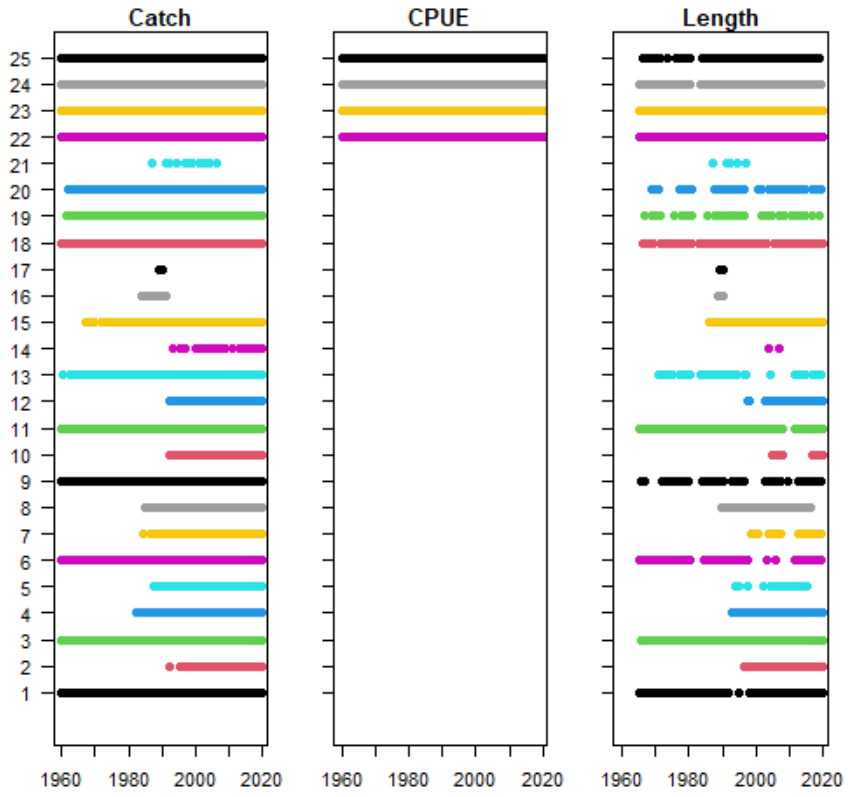

Table 3: Structural uncertainty grid for the 2021 South Pacific albacore tuna stock assessment.

Axis	**1**	**2**	**3**
Steepness (S)	0.65	**0.80**	0.95
Movement (M)	**M1-Estimated, age-dependent**	M2-SEAPODYM	
Size data weight (D)	Low (50)	**Medium (25)**	High (10)
Recruitment distribution (R)	**R1-SEAPODYM**	R2-Regions 3 and 4	
Growth/M (G/M)	**Fixed otolith, Nat-M1**	Estimated from length frequency, Nat-M2	

Table 4: Description of symbols used in the yield and stock status analyses. For the purpose of this assessment, "recent" for F is the average over the period 2015–2018 and for SB is the average over the period 2016–2019 and "latest" is 2019

Symbol	Description
C_{latest}	Catch in the last year of the assessment (2019)
F_{recent}	Average fishing mortality-at-age for a recent period (2015–2018)
$YF_{current}$	Equilibrium yield at average fishing mortality for a recent period (2015–2018)
fmult	Fishing mortality multiplier at maximum sustainable yield (MSY)
F_{MSY}	Fishing mortality-at-age producing the maximum sustainable yield (MSY)
MSY	Equilibrium yield at F_{MSY}
$F_{recent}/F_{\mathrm{MSY}}$	Average fishing mortality-at-age for a recent period (2015–2018) relative to F_{MSY}
SB_{latest}	Spawning biomass in the latest time period (2019)
SB_{recent}	Spawning biomass for a recent period (2016–2019)
$SB_{F=0}$	Average spawning biomass predicted in the absence of fishing for the period 2009–2018
SB_{MSY}	Spawning biomass that will produce the maximum sustainable yield (MSY)
$SB_{\mathrm{MSY}}/SB_{F=0}$	Spawning biomass that produces maximum sustainable yield (MSY) relative to the average spawning biomass predicted to occur in the absence of fishing for the period 2009–2018
$SB_{latest}/SB_{F=0}$	Spawning biomass in the latest time period (2019) relative to the average spawning biomass predicted to occur in the absence of fishing for the period 2009–2018
$SB_{latest}/SB_{\mathrm{MSY}}$	Spawning biomass in the latest time period (2019) relative to that which will produce the maximum sustainable yield (MSY)
$SB_{recent}/SB_{F=0}$	Spawning biomass for a recent period (2016–2019) relative to the average spawning biomass predicted to occur in the absence of fishing for the period 2009–2018
$SB_{recent}/SB_{\mathrm{MSY}}$	Spawning biomass for a recent period (2016–2019) relative to the spawning biomass that produces maximum sustainable yield (MSY)
$20\%SB_{F=0}$	WCPFC adopted limit reference point – 20% of spawning biomass in the absence of fishing average over years $t-10$ to $t-1$ (2009–2018)

Table 5: Summary of reference points over all 72 individual models in the structural uncertainty grid

	Mean	Median	Min	10%	90%	Max
C_{latest}	87298	86649	83519	84666	87681	130936
F_{MSY}	0.06	0.06	0.05	0.05	0.07	0.08
fmult	4.20	3.83	2.11	2.64	6.44	7.84
$F_{recent}/F_{\text{MSY}}$	0.27	0.26	0.13	0.16	0.38	0.47
MSY	106058	99920	68200	73520	144168	166240
SB_0	569943	522650	361800	384700	813820	929300
$SB_{F=0}$	644789	603672	524886	530202	800968	873278
SB_{latest}/SB_0	0.41	0.40	0.34	0.35	0.45	0.48
$SB_{latest}/SB_{F=0}$	0.35	0.36	0.25	0.27	0.44	0.46
$SB_{latest}/SB_{\text{MSY}}$	2.46	2.33	1.44	1.62	3.79	4.28
SB_{MSY}	100726	95945	48040	51360.00	156390	190000
SB_{MSY}/SB_0	0.18	0.18	0.11	0.12	0.22	0.23
$SB_{MSY}/SB_{F=0}$	0.15	0.15	0.09	0.10	0.22	0.23
$SB_{recent}/SB_{F=0}$	0.48	0.47	0.37	0.40	0.56	0.59
$SB_{recent}/SB_{\text{MSY}}$	3.34	3.22	2.07	2.25	4.84	5.33
$Y\ F_{recent}$	77817	76840	58440	61924	93788	101400

Table 6: Summary of reference points over all 72 individual models in the structural uncertainty grid for combined regions 1,2 and 3 - WCPFC-CA

	Mean	Median	Min	10%	90%	Max
C_{latest}	78946	78434	75673	76740	79163	118706
$SB_{F=0}$	457559	452323	415746	432039	483703	501602
$SB_{latest}/SB_{F=0}$	0.35	0.36	0.26	0.28	0.43	0.44
$SB_{recent}/SB_{F=0}$	0.49	0.47	0.39	0.42	0.58	0.61

Table 7: Summary of reference points over all 72 individual models in the structural uncertainty grid for combined region 4 - EPO (IATTC-CA)

	Mean	Median	Min	10%	90%	Max
C_{latest}	8351	8166	7845	7903	8773	12229
$SB_{F=0}$	187230	157583	92190	95879	336838	379718
$SB_{latest}/SB_{F=0}$	0.35	0.36	0.22	0.24	0.46	0.48
$SB_{recent}/SB_{F=0}$	0.43	0.43	0.28	0.31	0.56	0.57

12 Figures

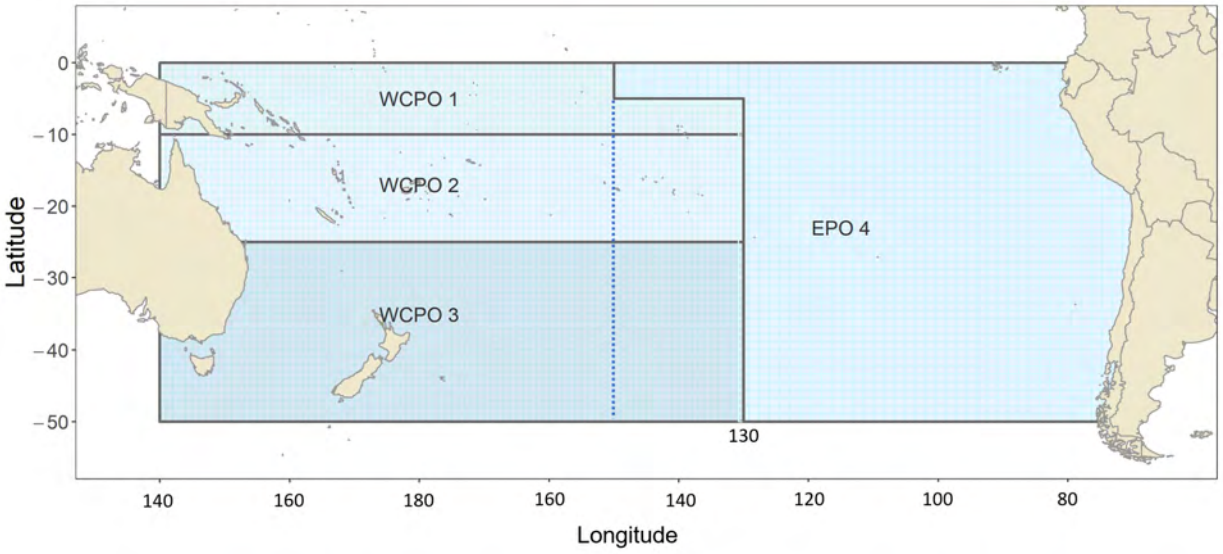

Figure 1: The geographical area covered by the stock assessment and the boundaries of the four model regions used for South Pacific-wide 2021 albacore assessment. The overlap region is the area between 130°- 150° west demarcated by the dashed line.

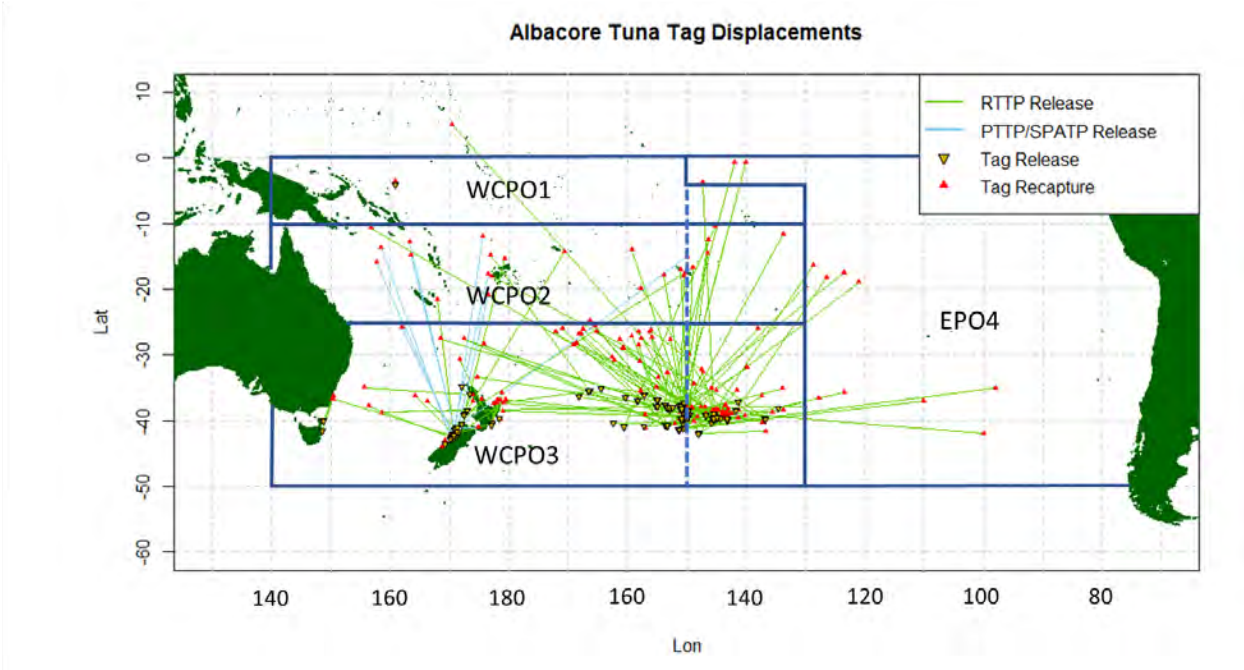

Summary

	RTTP-era											PTTP-era		
Year	1979	1980	1982	1986	1987	1988	1989	1990	1991	1992	→	2009	2010	2011
Released	19	1	4	861	1561	1274	1806	989	3701	5384		2766	111	5
Recaptured	0	0	0	3	11	3	6	7	56	83		32	1	1
Return rate				0.003	0.007	0.002	0.003	0.007	0.015	0.015		0.012	0.009	0.200

Figure 2: Map of tag displacements for South Pacific albacore tagged under the different tagging programs (top), and (bottom) table of tag-releases and recaptures for the various tagging programs 1979 to 1992.

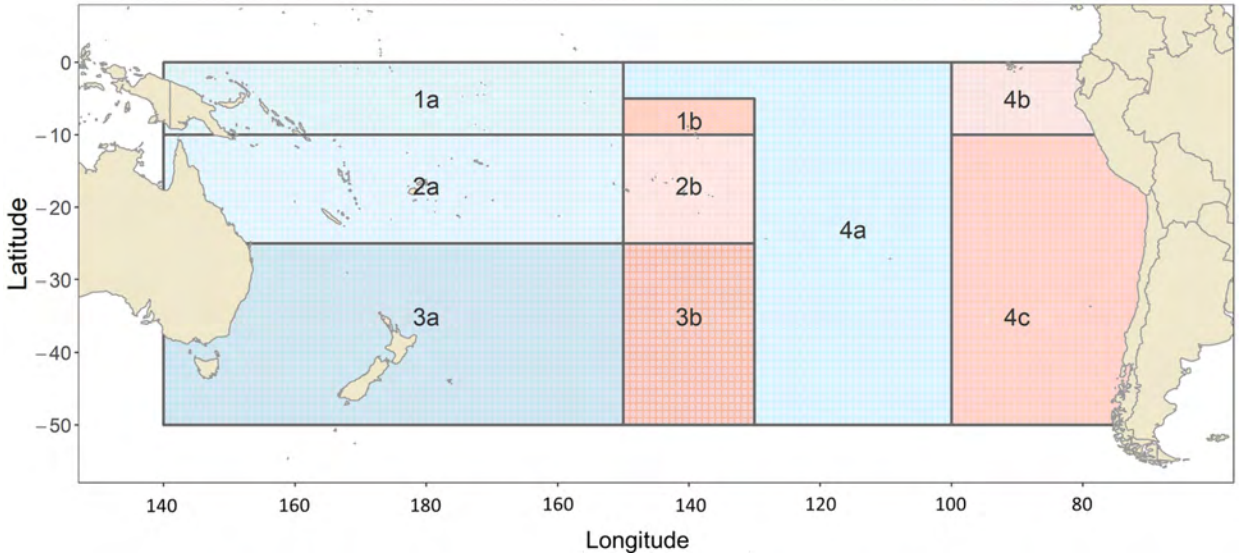

Figure 3: Map of model regions with addition of the fishery strata applied for the EPO and overlap regions. The overlap region is the area between 130°- 150° west.

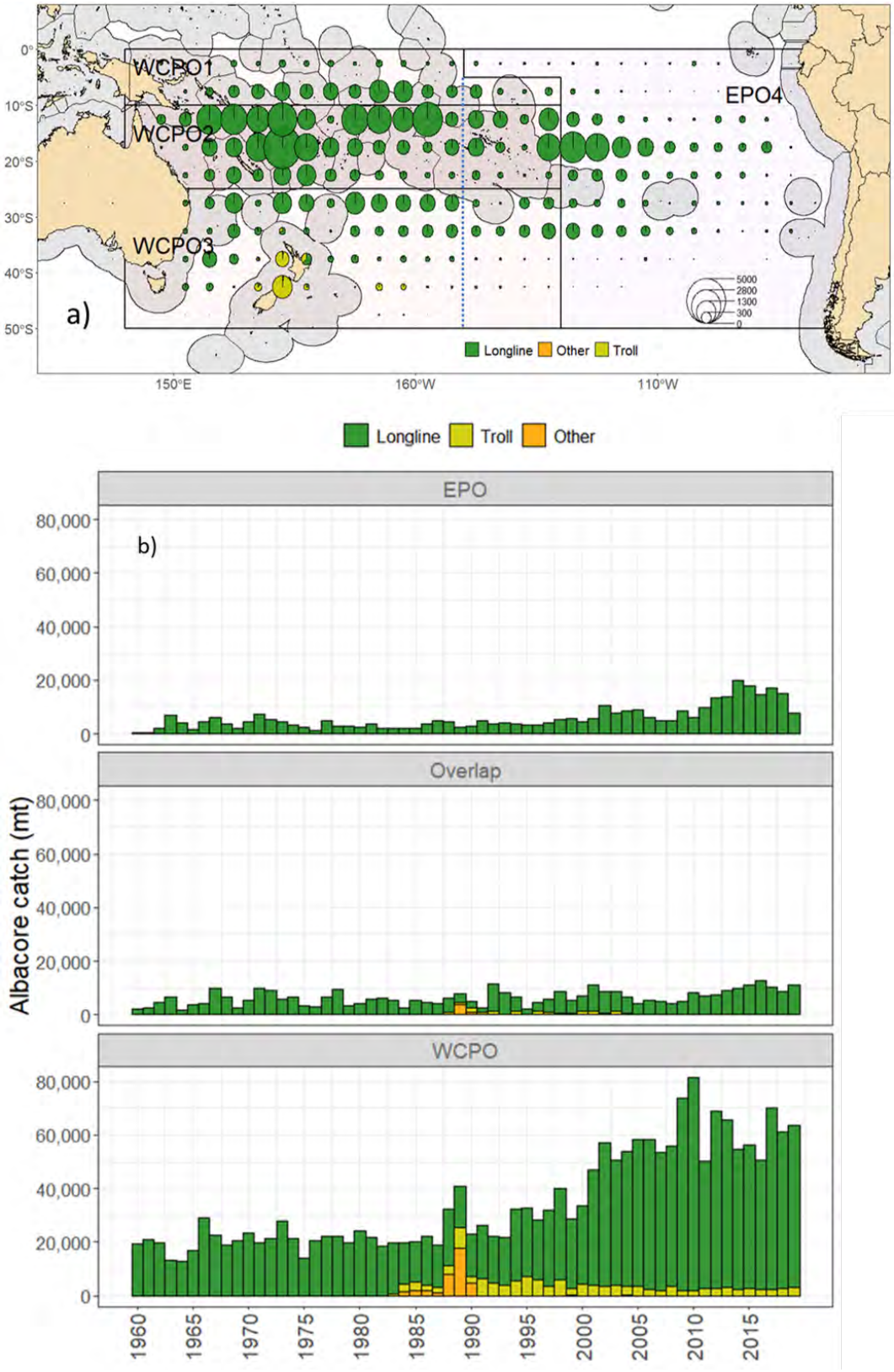

Figure 4: a) Spatial pattern of albacore catch by gear type over the last decade, and b) historical catches of albacore across the model region from 1952-2019 by gear type.

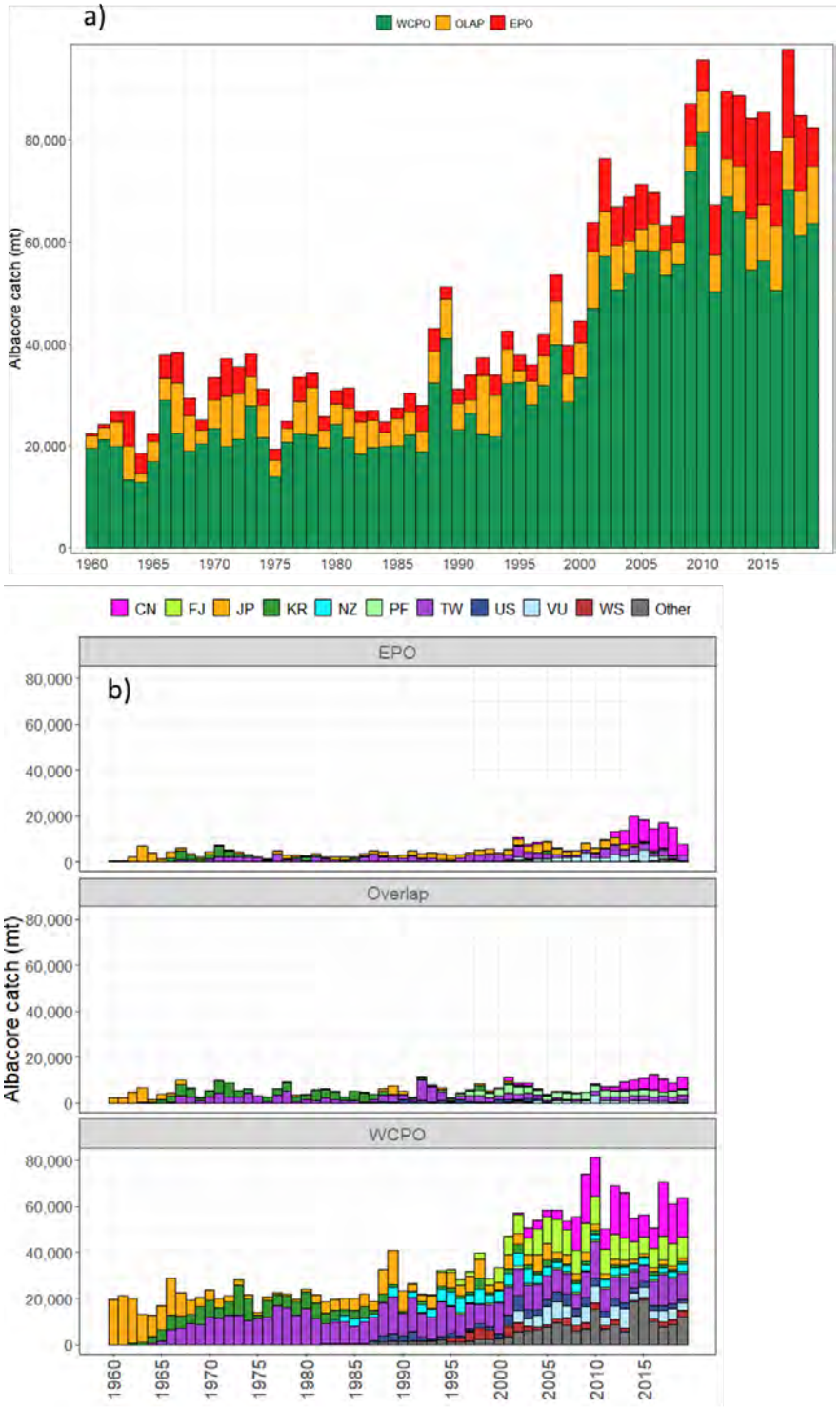

Figure 5: a) Annual catches of albacore from 1952-2019 separated by the WCPO, IATTC (EPO) and the convention area 'overlap'(OLAP) region, b) annual catches of albacore from 1952-2019 separated by flag for the WCPO, the overlap, and the IATTC regions.

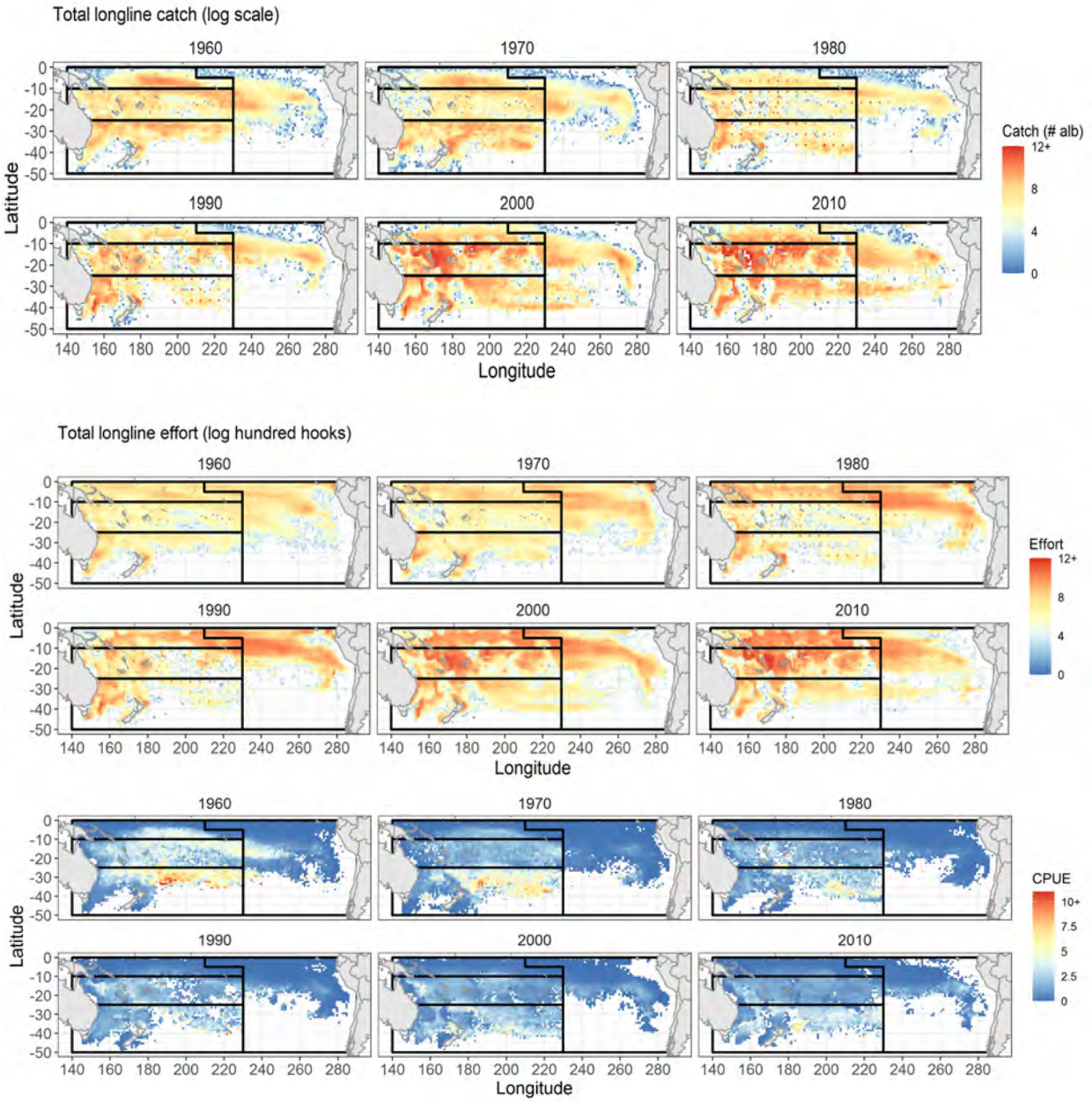

Figure 6: (top) Spatial distribution of albacore catches, (middle) longline effort and (bottom) longline nominal albacore CPUE in the South Pacific by decade. Model regions indicated by black lines.

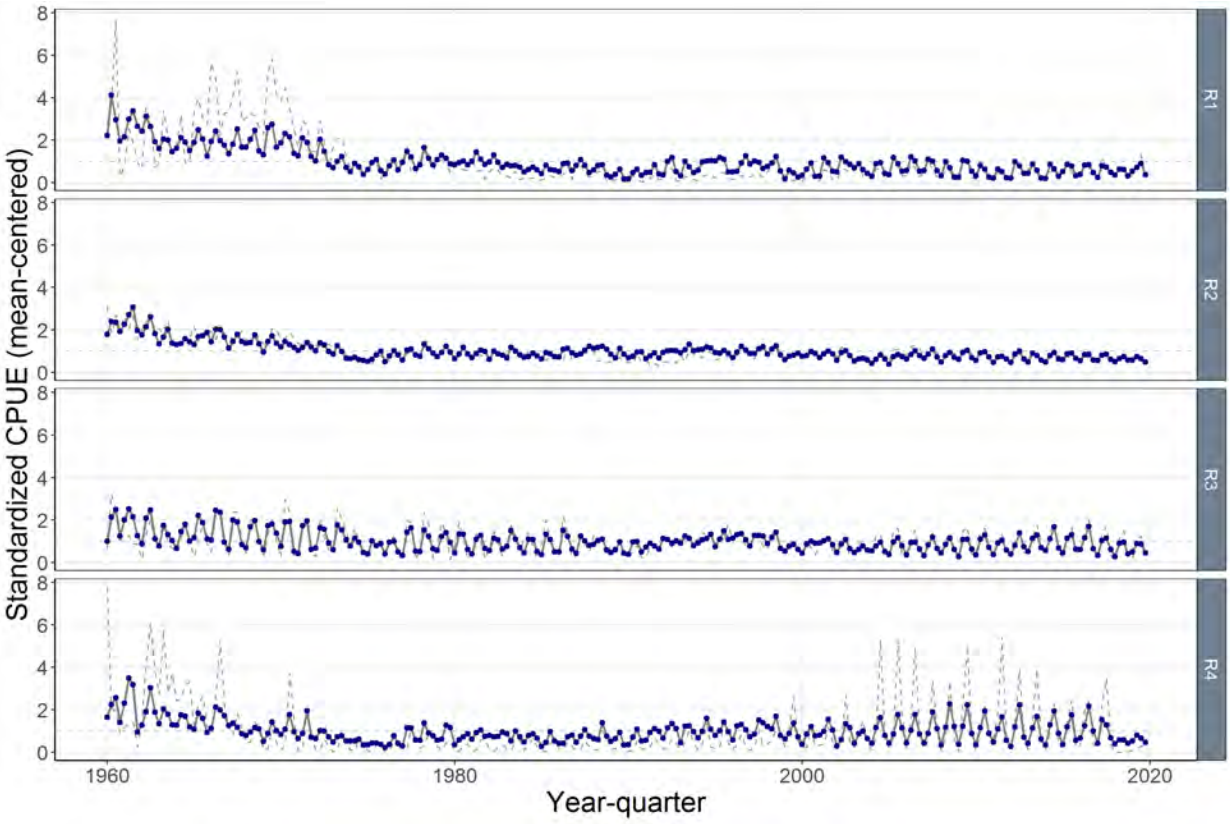

Figure 7: Standardized relative abundance indices, by region (gray with blue points) plotted alongside the nominal CPUE (gray dashed line), from 1960-2019.

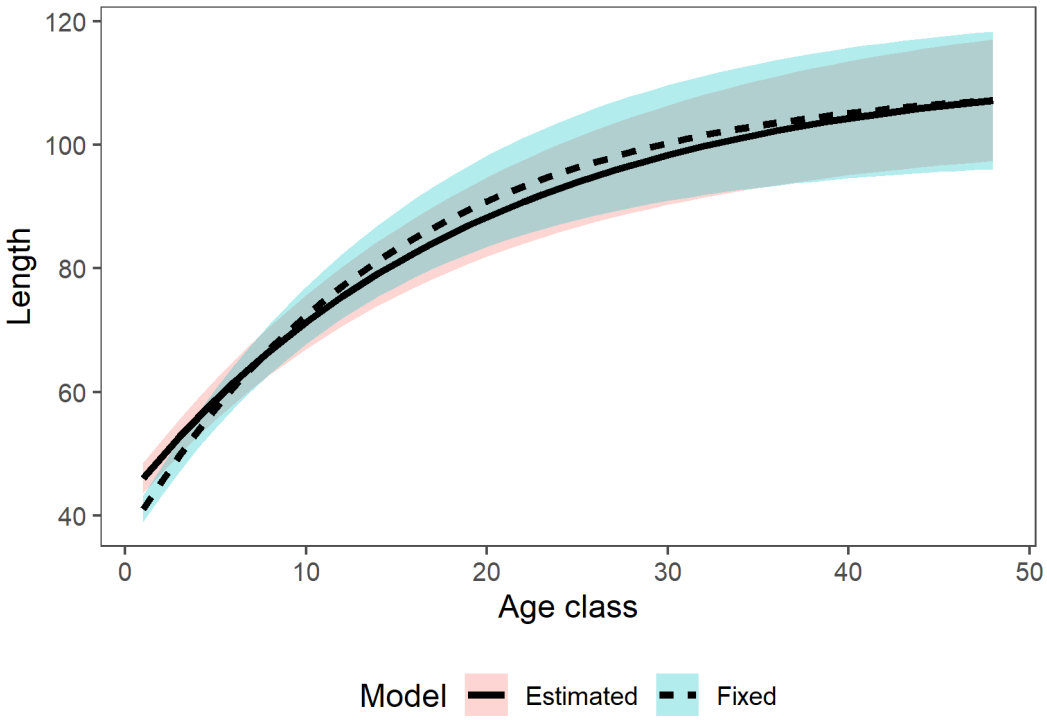

Figure 8: Comparison of VB Growth curves based on ages from otoliths (fixed) and length-frequency analysis (estimated).

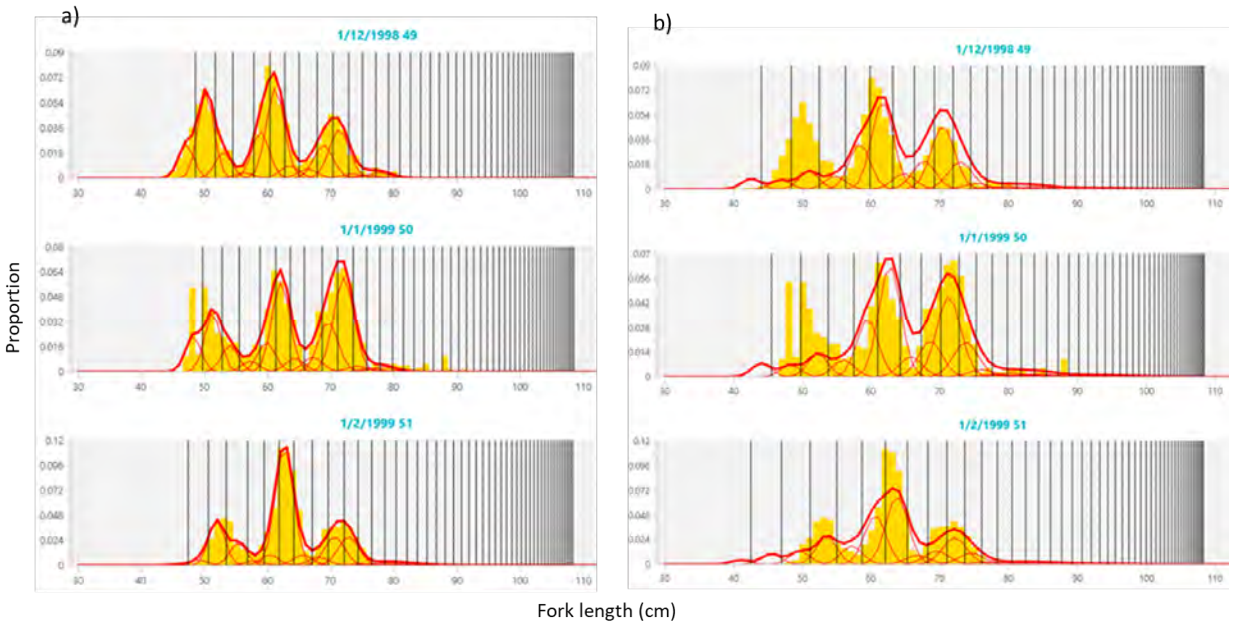

Figure 9: Model fits to a segment of the New Zealand troll fishery length-frequency data based on, a) growth estimated from length-frequency data, and b) growth from otolith ageing. The mean length of the 48 quarterly age classes are shown by the vertical lines, four quarterly age classes are expected between modes in the length frequency data.

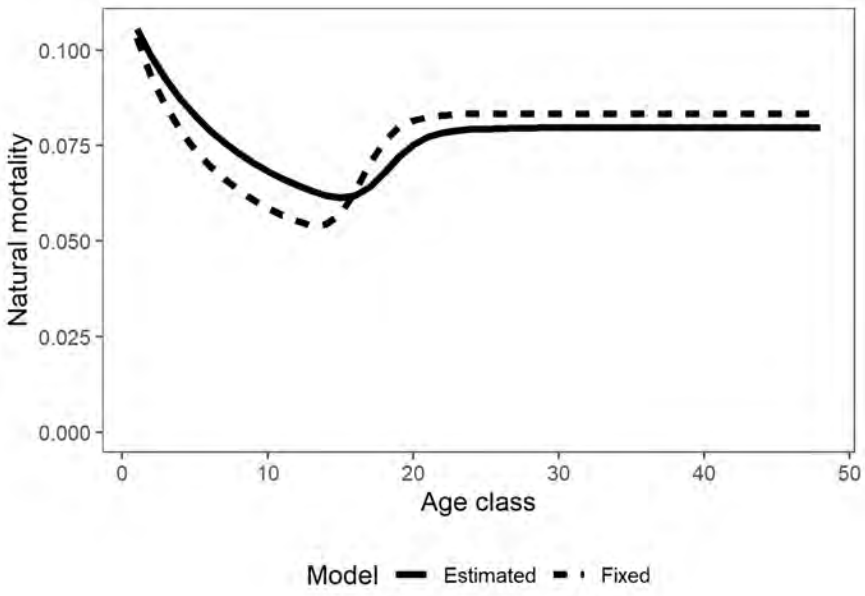

Figure 10: Natural mortality-at-age (quarterly) functions associated with each of the two growth hypotheses considered in the assessment.

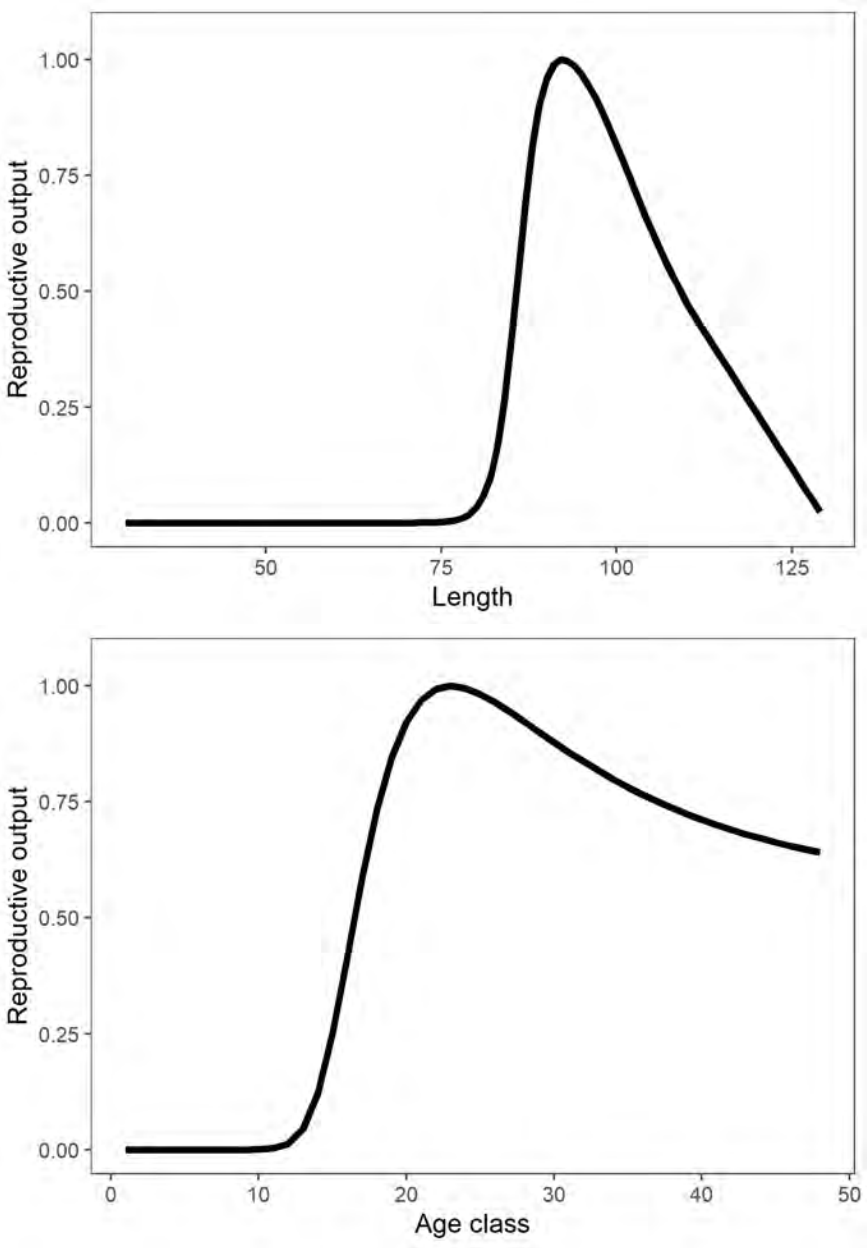

Figure 11: Reproductive potential ogives for South Pacific albacore by length (top) and converted to age (quarters) (bottom).

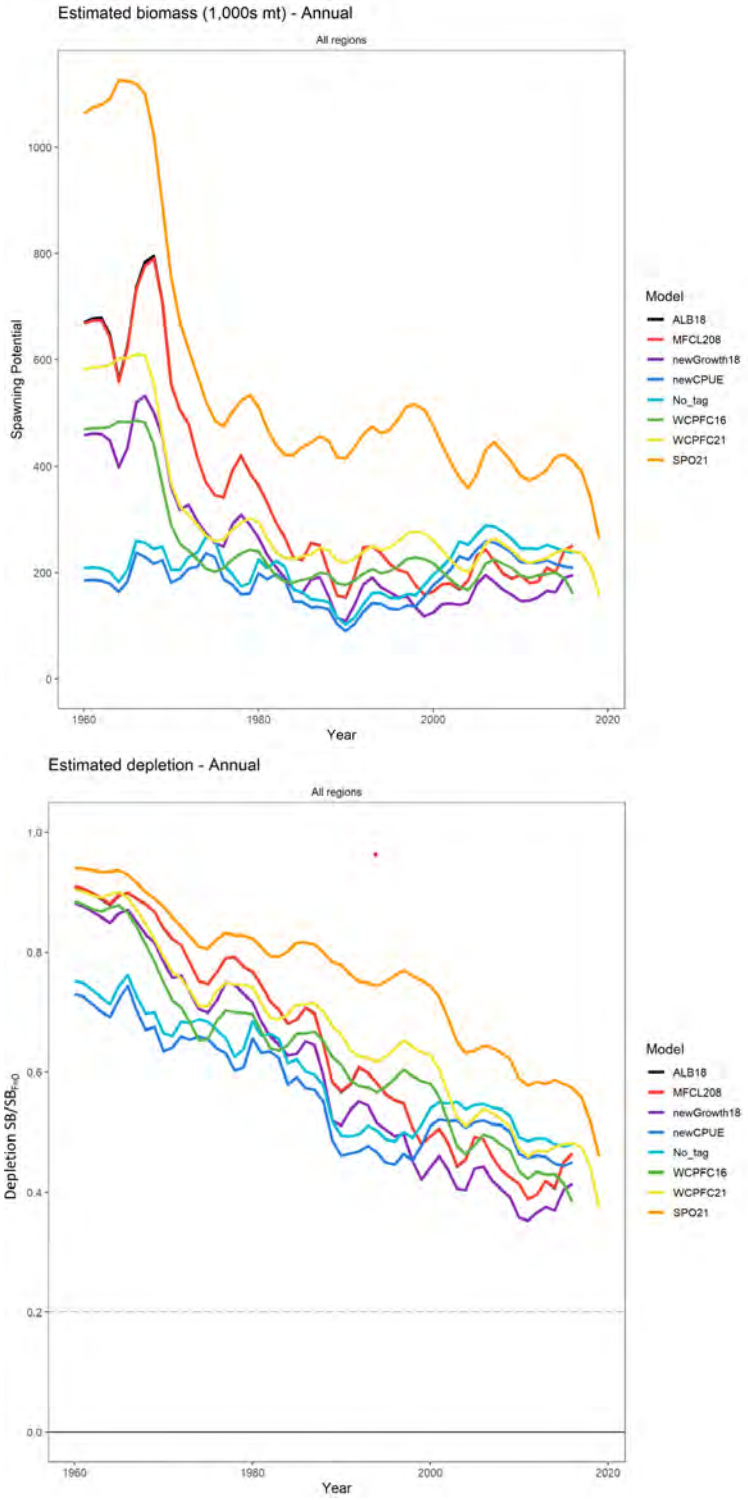

Figure 12: (top) Stepwise change in spawning potential from the 2018 reference model to the 2021 diagnostic case model, and (bottom), stepwise change in depletion from the 2018 reference model to the 2021 diagnostic case model.

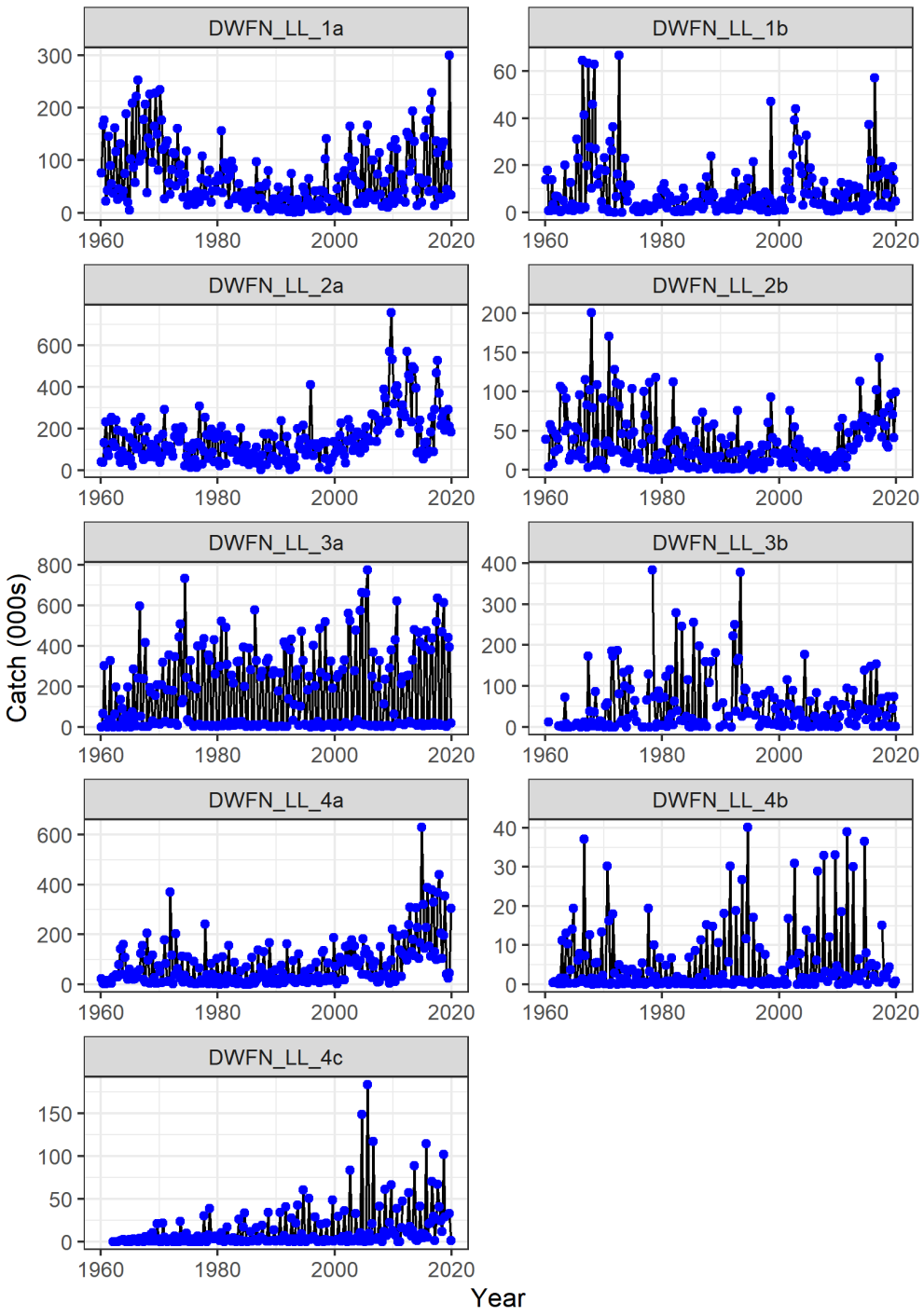

Figure 13: Model fits to longline catches for the Distant Water Fishing Nations (DWFNs) where the blue dots are the observed catches and the black lines are model predictions.

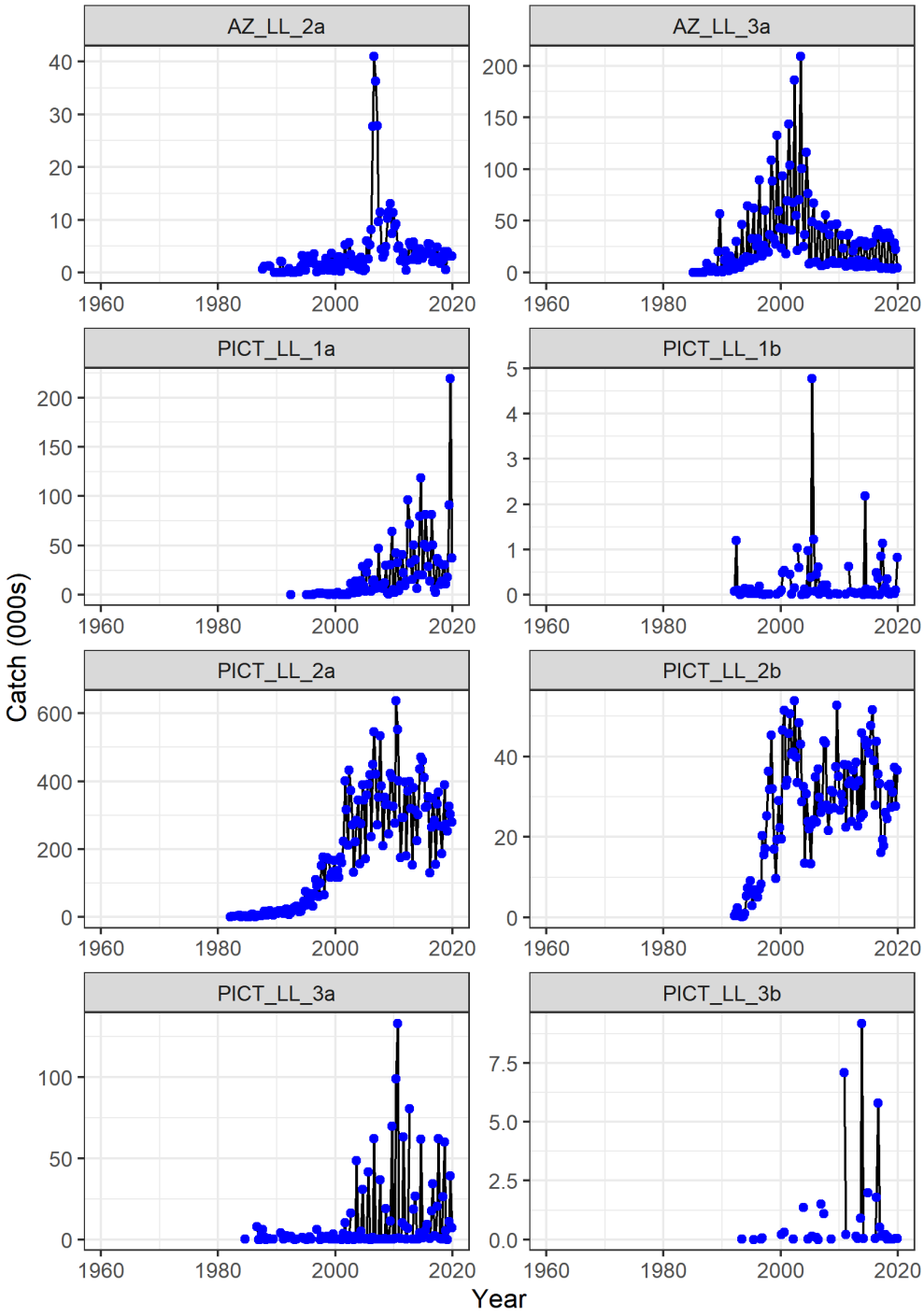

Figure 14: Model fits to longline catches for the PICT (Pacific Island Countries and Territories) and Australian and New Zealand (AZ) longline fisheries where the blue dots are the observed catches and the black lines are model predictions.

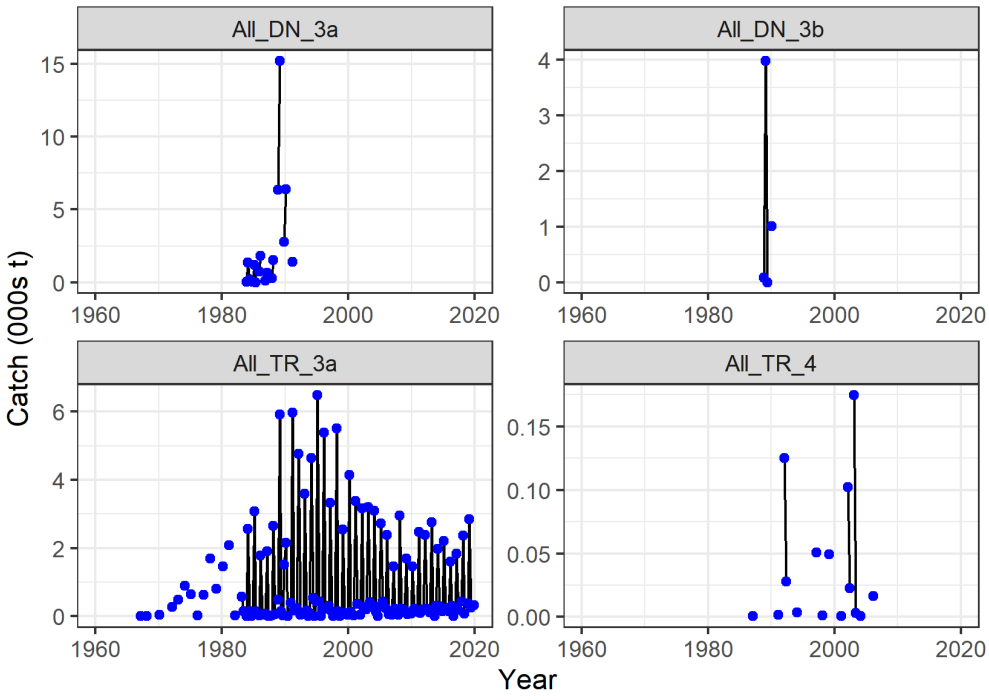

Figure 15: Model fits to the troll and driftnet fishery catches where the blue dots are the observed catches and the black lines are model predictions.

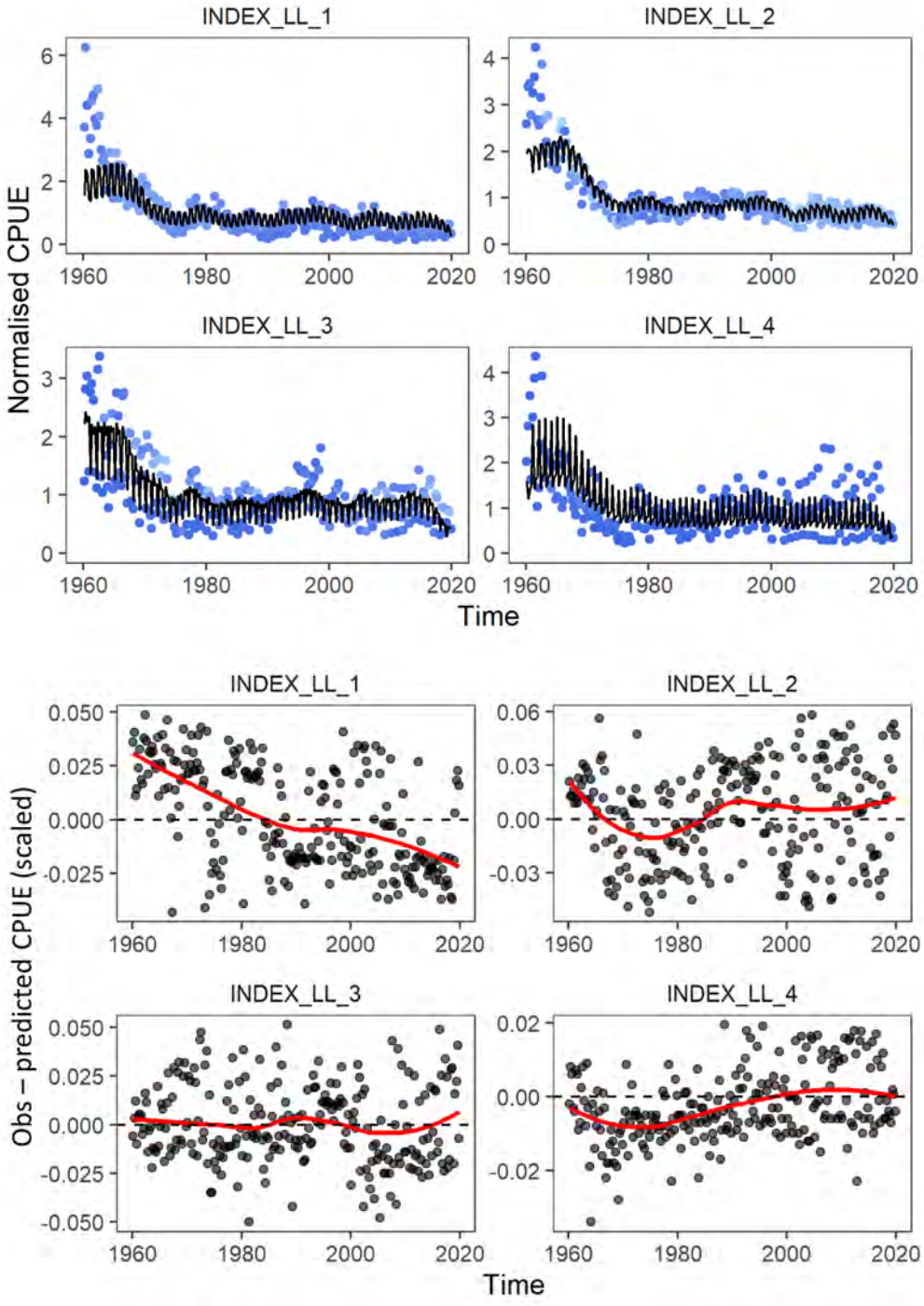

Figure 16: (top) Model fits (black line) to observed standardised CPUE (blue dots) for the four index fisheries, and (bottom) scaled residuals of model fits to observed CPUE indices. The red line represents a lowess smoothed fit to the scaled residuals.

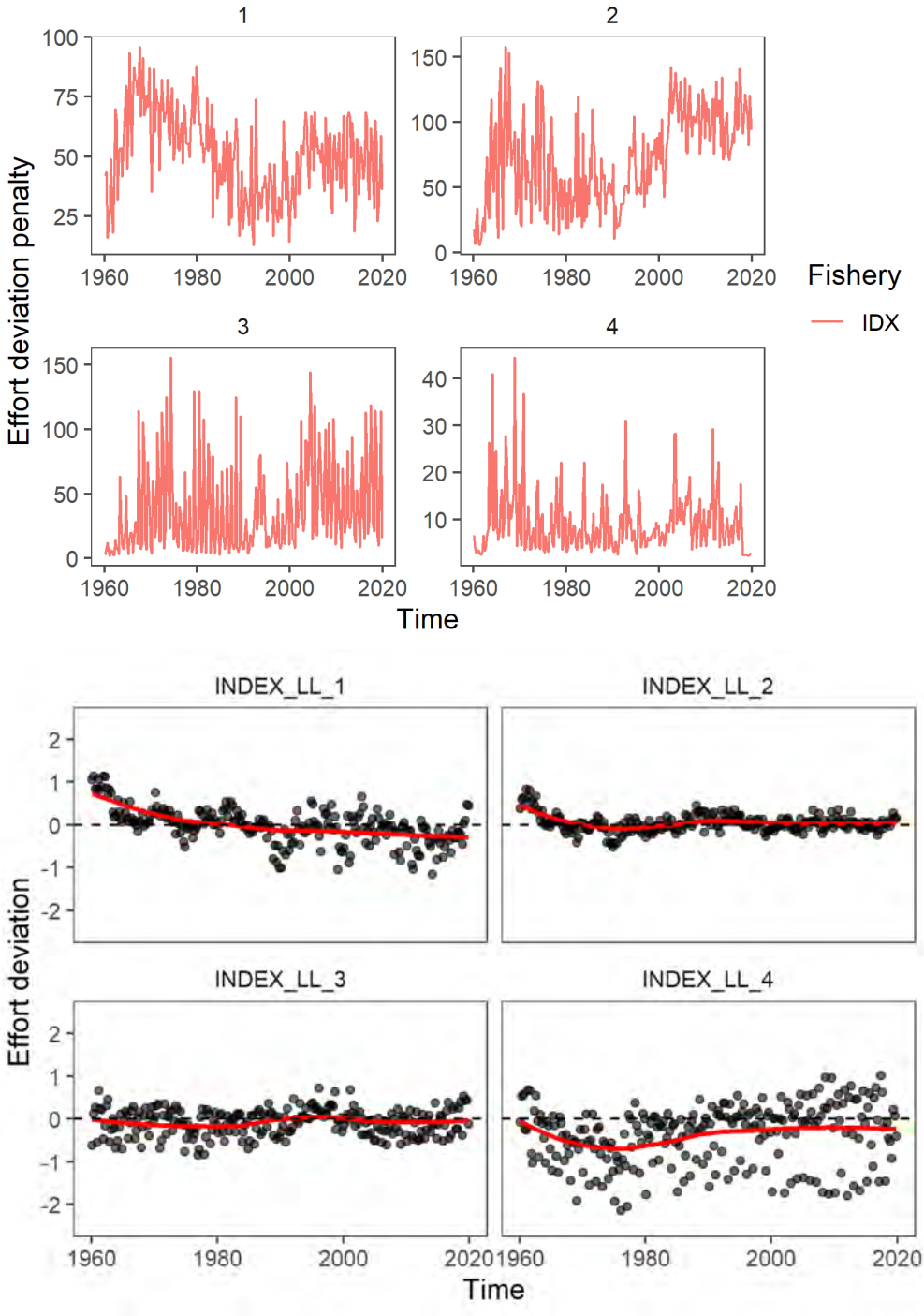

Figure 17: (top) Plot of the effort deviation penalties applied to each index fishery. A higher penalty gives more weight to the CPUE, and (bottom) effort deviations by time period for each of the index fisheries receiving standardised CPUE in the diagnostic case model. The red line represents a lowess smoothed fit to the effort deviations.

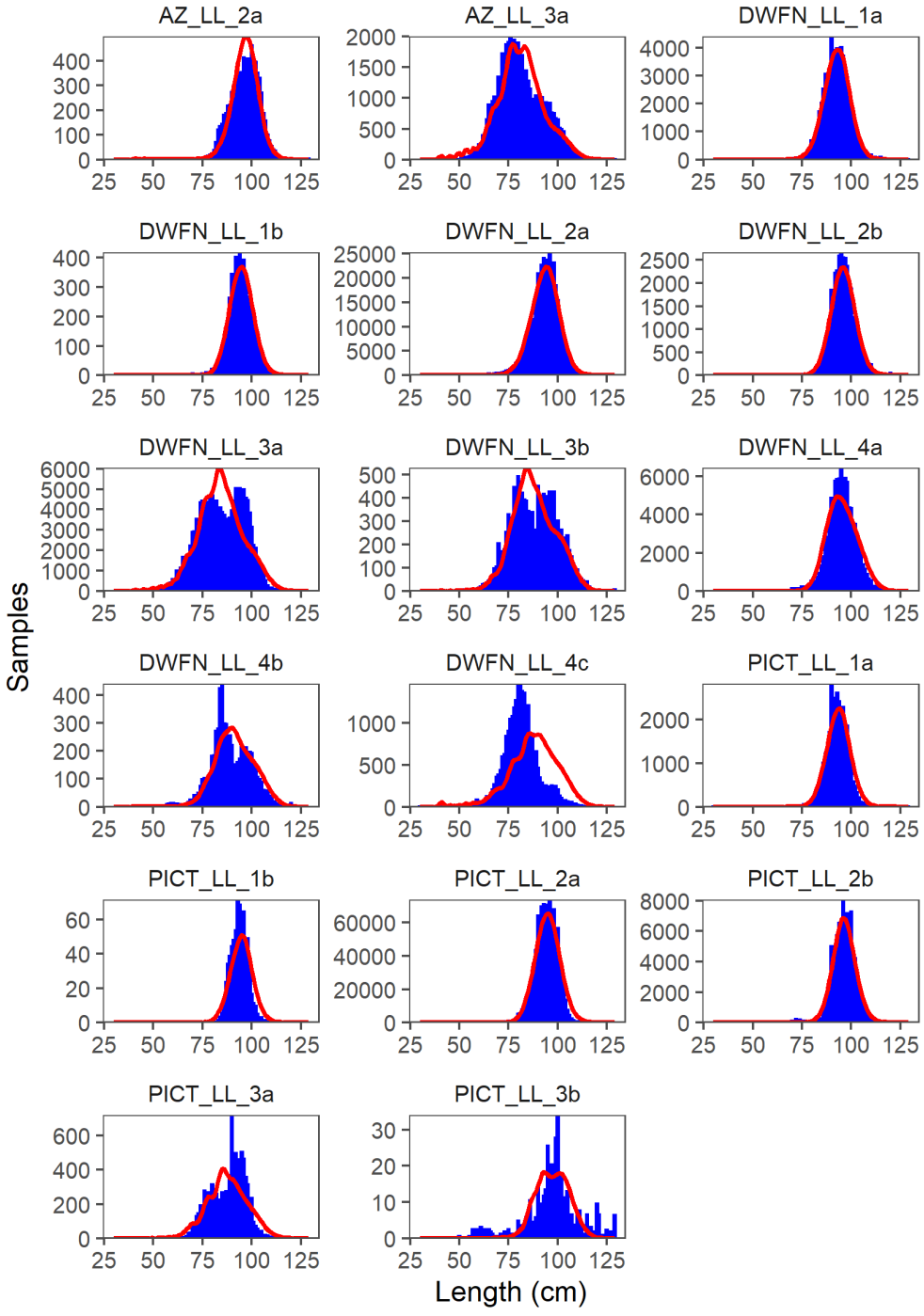

Figure 18: Composite (all time periods combined) observed (blue histograms) and predicted (red lines) catch-at-length for all longline fisheries with samples for the diagnostic case model.

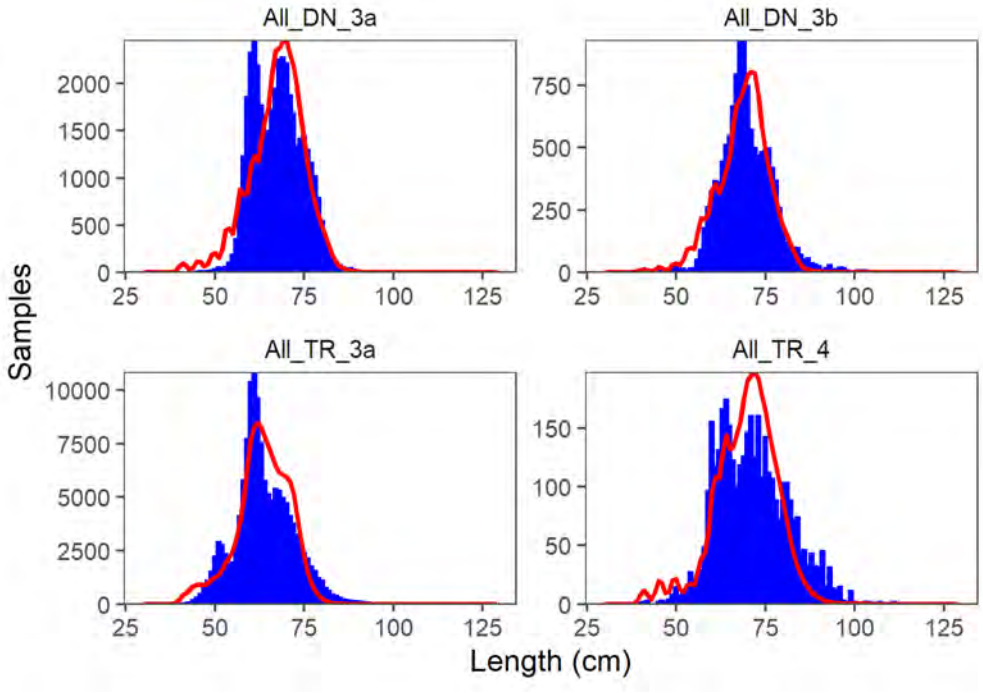

Figure 19: Composite (all time periods combined) observed (blue histograms) and predicted (red lines) catch-at-length for troll and driftnet fisheries with samples for the diagnostic case model.

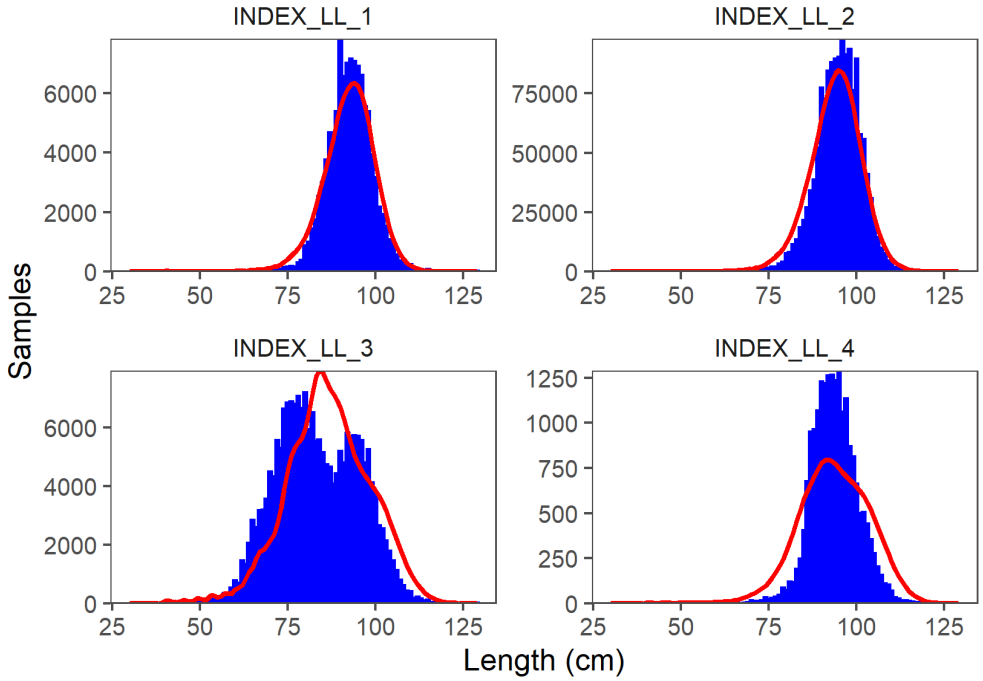

Figure 20: Composite (all time periods combined) observed (blue histograms) and predicted (red lines) catch-at-length for longline index fisheries for the diagnostic case model.

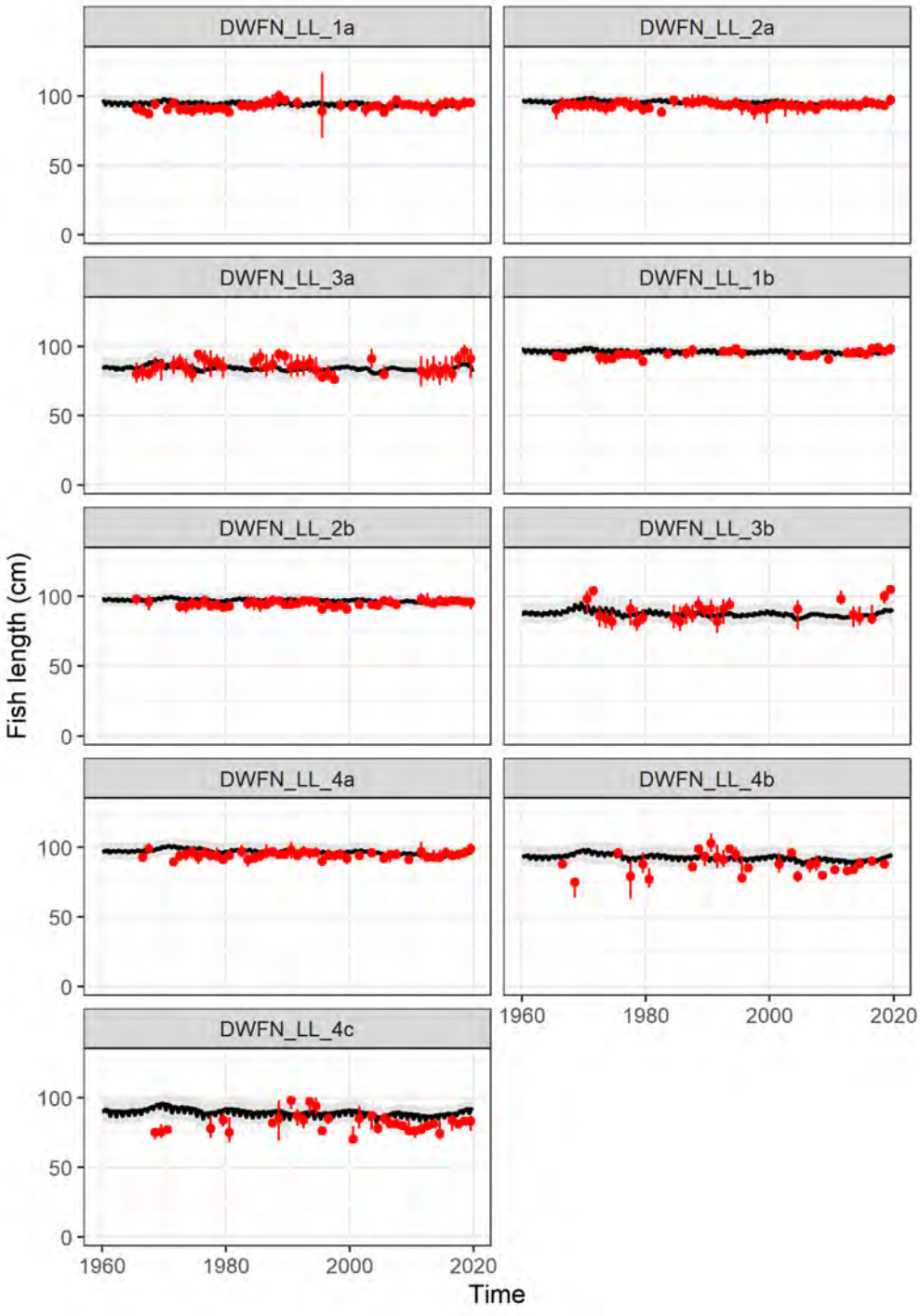

Figure 21: Comparison of the observed (red points) and predicted (grey line) median fish length for DWFN longline fisheries in the diagnostic case model. The uncertainty intervals (gray shading) represent the values encompassed by the 25% and 75% quantiles. Sampling data are aggregated by year and only length samples with a minimum of 30 fish per year are plotted.

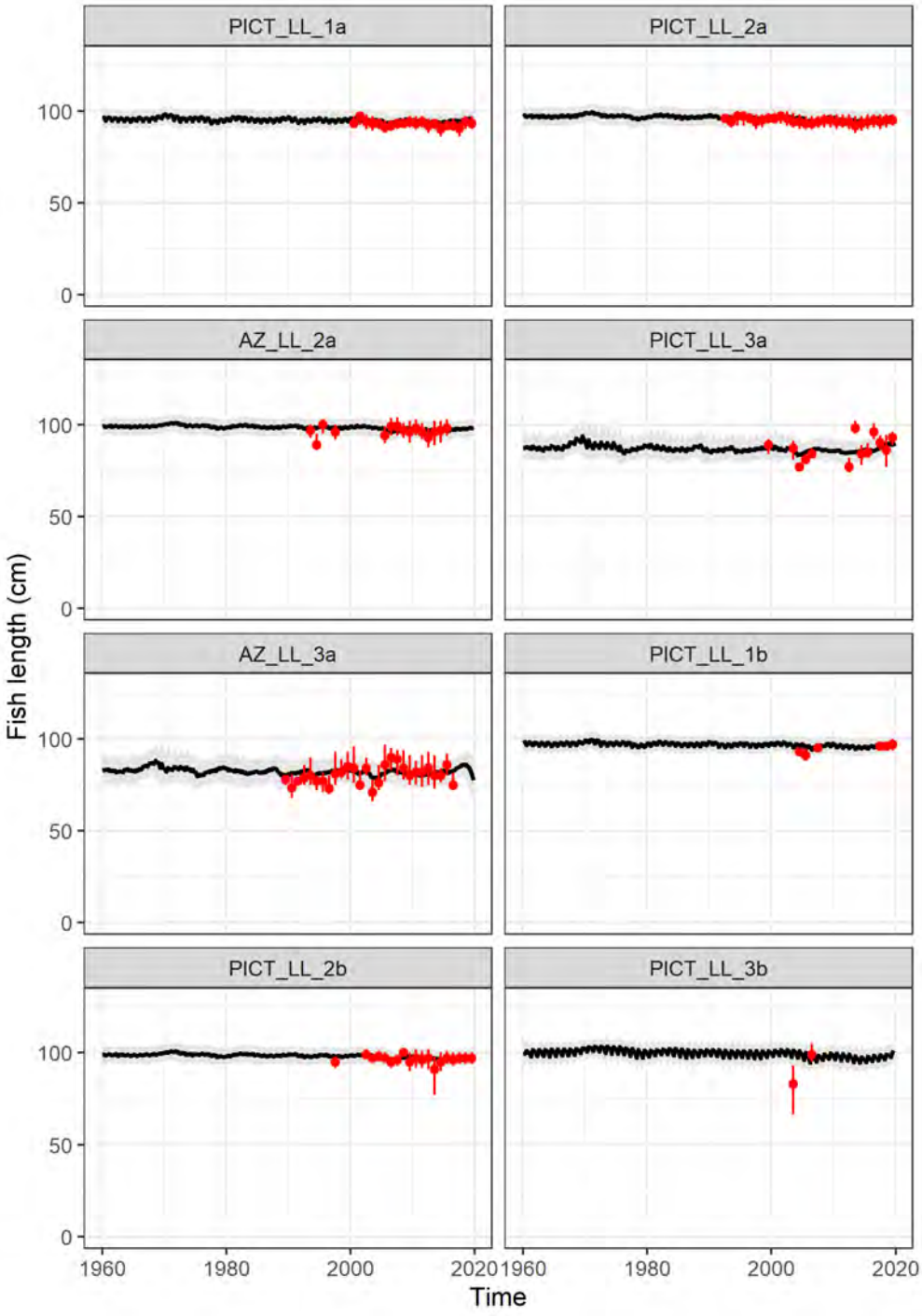

Figure 22: Comparison of the observed (red points) and predicted (grey line) median fish length for PICT and Australia/New Zealand (AZ) longline fisheries in the diagnostic case model. The uncertainty intervals (gray shading) represent the values encompassed by the 25% and 75% quantiles. Sampling data are aggregated by year and only length samples with a minimum of 30 fish per year are plotted.

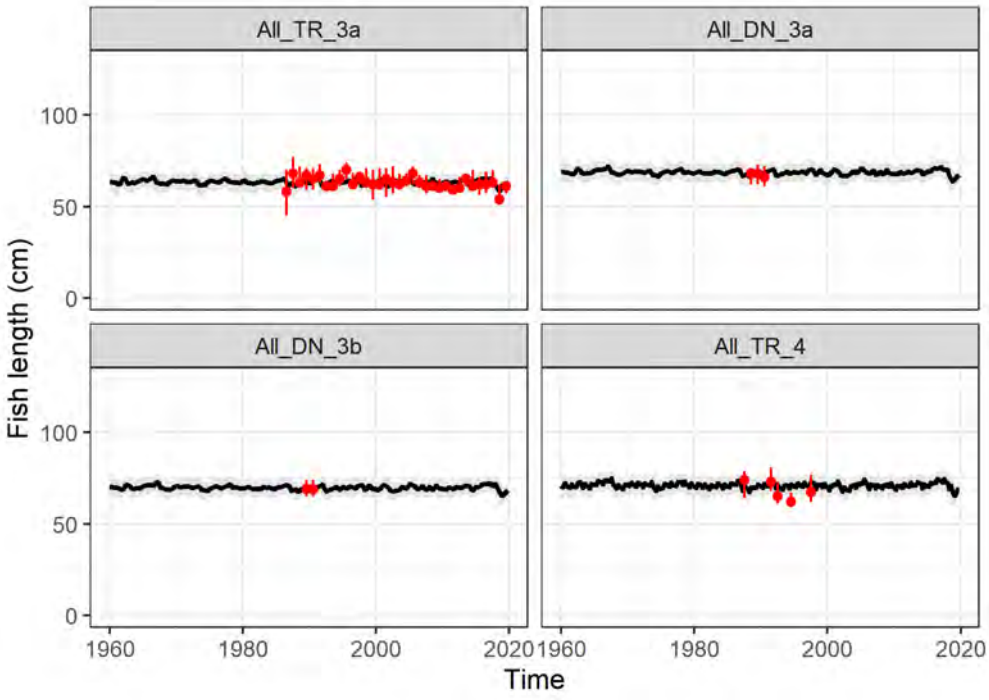

Figure 23: Comparison of the observed (red points) and predicted (grey line) median fish length for troll and drifnet fisheries in the diagnostic case model. The uncertainty intervals (gray shading) represent the values encompassed by the 25% and 75% quantiles. Sampling data are aggregated by year and only length samples with a minimum of 30 fish per year are plotted.

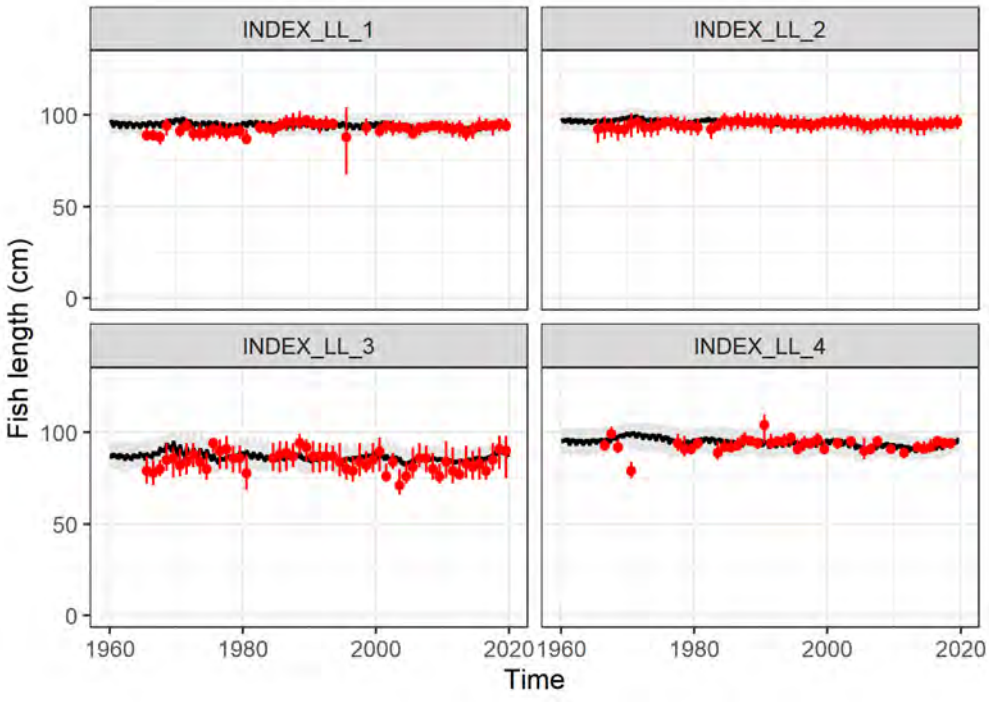

Figure 24: Comparison of the observed (red points) and predicted (grey line) median fish length for index fisheries in the diagnostic case model. The uncertainty intervals (grey shading) represent the values encompassed by the 25% and 75% quantiles. Sampling data are aggregated by year and only length samples with a minimum of 30 fish per year are plotted.

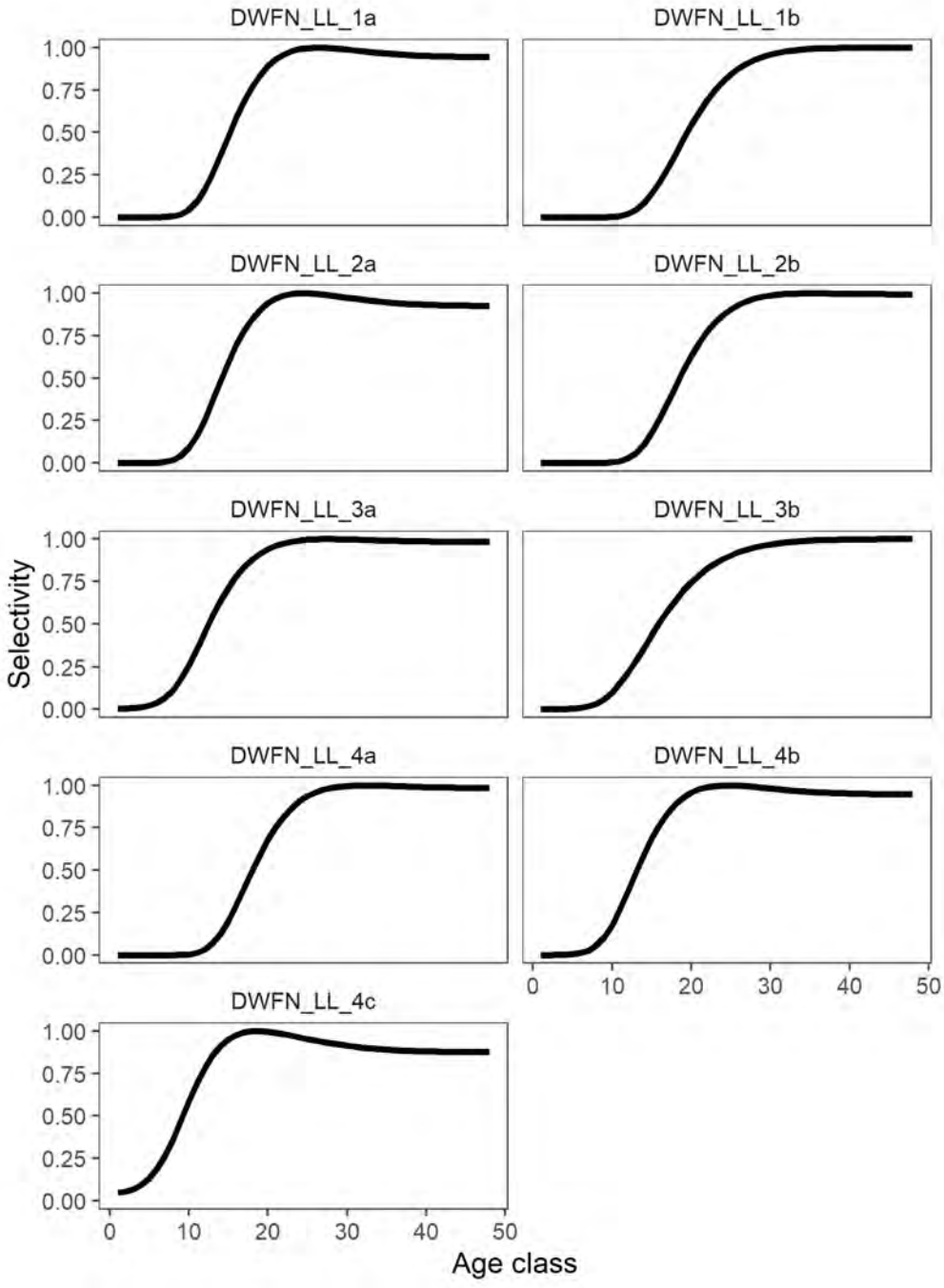

Figure 25: Estimated age-specific selectivity coefficients by DWFN longline fishery for the diagnostic case model.

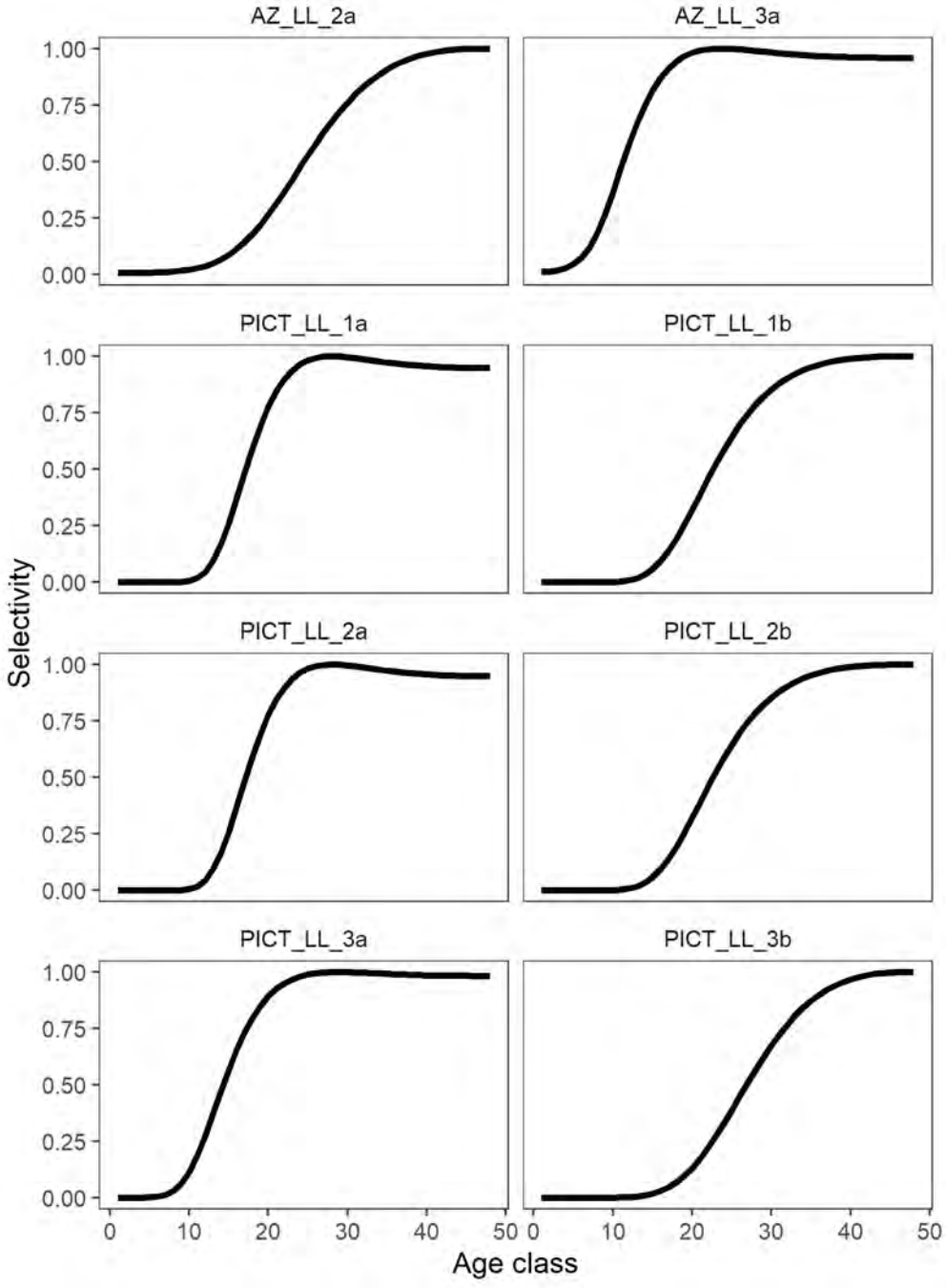

Figure 26: Estimated age-specific selectivity coefficients by fishery for PICT, Australian and New Zealand (AZ) longline fisheries for the diagnostic case model.

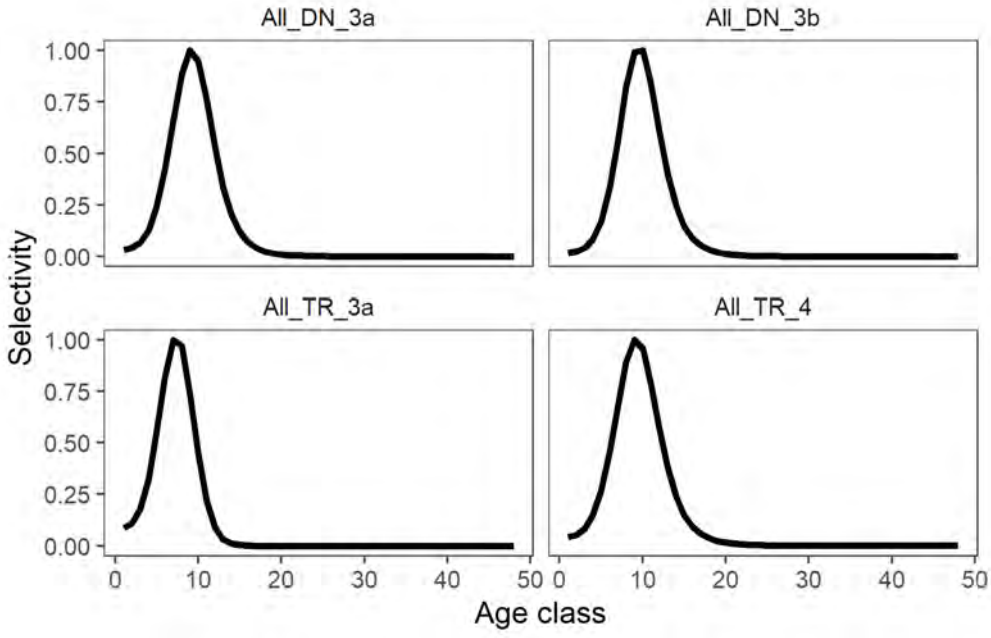

Figure 27: Estimated age-specific selectivity coefficients by fishery for troll and driftnet fisheries for the diagnostic case model.

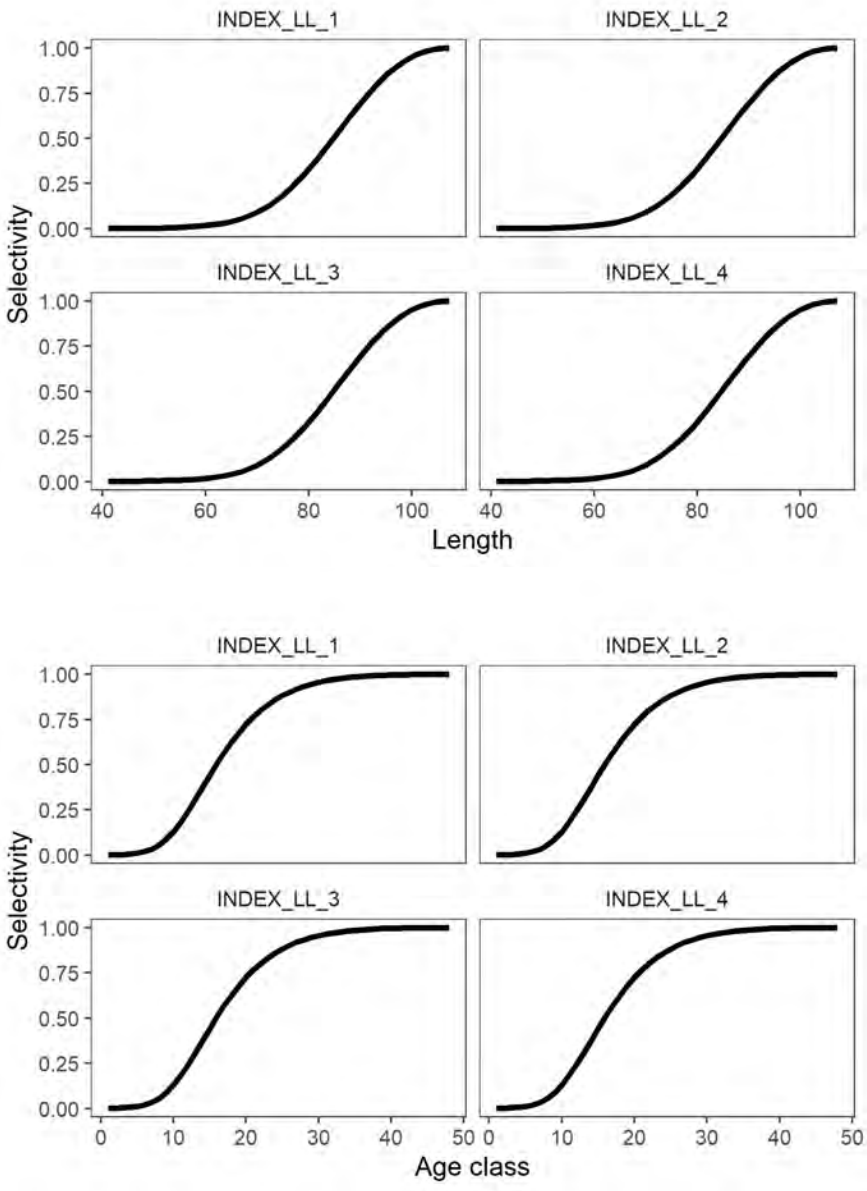

Figure 28: Estimated (top) length-specific and (bottom) age-specific selectivity coefficients by fishery for the index fisheries for the diagnostic case model.

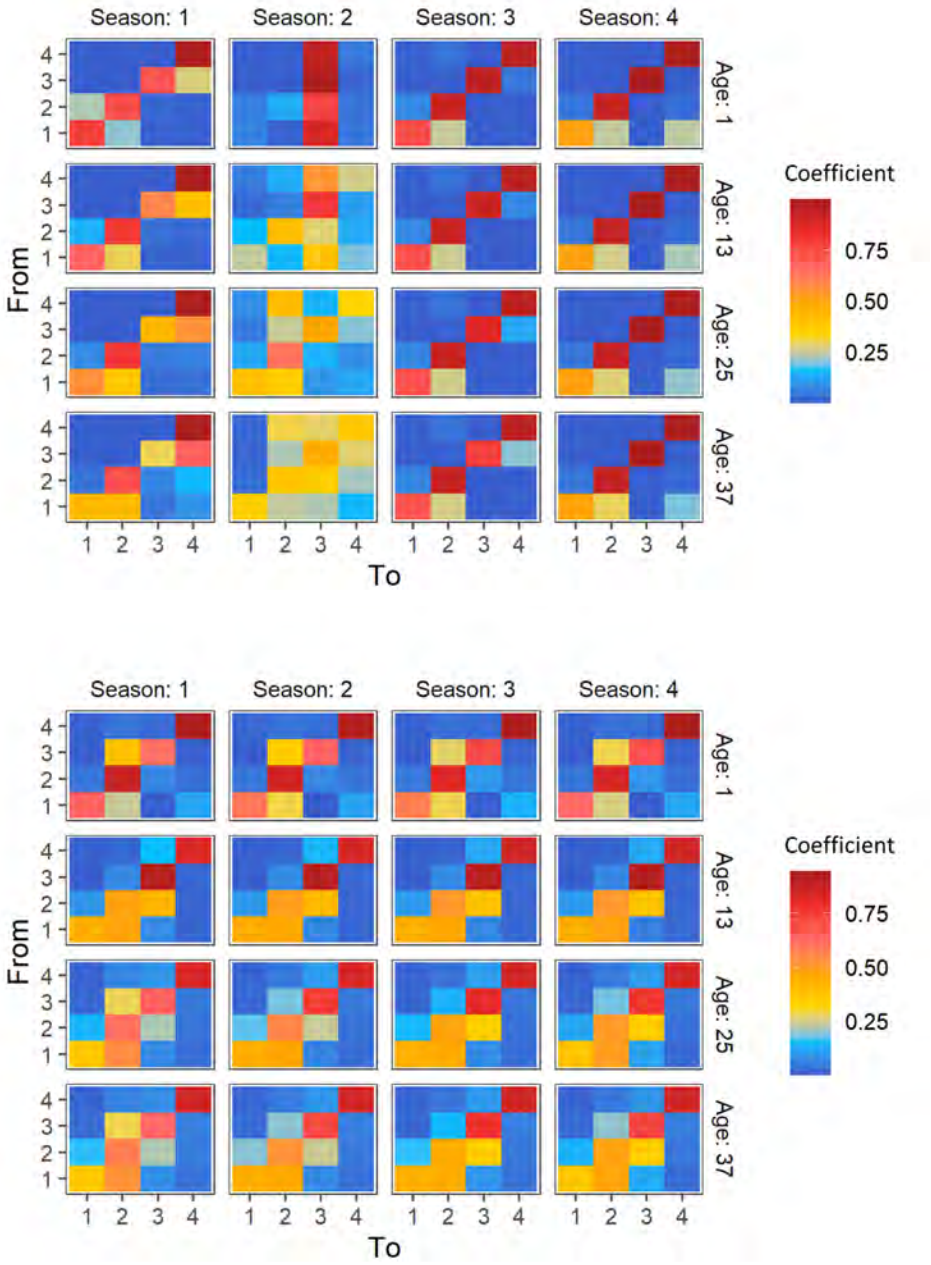

Figure 29: (top) Estimated movement coefficients (probabilities) by quarter (season) for the diagnostic case model. The colour of the tile shows the magnitude of the movement rate (probability of individuals of that age group from region x moving to region y in that quarter), with each row adding up to 1. (bottom) Equivalent plot for the fixed SEAPODYM movement coefficients.

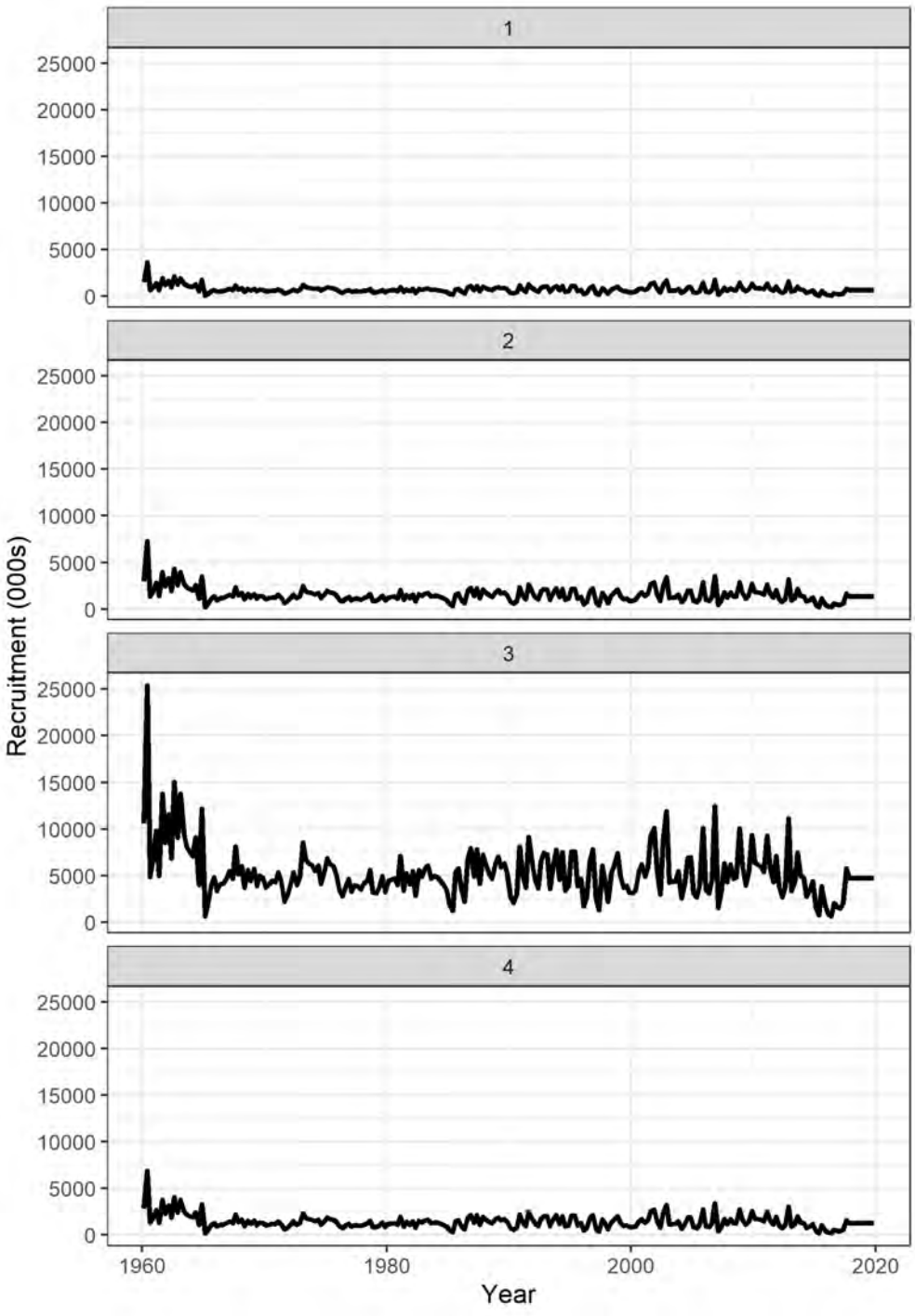

Figure 30: Estimated annual, temporal recruitment by model region for the diagnostic case model.

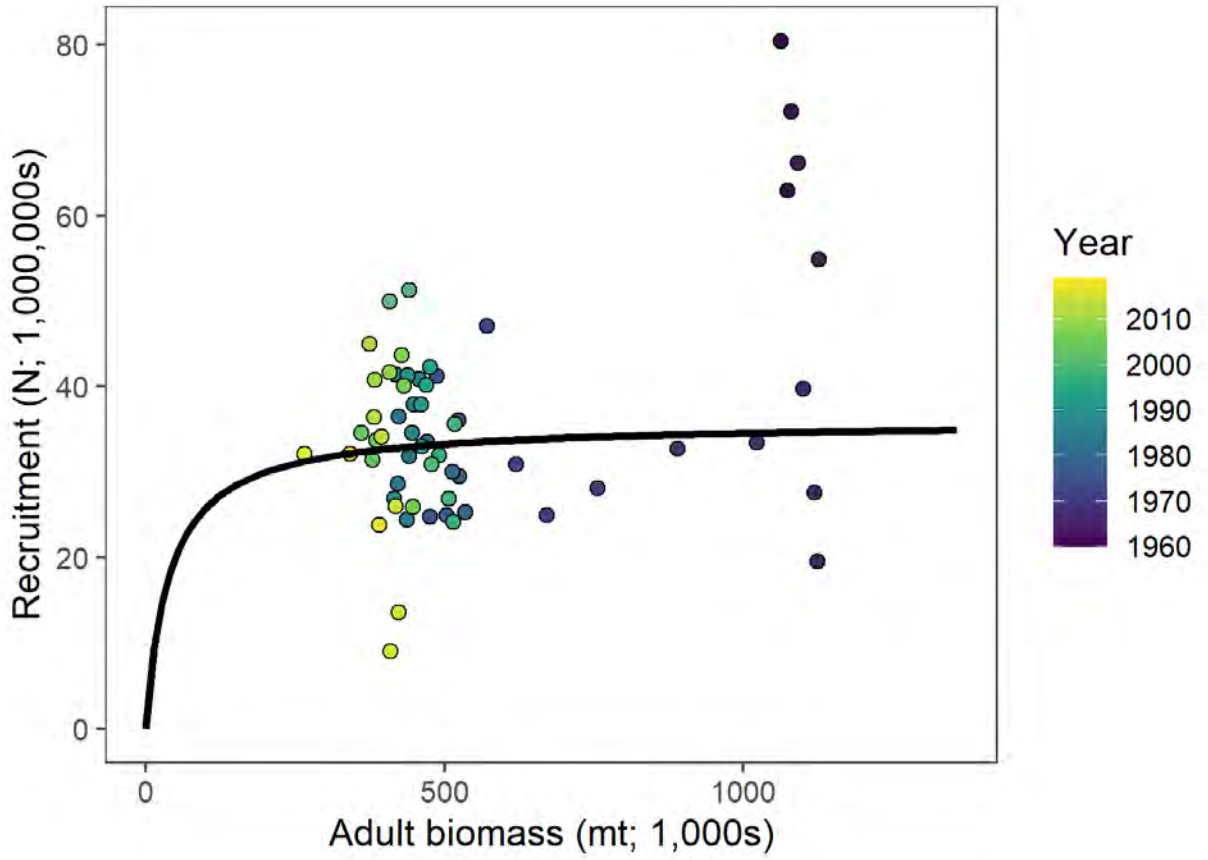

Figure 31: Estimated relationship between recruitment and spawning potential based on annual values for the diagnostic case model. The shade of the circles changes from light (recent) to dark back through time.

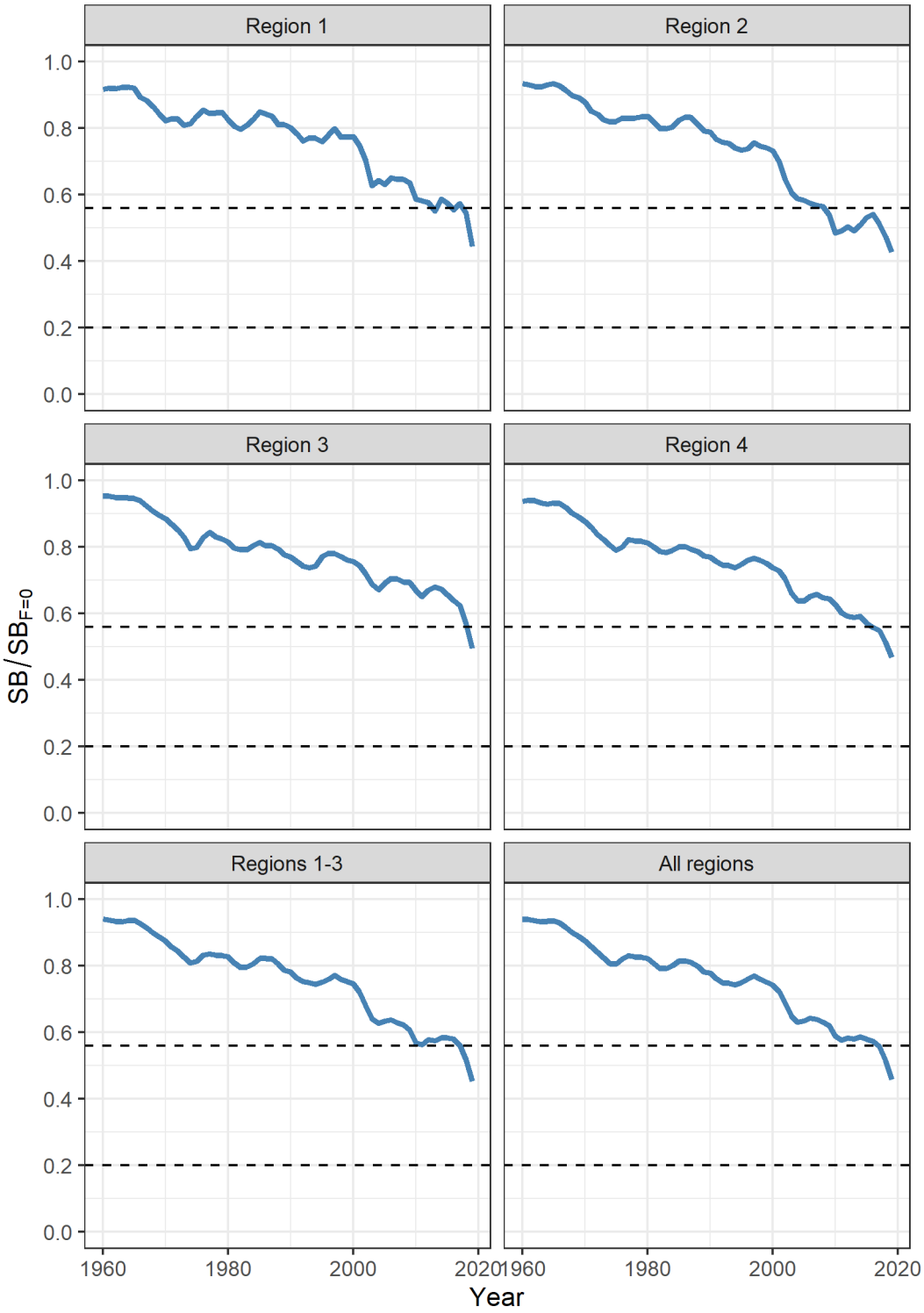

Figure 32: Estimated temporal spawning potential by model region, grouped by region (WCPFC-CA, EPO) and South Pacific as a whole, for the diagnostic case model. The dotted lines are included to indicate the SB/SB$_{F=0}$ interim TRP=0.56 and the LRP=0.2 for the WCPFC-CA albacore fishery.

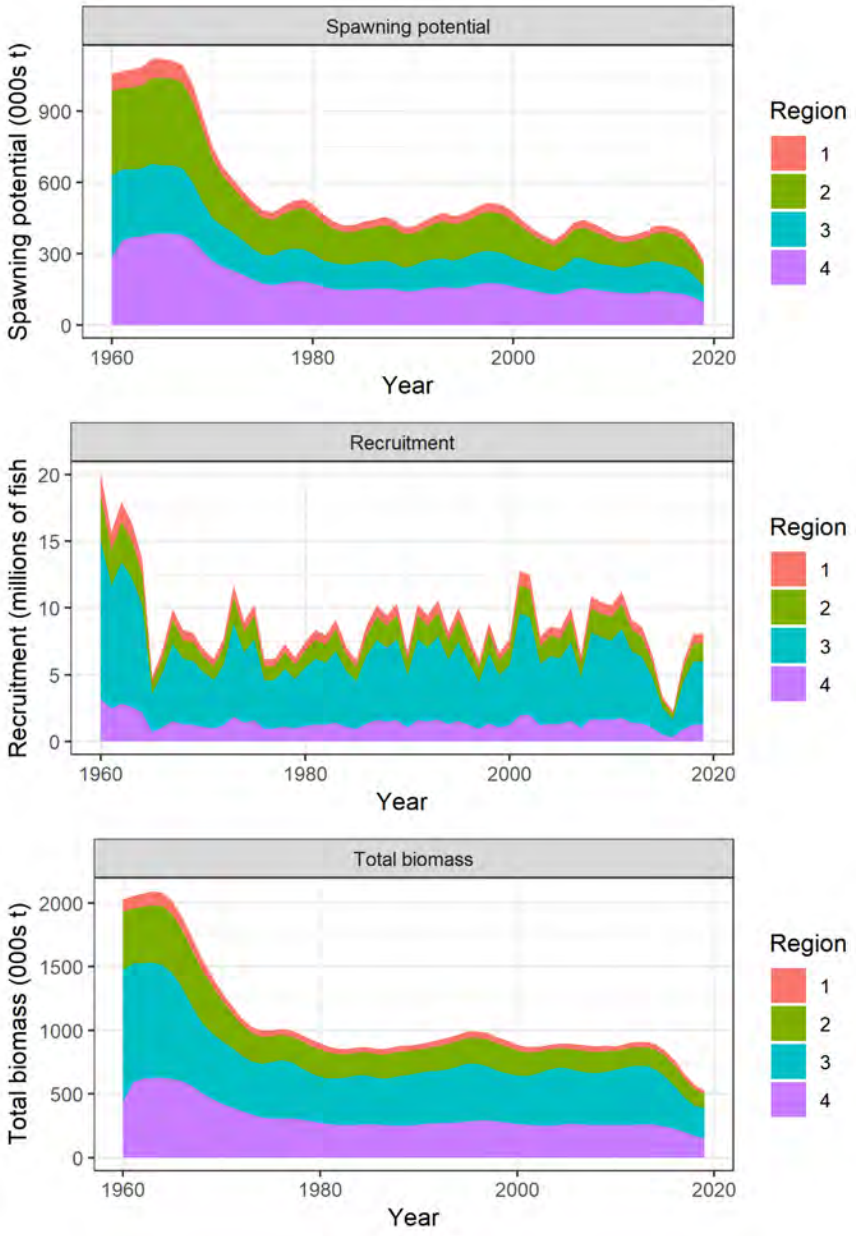

Figure 33: Estimated annual average, a) spawning potential b) recruitment, and c) total biomass by model region for the diagnostic case model, showing the relative levels among regions.

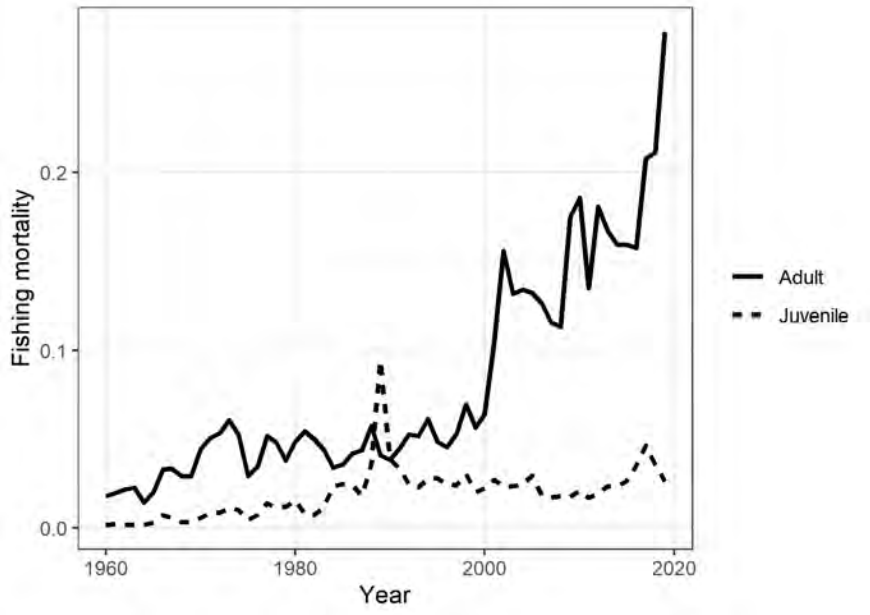

Figure 34: Estimated annual average juvenile and adult fishing mortality for the diagnostic case model.

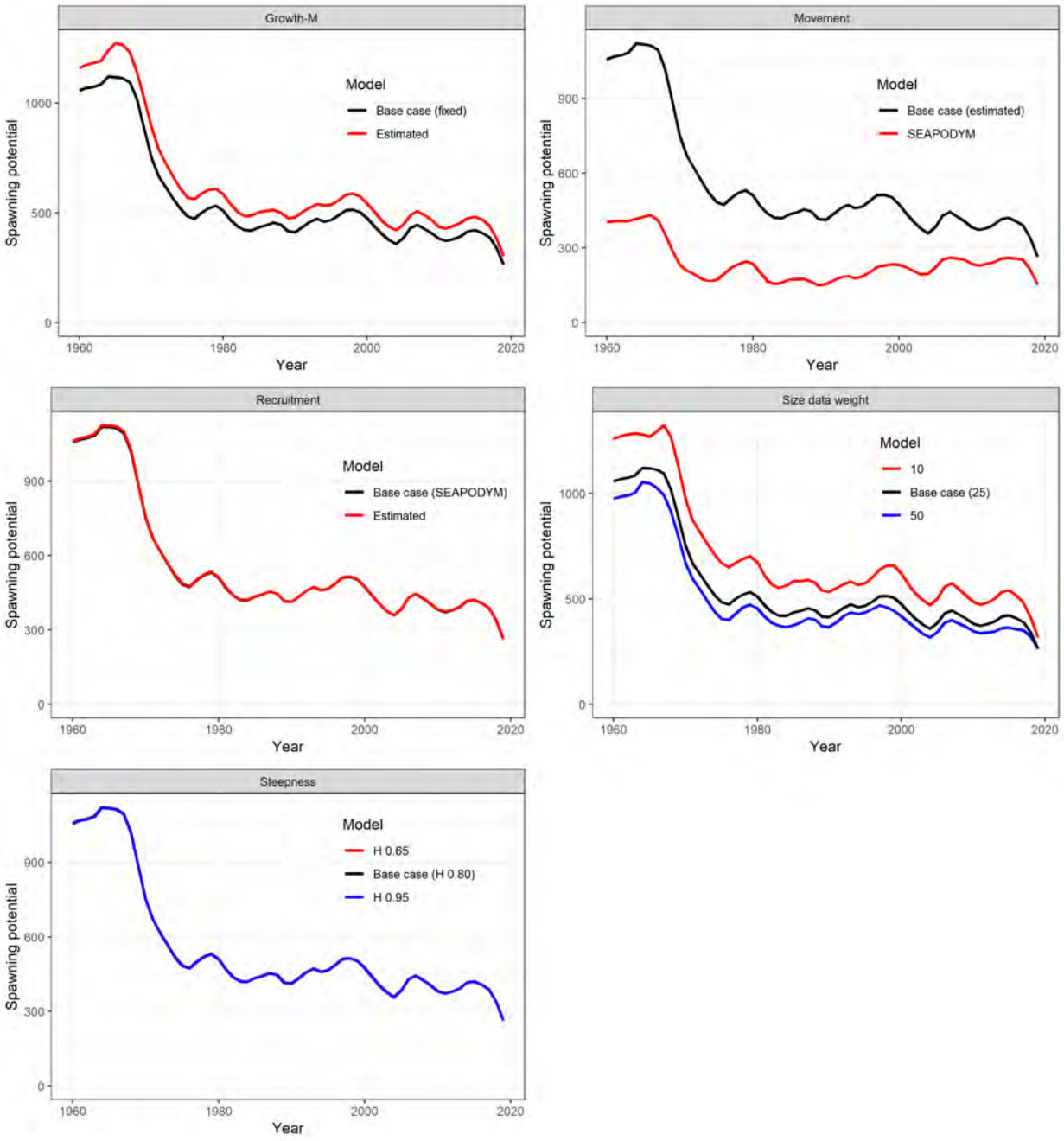

Figure 35: Estimated spawning potential for each of the one-off sensitivity models investigated in the assessment. Note in some cases the models lie on top of each other.

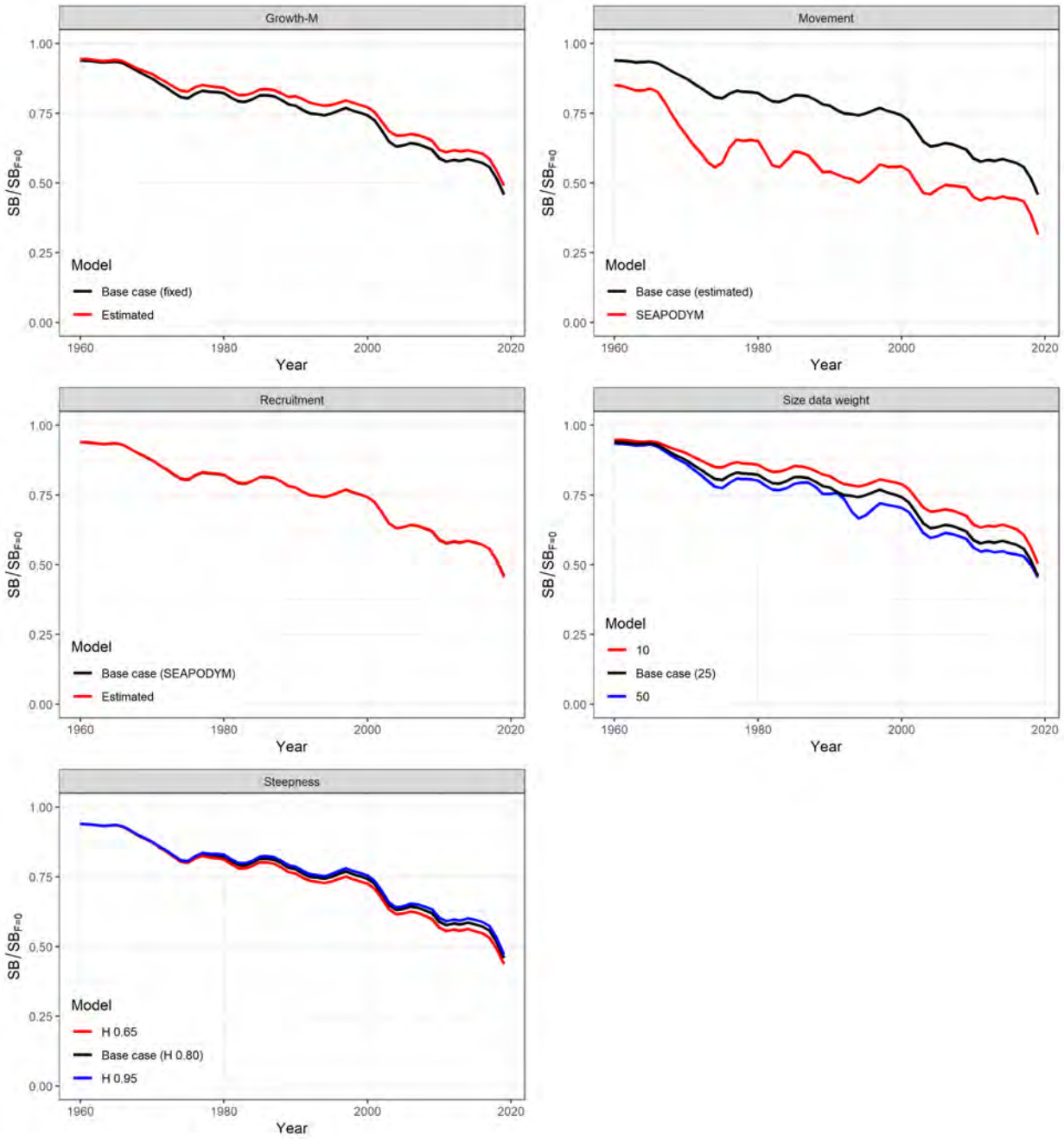

Figure 36: Estimated spawning depletion for each of the one-off sensitivity models investigated in the assessment.

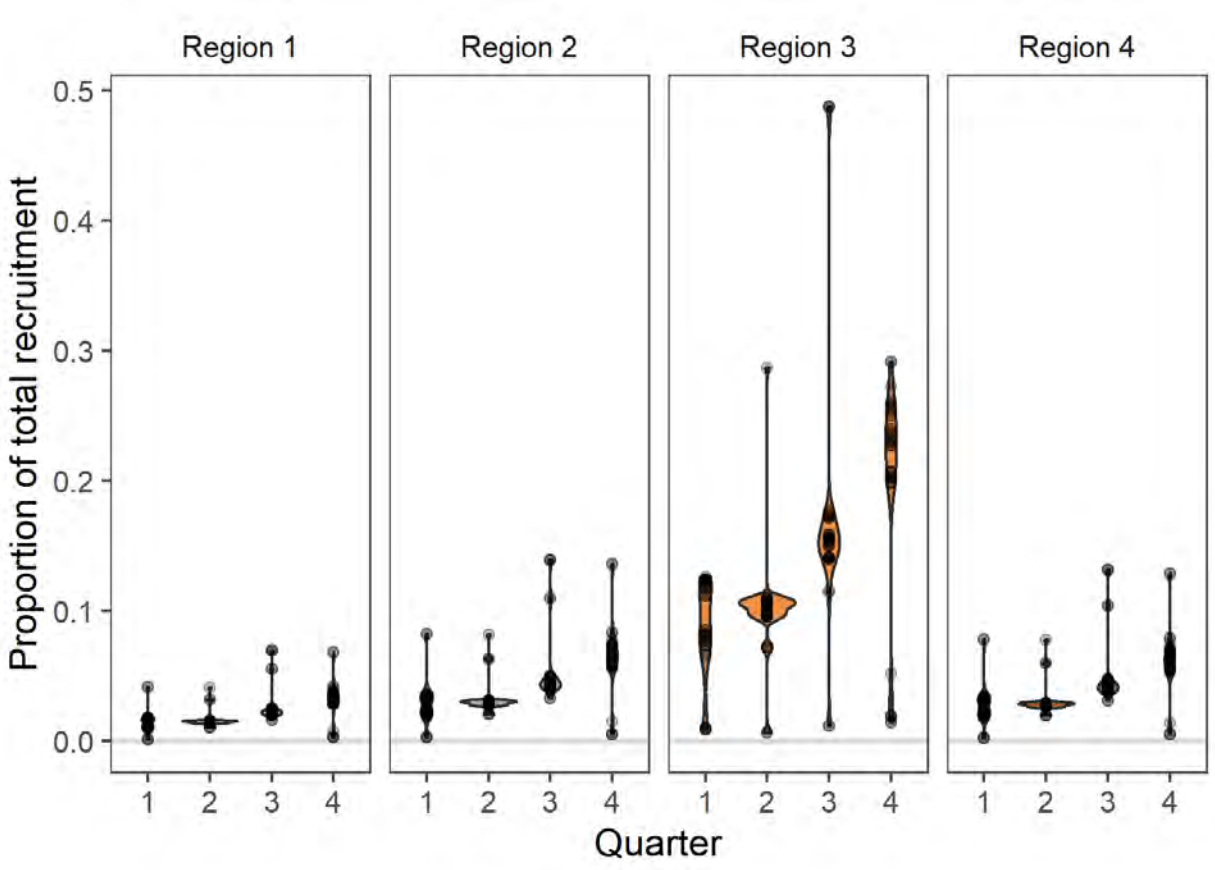

Figure 37: Distribution of annual proportions of recruitment by region (panels) and quarter (within panel group) for all years in the diagnostic case model under the SEAPODYM recruitment scenario R1.

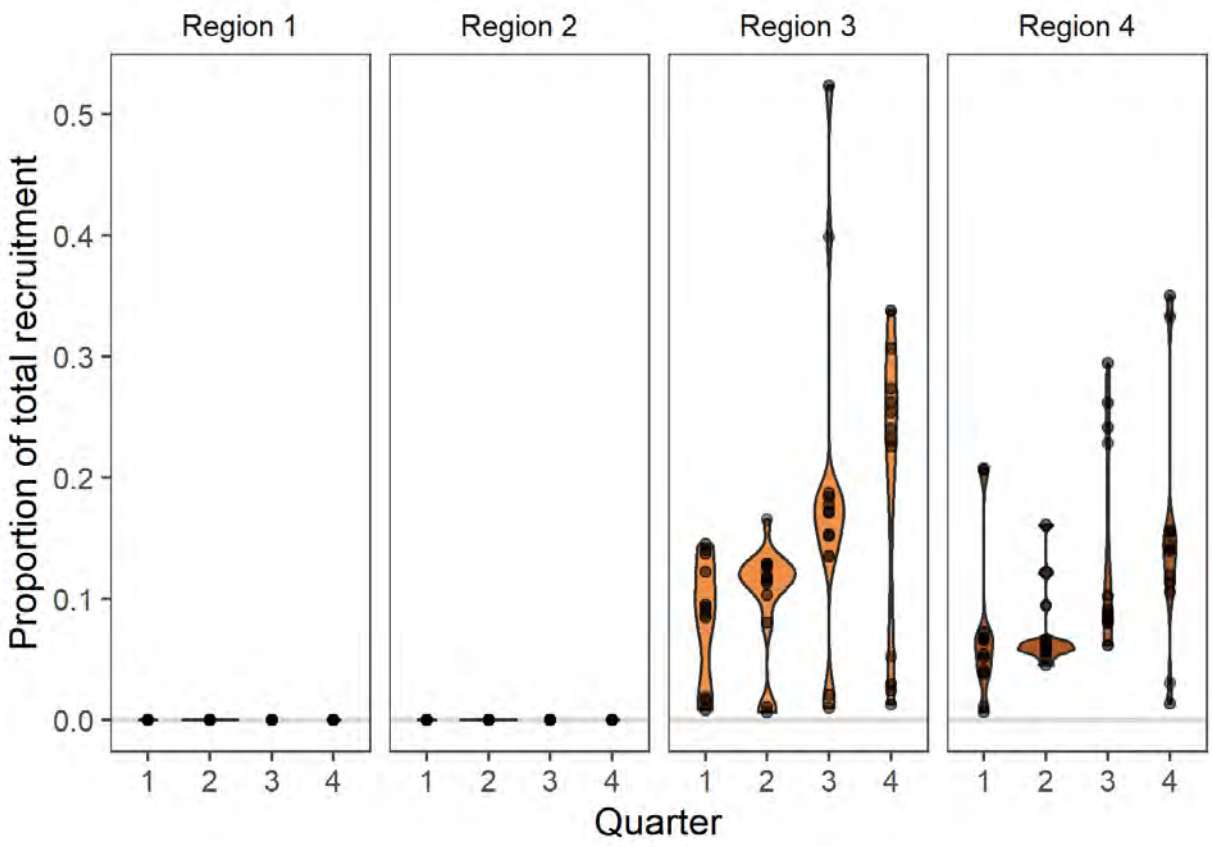

Figure 38: Distribution of annual proportions of recruitment by region (panels) and quarter (within panel group) for all years in the sensitivity model under the recruitment scenario, R2, where recruitment only occurs in model region 3 and 4.

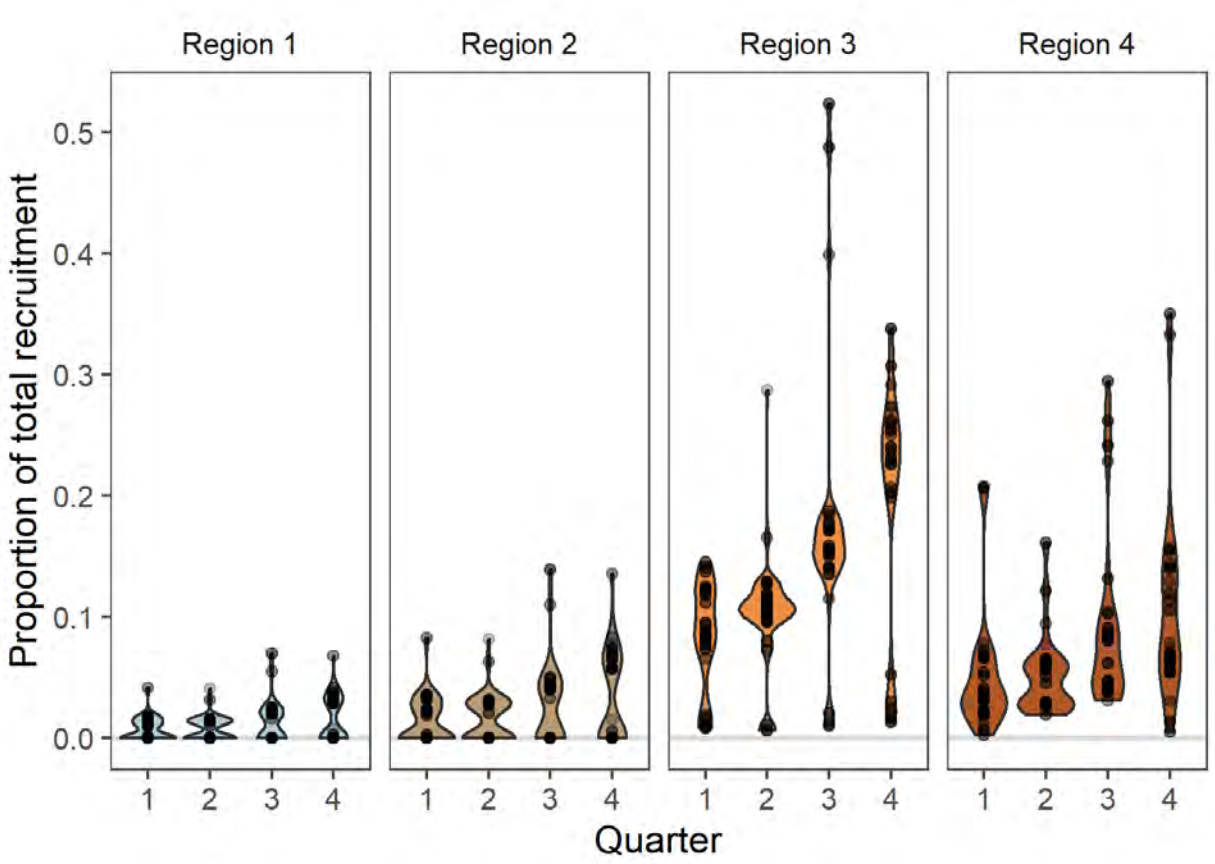

Figure 39: Distribution of annual proportions of recruitment by region (panels) and quarter (within panel group) for all years and all models in the structural uncertainty grid.

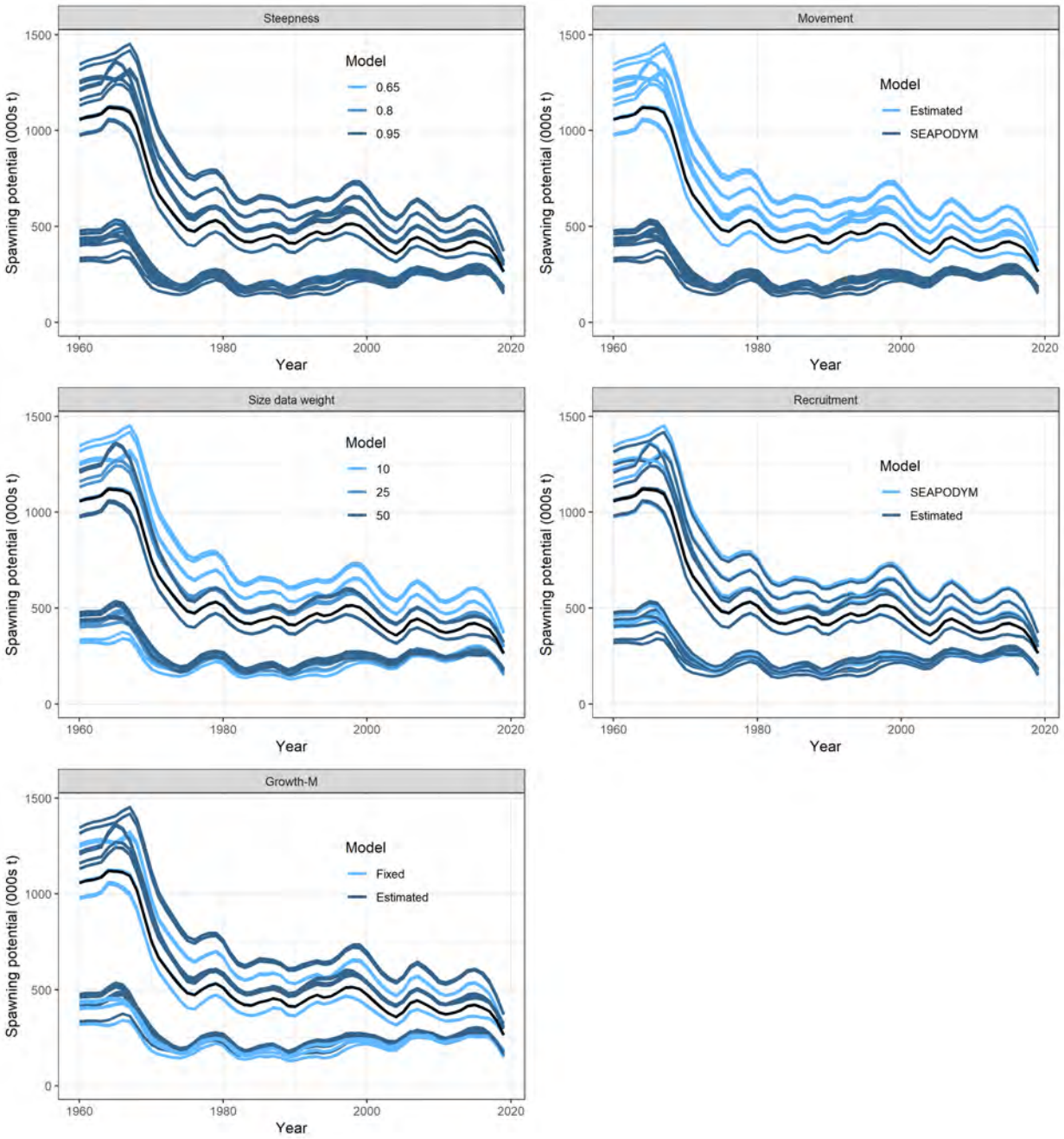

Figure 40: Trajectories of spawning potential for the model runs included in the structural uncertainty grid. The five panels show the models separated on the basis of the five axes used in the grid, with the colour denoting the level within the axes for each model. The black line is the diagnostic case model.

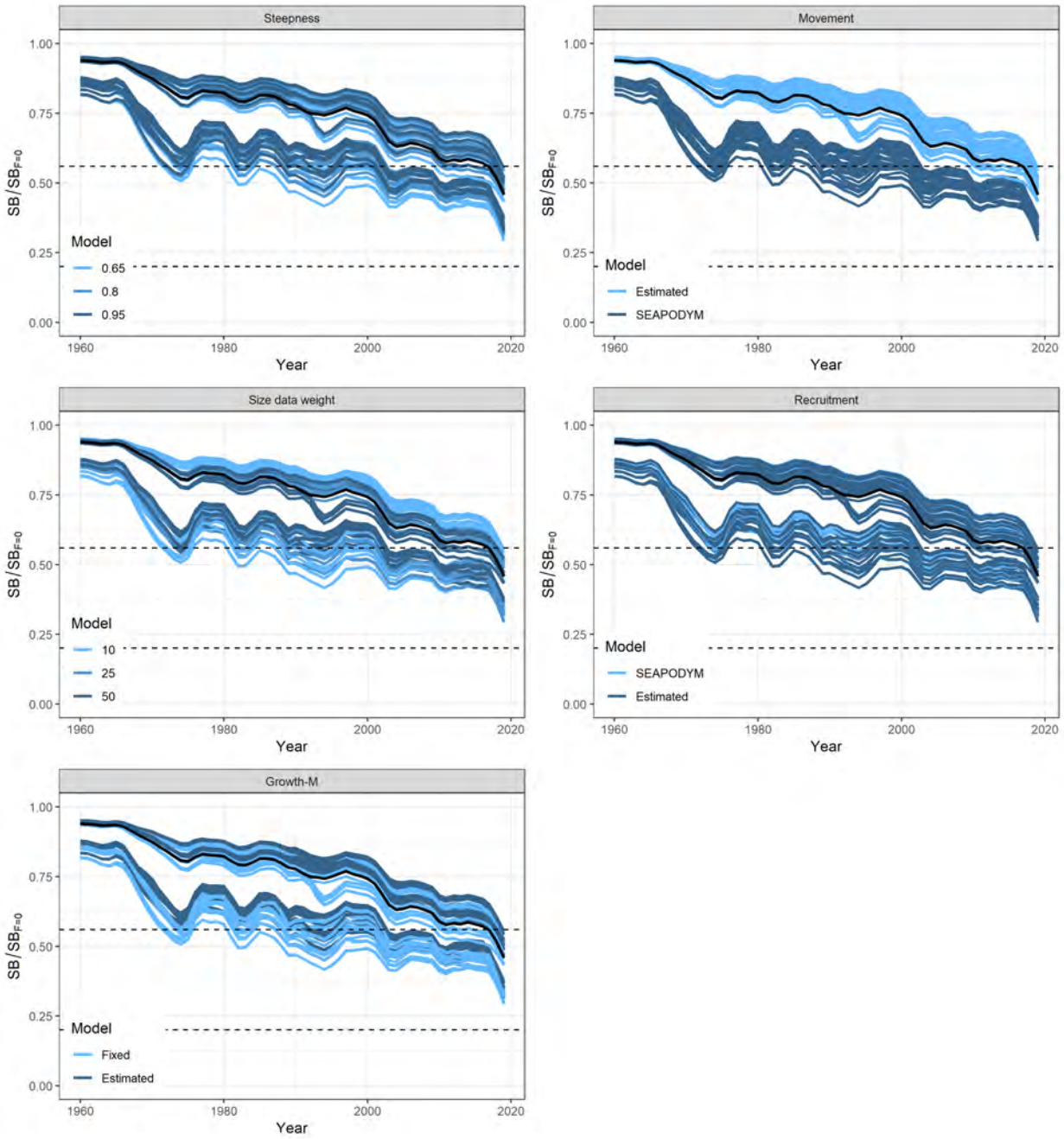

Figure 41: Trajectories of spawning depletion for the model runs included in the structural uncertainty grid. The five panels show the models separated on the basis of the five axes used in the grid, with the colour denoting the level within the axes for each model.The black line is the diagnostic case model.

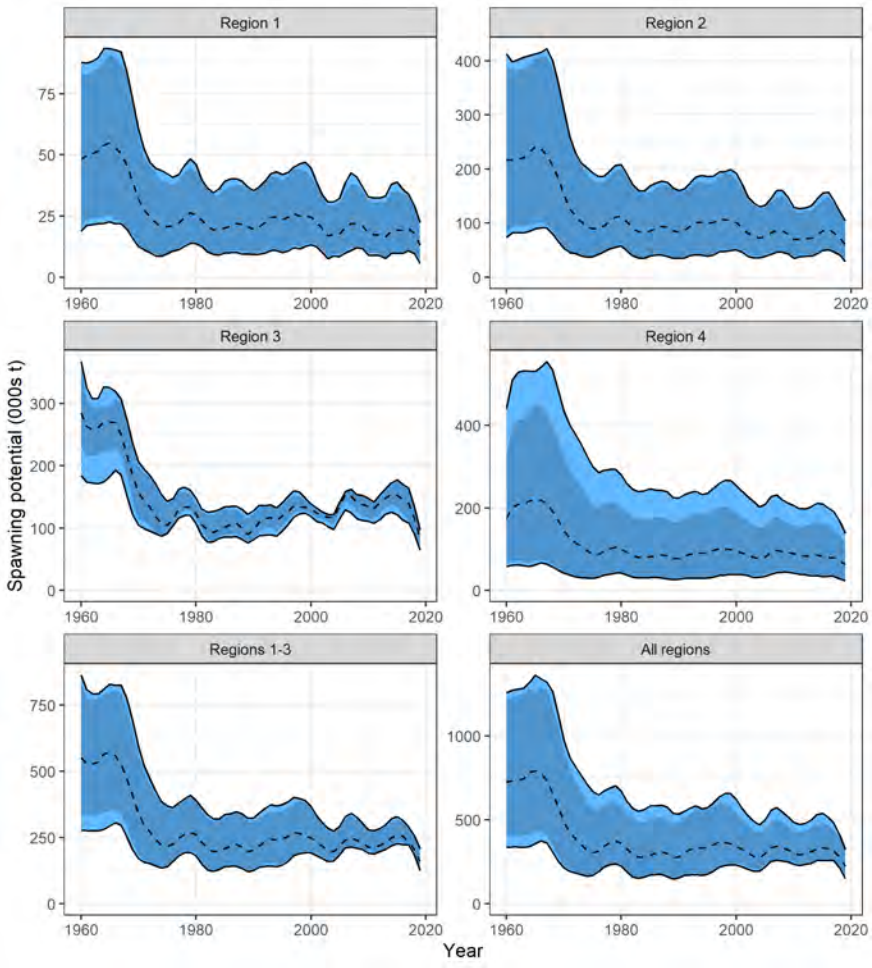

Figure 42: Estimated spawning potential across all models in the structural uncertainty grid over the period 1960-2019. The dashed line represents the median. The lighter band shows the 80^{th} percentile, and the dark band shows the 50^{th} percentile of the model estimates. Area 1-3 refers to the model regions in the WCPFC-CA and so covers the area that was included in the 2018 assessment, Area 1-4 is the entire South Pacific model region, Area 4 is the EPO region.

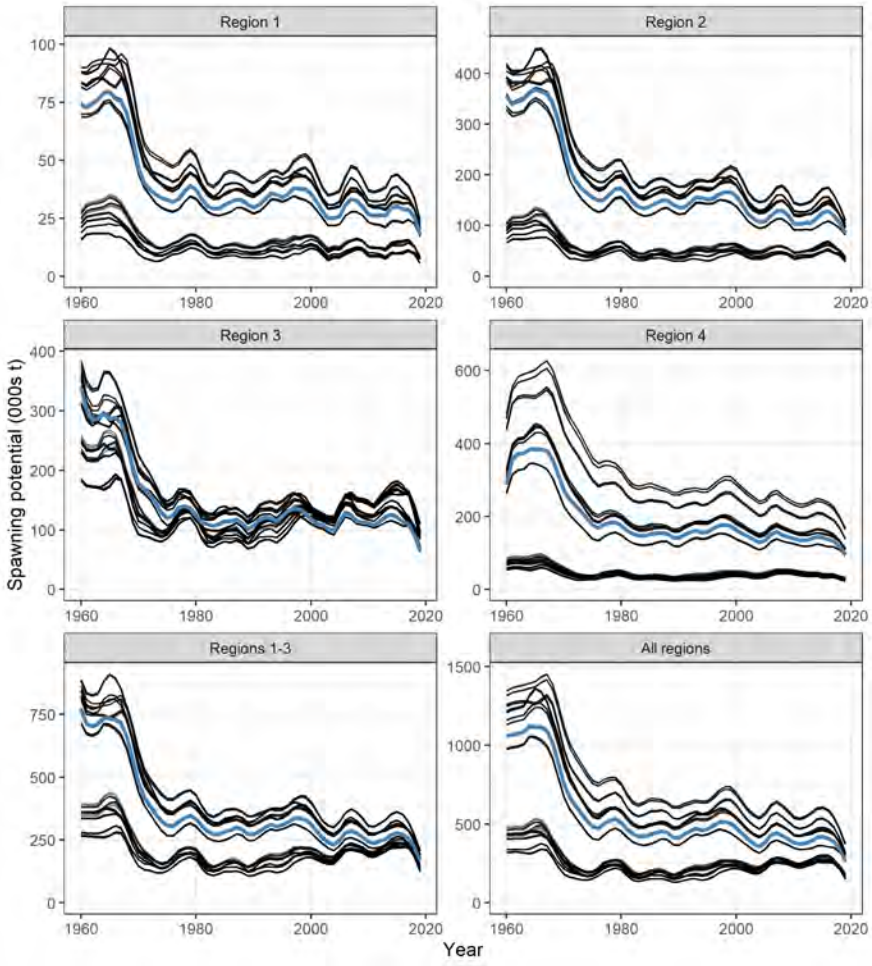

Figure 43: Estimated spawning potential for all individual models in the structural uncertainty grid over the period 1960-2019. The blue line represents the diagnostic case model. Area 1-3 refers to the model regions in the WCPFC-CA and so covers the area that was included in the 2018 assessment, Area 1-4 is the entire South Pacific model region, Area 4 is the EPO region.

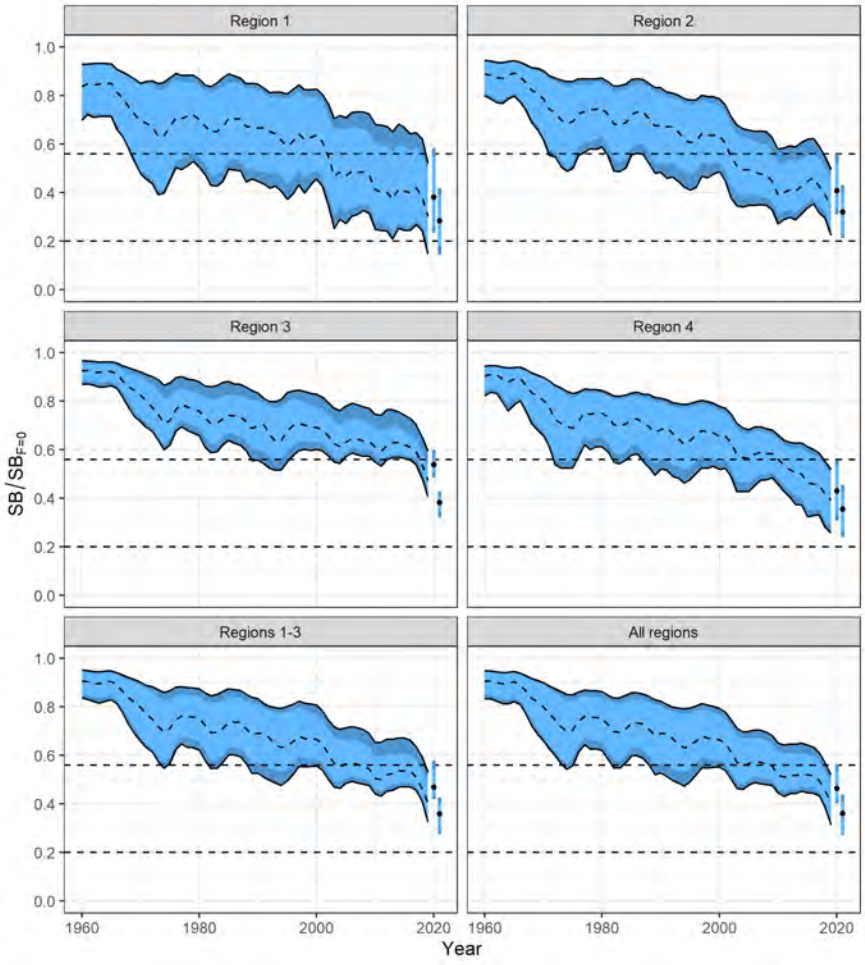

Figure 44: Estimated spawning depletion across all models in the structural uncertainty grid over the period 1960-2019. The dashed line represents the median. The lighter band shows the 80^{th} percentile, and the dark band shows the 50^{th} percentile of the model estimates. Area 1-3 refers to the model regions in the WCPO and so covers the area that was included in the 2018 assessment, Area 1-4 is the entire South Pacific model region, Area 4 is the EPO region. The dashed horizontal lines indicate the depletion limit reference point (LRP) (0.2) and the WCPFC-CA interim target reference point (TRP) for $SB/SB_{F=0}$ (0.56).The bars at right in each plot are the median values (points) and 80^{th} and 50^{th} percentiles for $SB_{recent}/SB_{F=0}$ (left) and $SB_{latest}/SB_{F=0}$ (right).

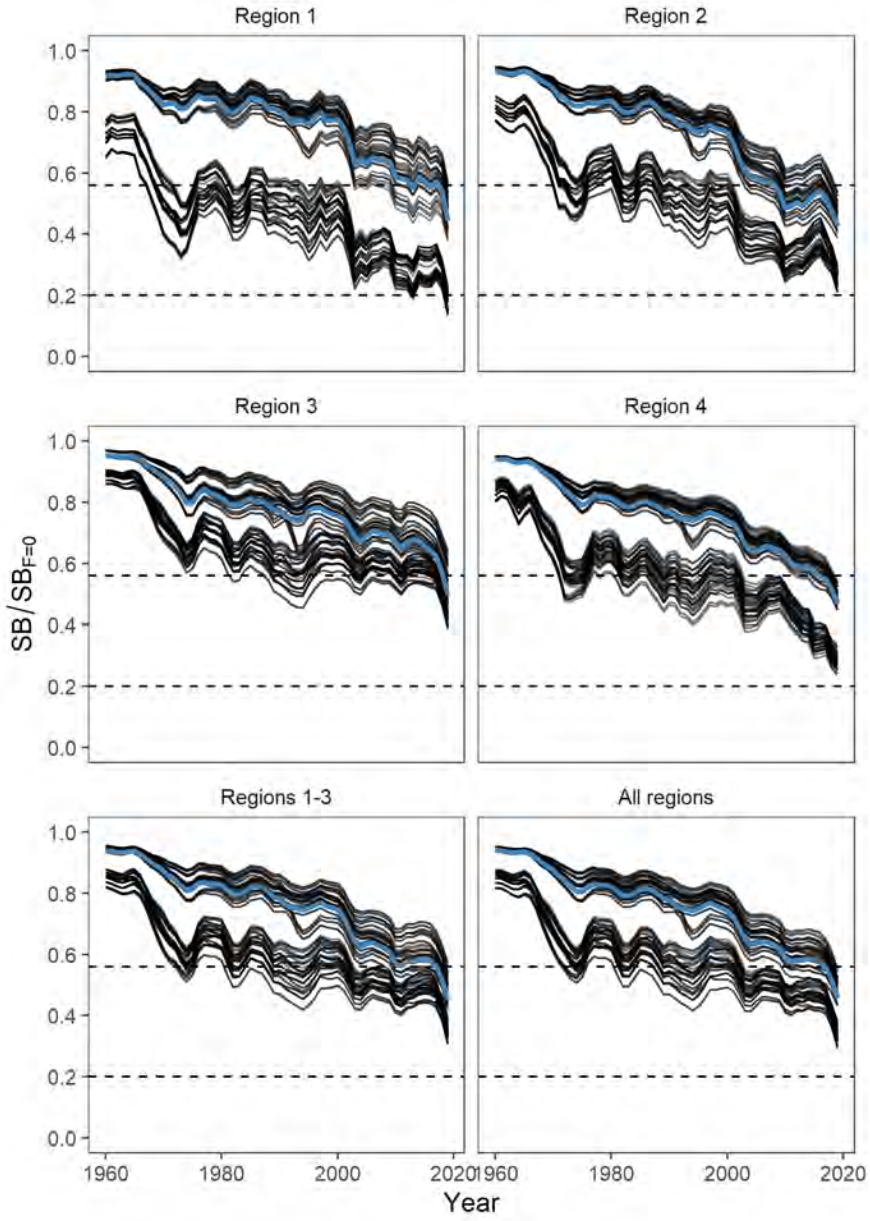

Figure 45: Estimated spawning depletion for all individual models in the structural uncertainty grid over the period 1960-2019. The blue line represents the diagnostic case model. Area 1-3 refers to the model regions in the WCPFC-CA and so covers the area that was included in the 2018 assessment, Area 1-4 is the entire South Pacific model region, Area 4 is the EPO region. The dashed horizontal lines indicate the depletion limit reference point (LRP) (0.2) and the WCPFC-CA interim target reference point (TRP) for $\mathrm{SB/SB}_F = 0$ (0.56).

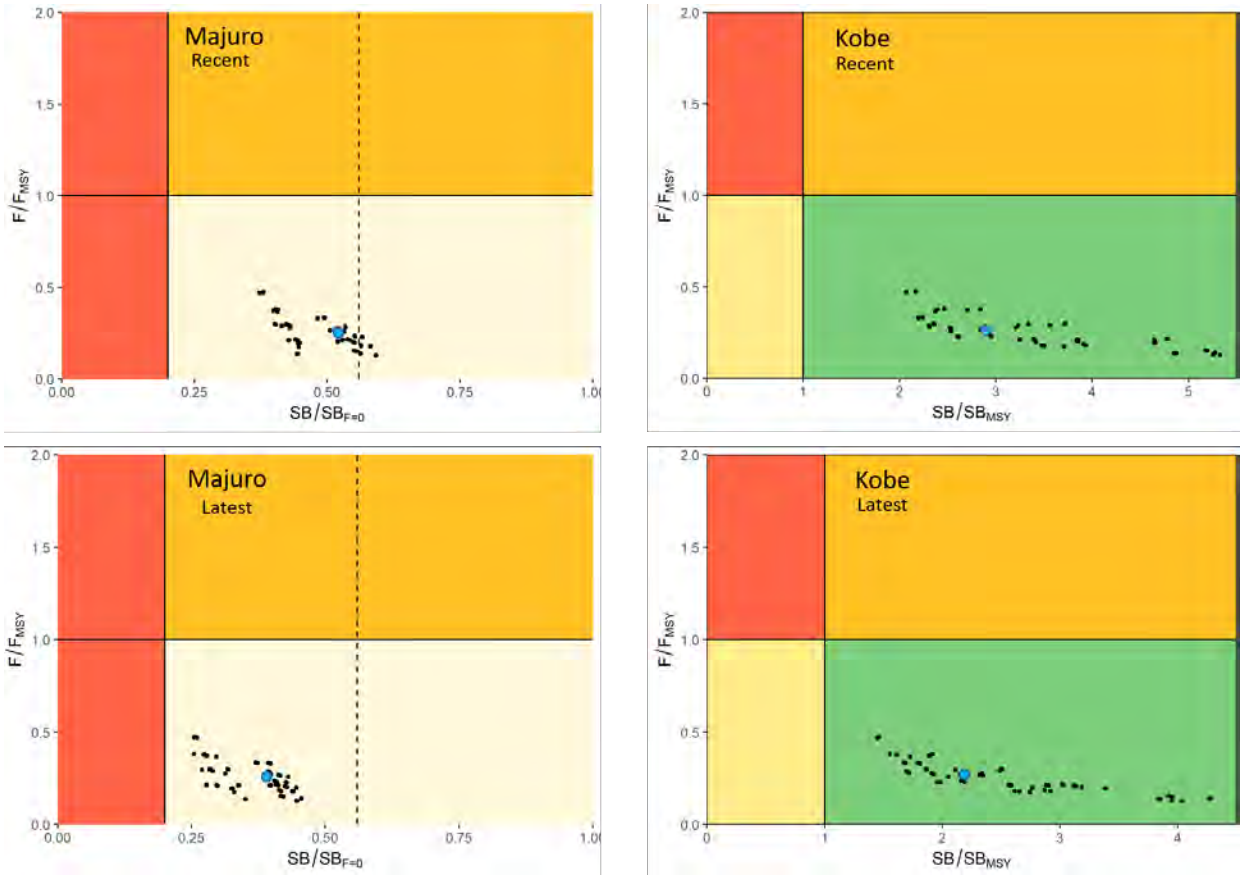

Figure 46: Majuro (left) and Kobe (right) plots summarising the results for each of the models in the structural uncertainty grid for the recent (2016-2019) and latest (2019) periods. The vertical dotted line on the Majuro plots is included to indicate the interim TRP of 0.56 $SB_{F=0}$ for the WCPFC-CA albacore fishery, but note that these data represent the estimates for the entire model area. The blue point is the diagnostic case model.

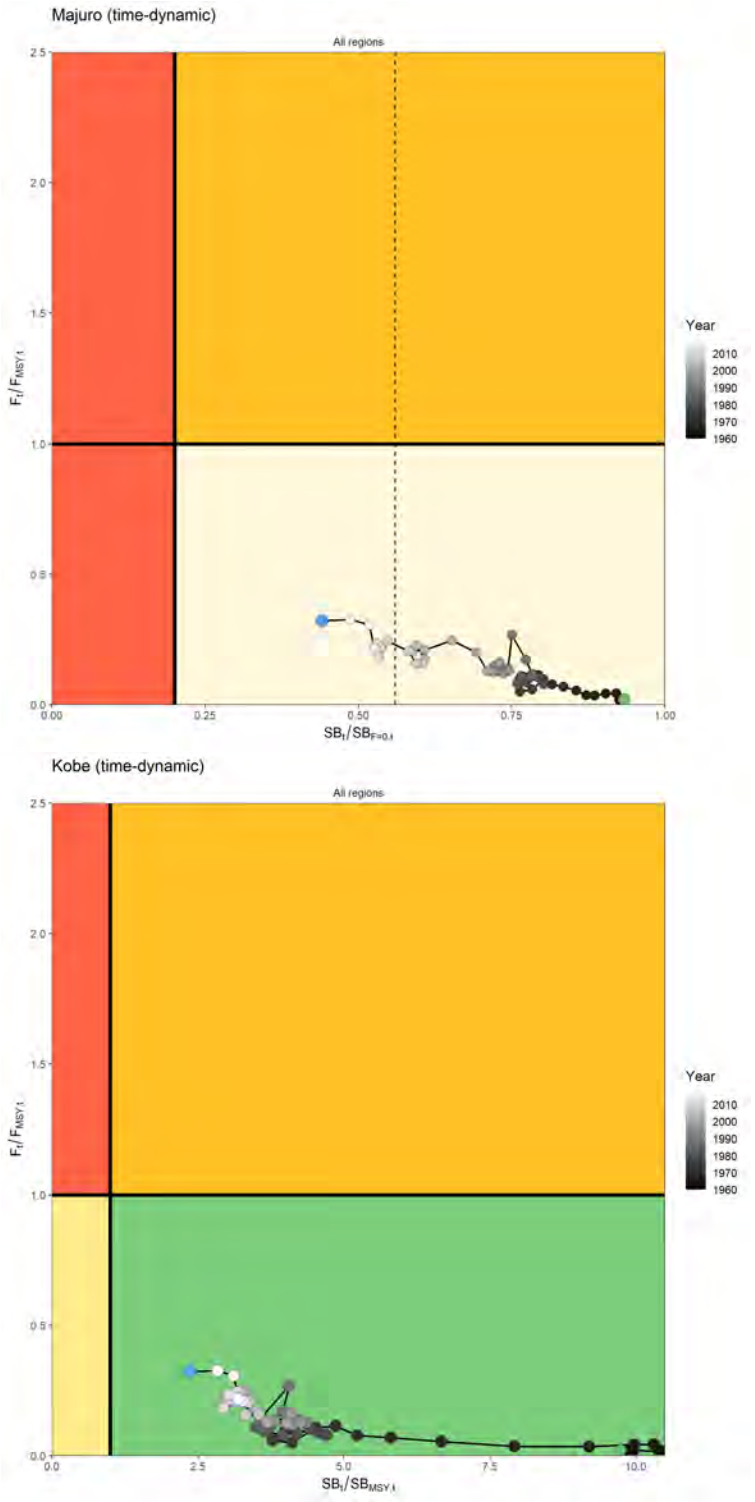

Figure 47: Time dynamic Majuro (top) and Kobe (bottom) plots summarising the results for the diagnostic case model over the model period. The vertical dotted line on the Majuro plot is included to indicate interim TRP of 0.56 $SB_{F=0}$ for the WCPFC-CA albacore fishery, but note that these data represent the estimates for the entire model area. The blue point is the estimated 2019 status.

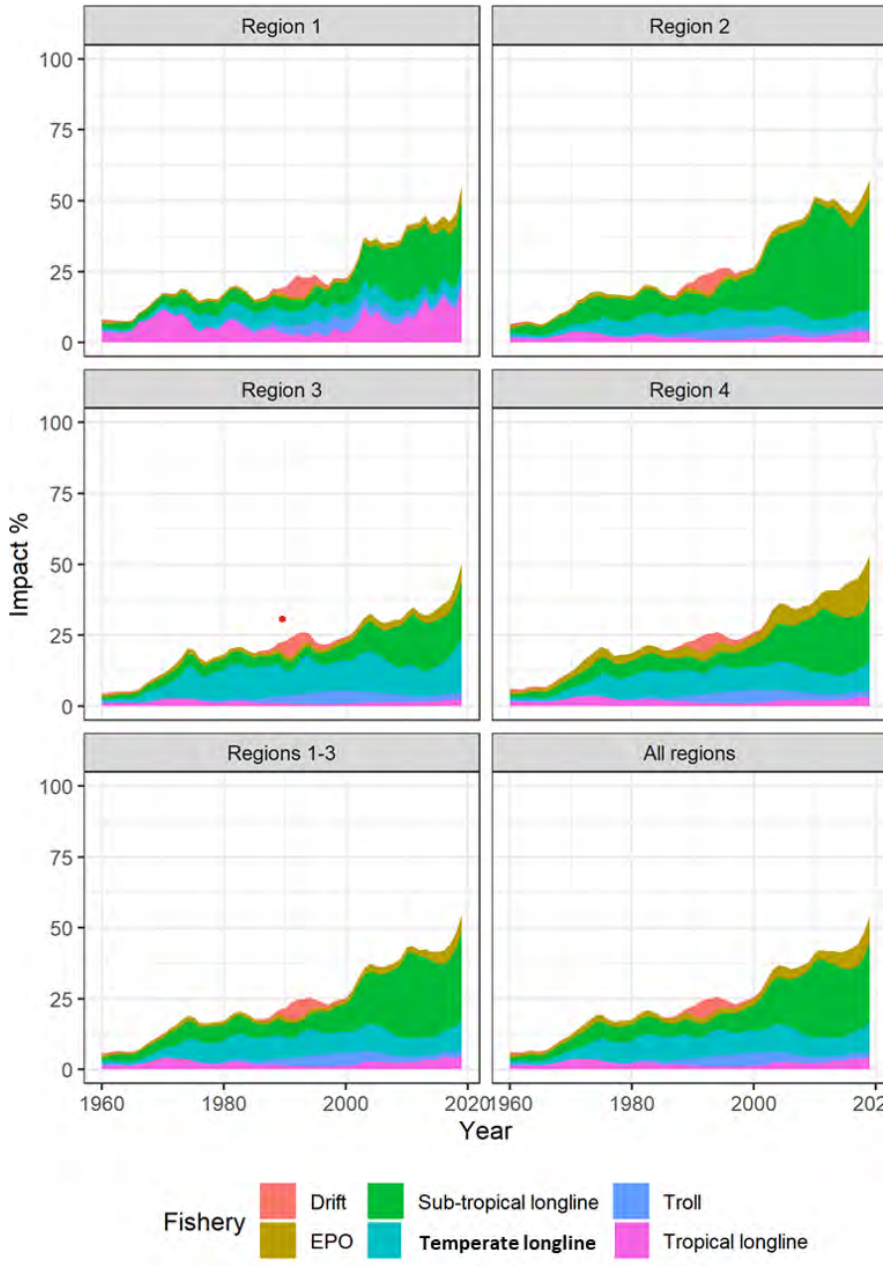

Figure 48: Estimates of reduction in spawning potential due to fishing (fishery impact=1–$SB_{latest}/SB_{F=0}$) by region, and over all regions (lower right panel), attributed to various fishery groups for the diagnostic case model.

13 Appendix 1

M-at-age method: From: *A review of estimation methods for natural mortality and their performance* Mark N. Maunder, Hui-Hua Lee, Kevin R. Piner, Owen S. Hamel, Jason M. Cope, André E. Punt, James N. Ianelli, Richard D. Methot. Manuscript submitted to Fisheries Research.

Approach based on Maunder et al. submitted manuscript for estimating natural mortality age using the alternative growth models (Fixed -otolith, Estimated – length frequency).

A general model for age- and sex-specific natural mortality that expands that developed by Maunder et al. (2009) and Maunder (2011), and is based on the assumptions outlined in the main text:

$$M_{s,a} = M_{juv}\left(\frac{L_{s,a}}{L_{mat*}}\right)^{\lambda} + \frac{M_{mat,s} - M_{juv}\left(\frac{L_{s,a}}{L_{mat*}}\right)^{\lambda}}{1 + exp\left[\beta_s\left(L_{s,a} - L_{50,s}\right)\right]}$$

with the defaults $\lambda = -1.5$ from Gulland(1987), β_s and $L_{50,s}$ from the maturity curve, $M_{mat,s}$= 5.4/$t_{max,s}$ (Hamel this issue) if t_{max} is available otherwise $M_{mat,s} = 4.118K_s^{0.73}Linf_s^{-0.33}$ (Then et al. 2015) and $M_{juv} = 3W_{mat*}^{-0.288}$ from Lorenzen (1996), L_{mat*} and W_{mat*} are the length and weight of a fish when they first become mature for either sex (could be set at the minimum length over both sexes when 5% of the fish are mature) or some other convenient corresponding length and weight of a fish before it becomes mature.

Maunder, M.N., Wong, R.A., 2011. Approaches for estimating natural mortality: Application to summer flounder (*Paralichthys dentatus*) in the U.S. mid-Atlantic. Fish. Res. 111, 92–99.

Maunder, M.N., Aires-da-Silva, A. Deriso, R.B., Schaefer, K. and Fuller, D., 2009. Preliminary estimation of age- and sex-specific natural mortality for bigeye tuna in the eastern Pacific Ocean by applying cohort analysis with auxiliary information to tagging data. Inter-Amer. Trop. Tuna Comm., Stock Assessment Report, 10: 253-278.

14 Appendix 2

Change in the total, and individual data component log-likelihoods with respect to the derived parameter, mean total biomass over the assessment period, across a range of values at which this parameter was penalised to fit, for the diagnostic case model.

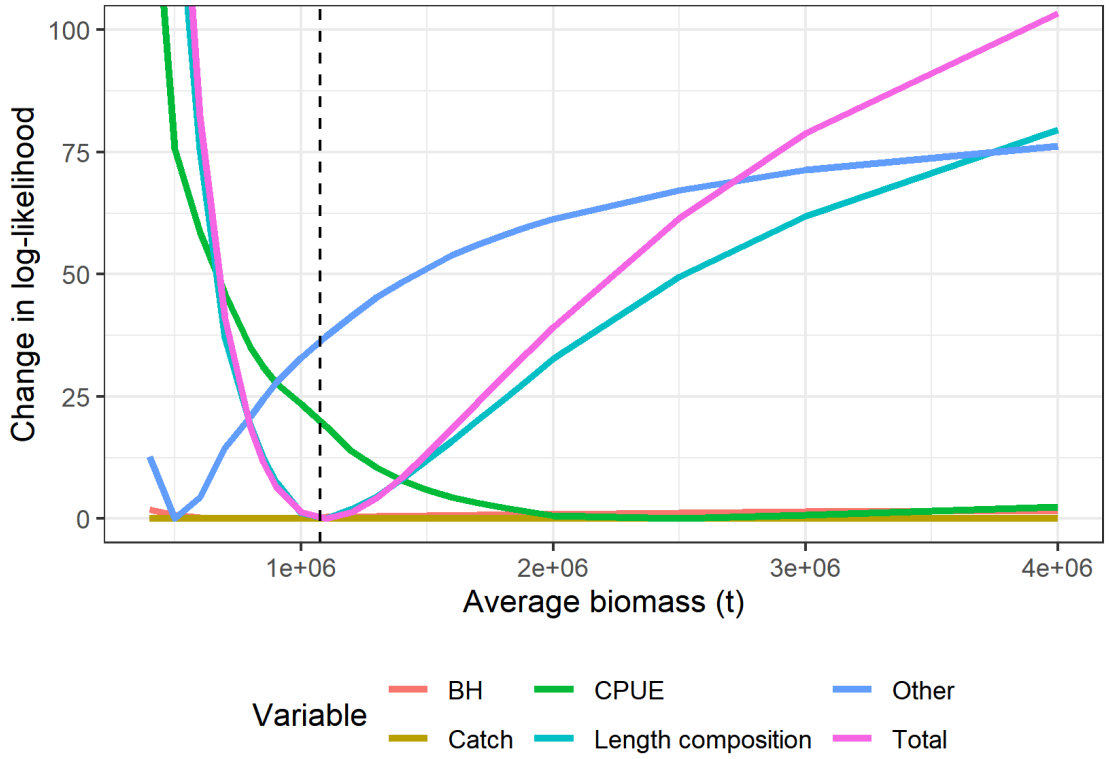

15 Appendix 3

Sensitivity of population scaling to alternative settings for the movement coefficients priors and penalty weightings.

CV settings	Movement scale Prior mean = 0 Age-dependency Prior mean = 0	Movement scale Prior mean = 0.1 Age-dependency Prior mean = 0
CV (movement scale) = 0.32 CV (age-dependency) = 0.32	1.076	1.072
CV (movement scale) = 2.20 CV (age-dependency) = 0.32	1.058	1.058
CV (movement scale) = 0.32 CV (age-dependency) = 2.20	1.188	1.179
CV (movement scale) = 2.20 CV (age-dependency) = 2.20	1.150	1.155

16 Appendix 4

Sensitivity of the SPO21 diagnostic case model to inclusion of tagging data. Spawning biomass (left), Spawning depletion (right).

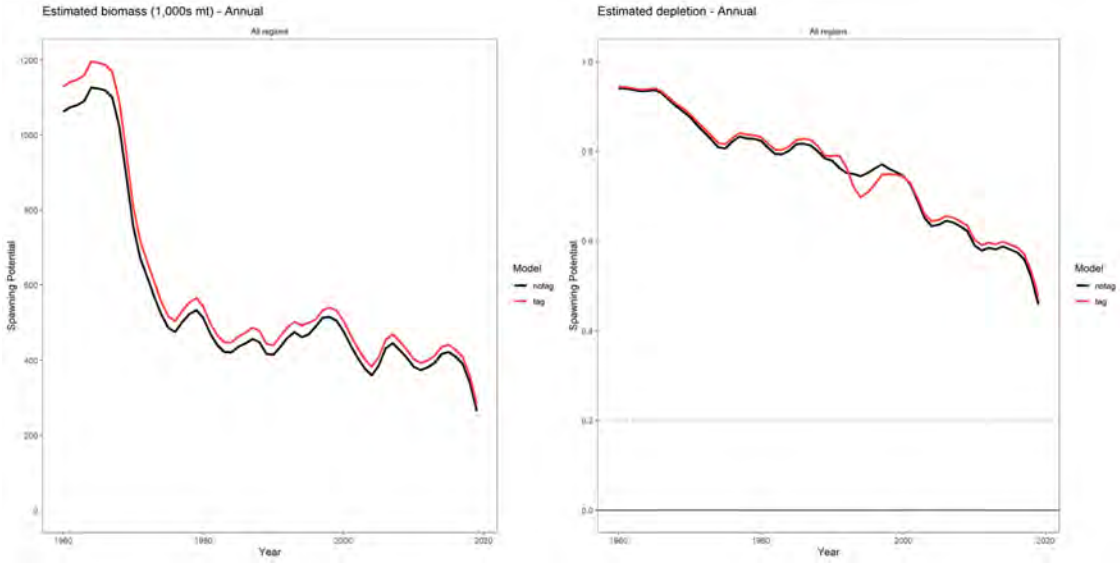

17 Appendix 5

Retrospective models for the diagnostic case.

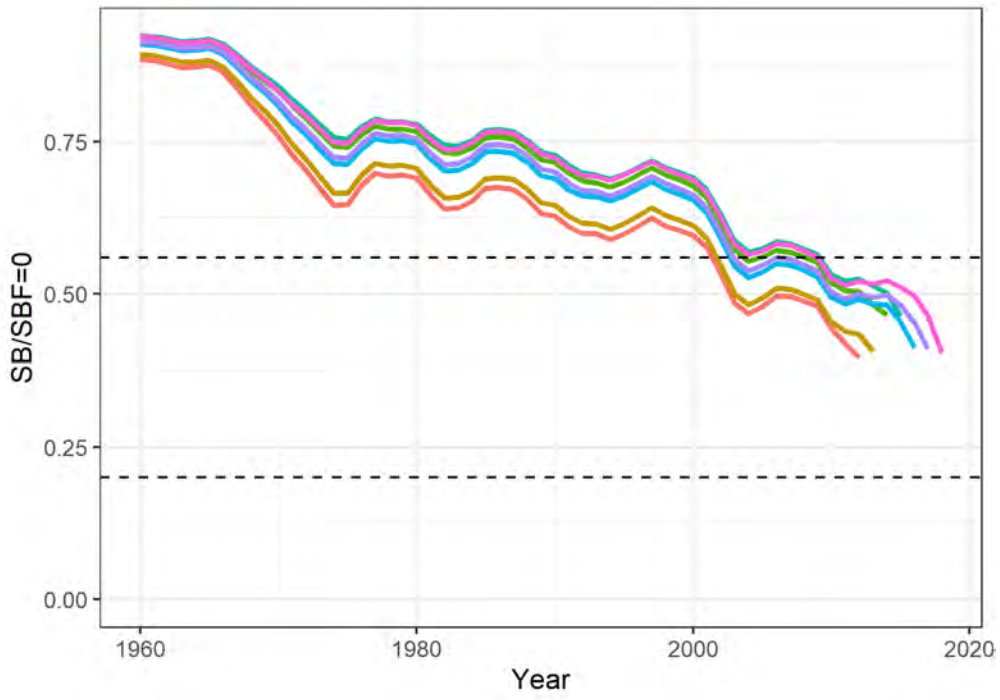

Retrospective analyses involve rerunning the selected model by consecutively removing successive years of data to estimate model bias. A series of seven additional models were fitted with the retrospective removal of all input data consecutively for the last seven years of the model time period. The estimated depletion does not change much across the retrospective analyses when the last one to five years are removed, however it shows an increased bias towards a more depleted state when the last six and seven years of data are removed.

18 Appendix 6

The potential stock consequences of fishing at alternative "status quo" conditions (i.e. at recent average fishing levels) were evaluated, where future longline fishing was projected based upon recent catch levels and recent effort levels (see Table 5). For both alternatives all other fisheries were projected based upon catch (e.g. troll). A summary of the approach is as follows:

- Catch-based projections: Two scenarios for future longline and troll catches were considered: 2017-2019 average catches across the South Pacific; 2020 average catches within the WCPFC-CA, and 2017-2019 average catches in the EPO (given EPO data for 2020 are likely still incomplete).
- Effort-based projections: Two scenarios for future longline effort and troll catch were considered: 2017-2019 average levels across the South Pacific; 2020 average levels within the WCPFC-CA, and 2017-2019 average levels in the EPO (given EPO data for 2020 are likely still incomplete). All other settings were as assumed for the catch-based projections.
- Stochastic 30 year projections were conducted from each assessment model within the uncertainty grid developed for the 2021 South Pacific albacore assessment.
- For each model, 100 stochastic projections were conducted, with future recruitments randomly sampled from historical deviates across the period used to estimate the stock-recruitment relationship within the assessment.
- The outputs of the projections (median $SB_{year}/SB_{F=0}$) for specific years of the projection period, F_{recent}/F_{MSY}, and risk $SB_{2049}/SB_{F=0}$ <LRP, were calculated across the model grid for the whole of the South Pacific.
- Median $SB_{year}/SB_{F=0}$ for specific years of the projection period and risk $SB_{2049}/SB_{F=0}$ <LRP were also calculated across the model grid for the southern WCPFC-CA region only.
- Catchability (which can have a trend in the historical component of the model) was assumed to remain constant in the projection period at the level estimated in the terminal year of the assessment model.

Results of the catch-based projections are summarized in Tables 1 and 2 and Figure 1. Results of the effort-based projections are summarized in Tables 3 and 4 and Figure 2.

Table 1. **Catch-based:** Summary of median South Pacific-wide albacore tuna stock outcomes under alternative average future fishing conditions.

Fishing level	$SB_{2025}/SB_{F=0}$	$SB_{2035}/SB_{F=0}$	$SB_{2049}/SB_{F=0}$	Risk $SB_{2049}/SB_{F=0}$ < LRP	F/F_{MSY}	Risk $F>F_{MSY}$
2017-2019 average	0.33	0.38	0.35	30%	0.43	27%
2020	0.36	0.43	0.41	26%	0.37	26%

Table 2. **Catch-based:** Summary of median WCPFC-CA albacore tuna stock outcomes under alternative average future fishing conditions.

Fishing level	$SB_{2025}/SB_{F=0}$	$SB_{2035}/SB_{F=0}$	$SB_{2049}/SB_{F=0}$	Risk $SB_{2049}/SB_{F=0}$ < LRP
2017-2019 average	0.20	0.26	0.24	36%
2020	0.22	0.30	0.28	30%

Table 3.**Effort based:** Summary of median South Pacific-wide albacore tuna stock outcomes under alternative average future longline effort and troll catch fishing conditions.

Fishing (effort) level	$SB_{2025}/SB_{F=0}$	$SB_{2035}/SB_{F=0}$	$SB_{2049}/SB_{F=0}$	Risk $SB_{2049}/SB_{F=0}$ < LRP	F/F_{MSY}	Risk $F>F_{MSY}$
2017-2019 average	0.37	0.48	0.44	1%	0.26	0%
2020	0.39	0.51	0.48	0%	0.24	0%

Table 4.**Effort based:** Summary of median WCPFC-CA albacore tuna stock outcomes under alternative average future longline effort and troll catch fishing conditions.

Fishing (effort) level	$SB_{2025}/SB_{F=0}$	$SB_{2035}/SB_{F=0}$	$SB_{2049}/SB_{F=0}$	Risk $SB_{2049}/SB_{F=0}$ < LRP
2017-2019 average	0.26	0.35	0.32	4%
2020	0.26	0.36	0.32	3%

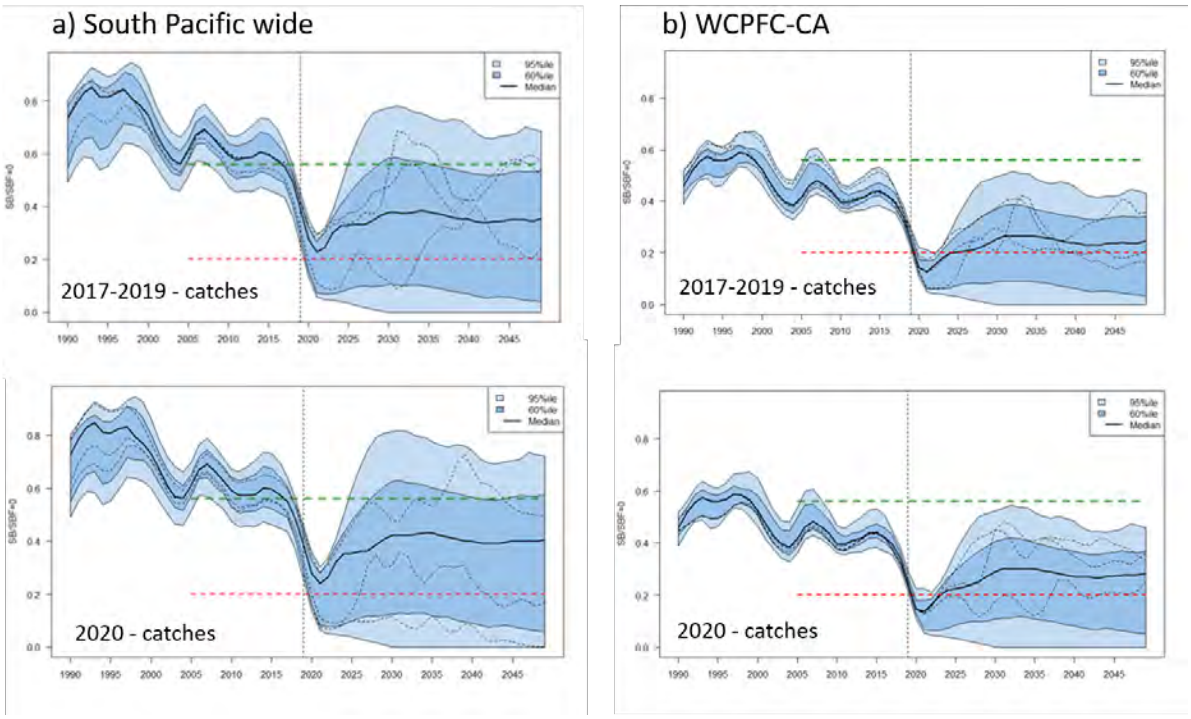

Figure 1. **Catch based:** Time series of South Pacific albacore tuna spawning potential $SB_t/SB_{F=0}$ for the whole of the South Pacific (left column) and the WCPFC-CA (right column) where $SB_{F=0}$ is the average SB from *t-10* to *t-1*, from the uncertainty grid of 2021 assessment models for the period 1990 to 2019, and stochastic projection results for the period 2020 to 2049 assuming 2017-2019 (top row) and 2020 (bottom row) catch levels continue. Vertical line at 2019 represents the last year of the assessment. During the projection period (2020-2049) levels of recruitment variability are assumed to match those over the period used to estimate the stock recruitment relationship (1960-2017). The dashed lines indicate three example trajectories (chosen randomly out of 7200) from the model grid; the dark and light blue areas contain 60 and 95th percentiles, respectively, of depletion estimates for each year. The red horizontal dashed line represents the agreed limit reference point, the green dashed line the interim target reference point.

We note that 13% of the stochastic catch-based projections failed to run to completion. This may result from a combination of particular grid models with lower stock productivity, low future recruitments sampled from the historical estimates within the projection period, and the assumption that fixed catch levels are assumed in the future regardless of the underlying stock status. Under those conditions the biomass can be reduced to zero. As per previous SC discussions, effort-based projections will also be examined as soon as possible.

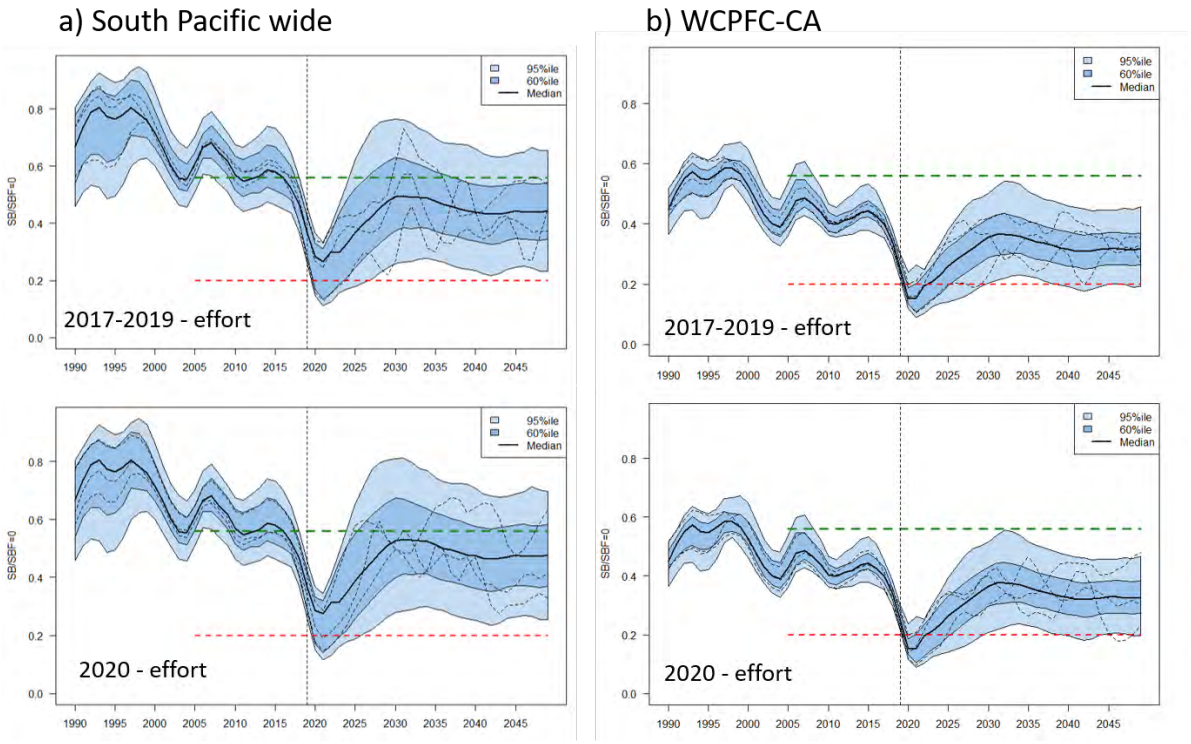

Figure 2. **Effort based:** Time series of South Pacific albacore tuna spawning potential $SB_t/SB_{F=0}$ for the whole of the South Pacific (left column) and the WCPFC-CA (right column) where $SB_{F=0}$ is the average SB from *t-10* to *t-1*, from the uncertainty grid of 2021 assessment models for the period 1990 to 2019, and stochastic projection results for the period 2020 to 2049 assuming 2017-2019 (top row) and 2020 (bottom row) effort levels continue. Vertical line at 2019 represents the last year of the assessment. During the projection period (2020-2049) levels of recruitment variability are assumed to match those over the period used to estimate the stock recruitment relationship (1960-2017). The dashed lines indicate three example trajectories (chosen randomly out of 7200) from the model grid; the dark and light blue areas contain 60 and 95th percentiles, respectively, of depletion estimates for each year. The red horizontal dashed line represents the agreed limit reference point, the green dashed line the interim target reference point.

Table 5. Values of catch and effort used to provide alternative "status quo" fishing for the stock projections. Note that effort in days for longline fisheries is not a requirement in the annual catch estimates nor aggregate data submission for WCPFC. That standard reporting of effort is in hooks set.

Period	Fishery	Catch (mt)	Effort (hooks)
WCPFC_CA			
2017-2019 average	longline	69,082	4,307,339
2020	longline	55,321	4,200,793
2017-2019 average	troll	2,753	na
2020	troll	4,772	na
South Pacific Wide			
2017-2019 average	longline	84,629	5,791,945
2020	longline	64,963	4,704,797
2017-2019 average	troll	2,753	na
2020	troll	4,772	na